DIPARTIMENTO SCIENZE DELLA VITA

DOTTORATO DI RICERCA IN SCIENZE DELLA VITA

CICLO XXXIV

COORDINATORE Prof. Massimo Valoti

Gut-brain axis: the role of microbiota in gut and brain ageing

SETTORE SCIENTIFICO-DISCIPLINARE: BIO/16

TUTOR: Prof. Eugenio Bertelli

DOTTORANDA: Annalisa Altera

Annalisa Altera

CO-RELATORE: Prof. Claudio Nicoletti

A.A. 2021-2022

Al mio mentore

INDEX

ABSTRACT

In the last decade there has been a growing interest in the reciprocal impact occurring between the gut and the brain and this is well conceptualized in the gut-brain axis notion. The gut-brain axis is the bidirectional communication route between the "little brain" (gut) and the "big brain" (brain). There are several factors that play an important role in this axis but it has become more and more evident that the gut bacteria represent a key component. This has led to the new concept of the microbiota-gut-brain axis, emphasizing the importance of the gut microbiota in this axis. The gut has evolved with bacteria in a symbiotic way and the human gut hosts about 10^{14} bacterial cells. Researches in the last years have highlighted the importance of the microbiota not only for gut functions but also for the central nervous system (CNS) development, physiology and pathology. However, there are different factors that influence the composition of the gut microbiota (mode of delivery, diet, stress and ageing). In particular, the composition of the gut microbiota changes with ageing: in the adults the majority of taxa are *Bacteroidetes* and *Firmicutes* while the elderly has a different composition of the gut microbiota. Some studies have reported a decrease in *Bifidobacteria* and an increase in *Escherichia*, *Enterobacteriaceae* and *Clostridium difficile* in the elderly. Interestingly, the centenarians apparently have no changes in gut microbiota in comparison to adult, further highlighting the importance of gut bacteria in longevity. Ageing is a physiological process related to the loss of function in different body systems and also associated with a decline in cognitive functions. It has become more and more evident that events taking place in the gut play a major role in the ageing process and in age-related diseases. Faecal microbial transplant (FMT) is a technique that consists in the transfer of gut microbiota from a donor to a recipient (usually *via* an oral gavage in rodents or colonoscopy in humans) and allows to establish a donor-like microbiota in the gastro-intestinal tract of the recipient. FMT is used to treat recurrent *Clostridium difficile* infections but there are studies trying to test this technique in the treatment of other pathologies such as irritable bowel syndrome, inflammatory bowel disease and constipation. It is also worth noticing that the

imbalance in the composition of the gut microbiota (dysbiosis) has been associated with a plethora of neurological disorders. In this context FMT is being investigated as a therapeutic option not only for treatment of gut disorders but also for diseases of the CNS. The present thesis illustrates a series of experiments by which we tested the impact of FMT from aged donor mice into young adult recipients. Controls were carried out operating FMT from young adult donor mice to age-matched recipients. Following transplantation, characterization of the microbiota and metabolomics profiles along with a series of cognitive and behavioural tests were carried out. Label-free quantitative proteomics was employed to evaluate protein expression in the hippocampus and gut after the transplant.

In addition, in the attempt to elucidate the mechanisms underlying microbiota-host interactions within the framework of the gut-brain axis, we worked on setting up a procedure to tracking down and visualize bacterial metabolites (such as peptides and lipids) that are thought to play a role acting as signaling molecules. To this end, we used copper-catalysed azide-alkyne cycloaddition (CuAAC) click chemistry, a biorthogonal reaction of widespread utility throughout medical chemistry and chemical biology. We sought to optimize click-based protocols to detect the production of lipids in gut-bacteria to track the metabolism of active bacterial cells. This technique use click chemistry to stain synthetic (e.g., noncanonical) precursors incorporated into bacterial cell biomass. After incorporation, the artificial molecules can be fluorescently detected via azide-alkyne reaction and visualized by confocal microscopy.

FMT from aged mice into adult recipients affected spatial learning and memory while we did not observe effects on locomotion and explorative behaviour. Alongside, there was an alteration in the expression of proteins related to synaptic plasticity and neurotransmission in the hippocampus which was not observed in controls. FMT from aged into young adult mice did not induce a significant increase in glial fibrillary acidic protein expression in hippocampal astrocytes suggesting the lack of an overt neuroinflammatory response. On the other hand, a significant increase in the expression of F4/80, a typical trait of the ageing brain, was observed in microglial cells resident in the fimbria. Gut permeability and levels of systemic and local (hippocampus, gut) cytokines were not affected. As regards click chemistry, we used

Bacteroides thetaiotaomicron grown in minimal medium supplemented with palmitic acid alkyne (PAA) and stained this molecule using an azide-containing fluorescent dye. After palmitic acid staining, co-culture experiments were performed to assess the transfer of this bacterial product to eukaryotic cell lines (CaCo2 and SK-N-SH cell lines). The successful transfer to host cells was confirmed by confocal microscopy. Results obtained in FMT experiments highlighted the importance of the gut microbiota on protein expression and functions of CNS. These results support the key role of microbiota in gut-brain axis and it would be of great importance to get more insight into the restoration of a young microbiota in the elderly to try to improve cognitive functions and the quality of life. Click chemistry experiments demonstrate that this technique could be employed to track molecules produced by gut bacteria to unveil their role in host-microbe interactions.

1. Introduction

1.1. Gastrointestinal (GI) tract

The gastrointestinal (GI) tract includes mouth, pharynx, oesophagus, stomach, small intestine (duodenum, jejunum, and ileum) and large intestine (cecum, colon, and rectum) (Fig. 1). Each part of the GI tract has specific functions and allows ingestion and digestion of food, absorption of nutrients and final disposal of the non-absorbable remains through the anus (Cheng et al., 2010).

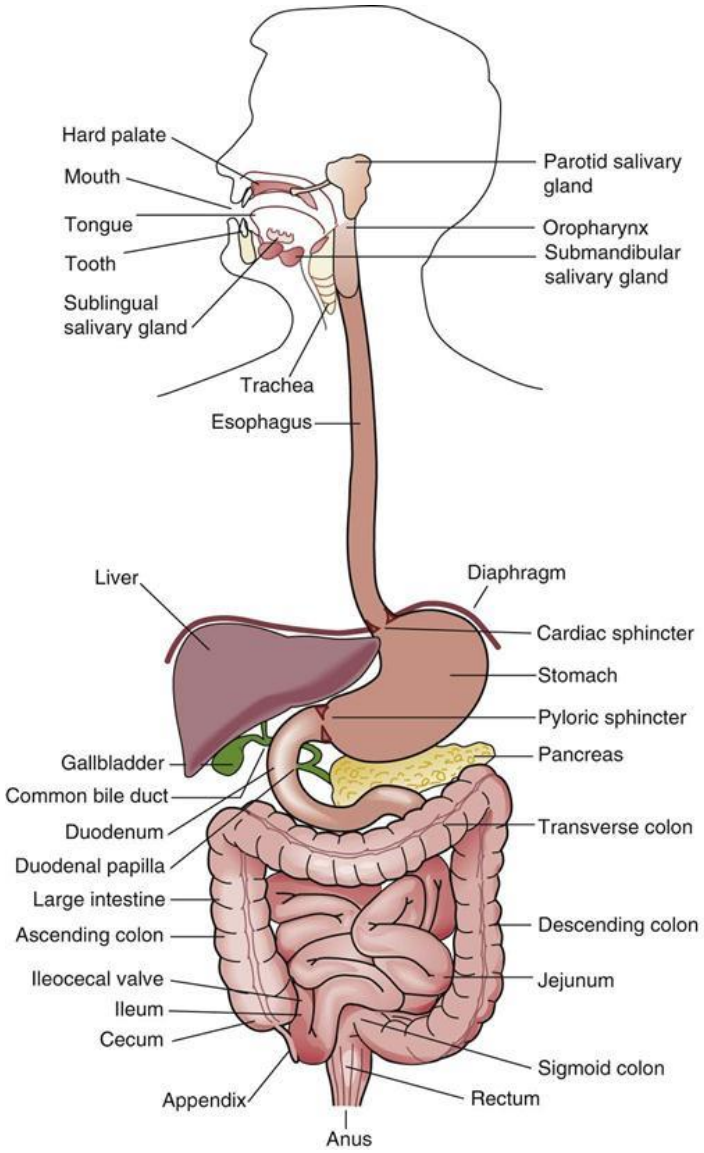

Figure 1. Anatomy of the human Gastro Intestinal (GI) tract and associated glands

The gut (small and large intestine) is a complex system where many events (nutrient absorption, immune modulation, antigen sampling) take place (Funk et al., 2020). The gut barrier includes a mucus layer, the epithelium and the cells that reside in the lamina propria (Conway and Duggal, 2021). The gut epithelium consists of a single layer of columnar cells arising from stem cells dwelling in the intestinal crypts and it is the first area of contact with antigens and many other types of *stimuli* (Funk et al., 2020) (Fig. 2).

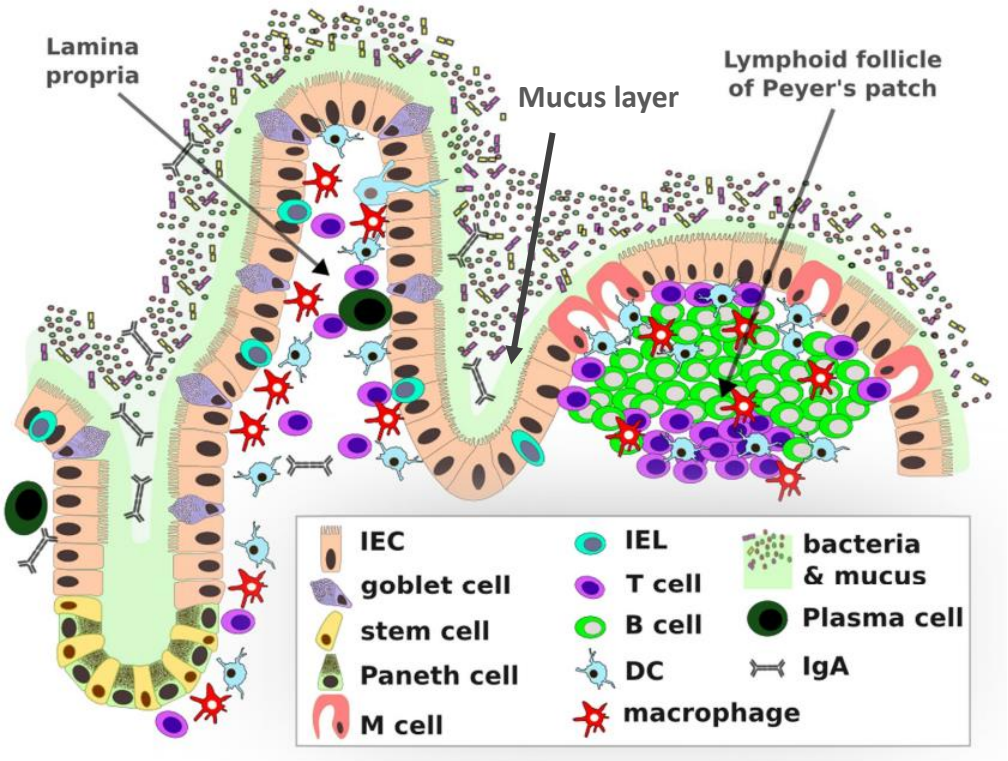

Figure 2. **Schematic representation of the gut barrier**. IEC= intestinal epithelial cell; IEL= intra-epithelial lymphocyte; DC= dendritic cell; M cell= microfold cell; IgA= immunoglobulin A. (Adapted from Man et al., 2014).

1.1.1. The intestinal crypt

The intestinal epithelium is exposed to a great variety of material, from the everyday ingested food to microbes. Microorganisms might either belong to the intestinal commensal population of bacteria (collectively called "microbiota") or other pathogen microorganisms that can reach the gut with the ingestion of infected nutrients and/or fluids. Such material, always in contact with the intestinal surface, can cause a damage to the epithelium with loss of intestinal epithelial cells (IECs). Intestinal epithelial stem cells (IESCs) are cells located in the intestinal crypt that ensure the replacement of damaged or senescent epithelial cells (Seishima and Barker, 2019). Since the small and large intestine have different epithelia arrangements to fulfill diverse functional demands, also the intestinal crypt organization varies depending on the different location. In particular, in the small intestine, epithelial cells cover the finger-like projections of the lamina propria into the intestinal lumen referred to as villi. IECs are also provided with long packed microvilli that allow to increase the absorptive area to maximize nutrient absorption. In this site, each villus is surrounded by a minimum of six crypts of Lieberkühn (Fig. 3A). In the large intestine, where faeces are ultimately formed also through the absorption of ions and water, IECs just cover the flat inner surface and have shorter microvilli. Here, each crypt is directly in continuity with the luminal surface *via* a circular opening (Fig. 3B). In the recent past, many studies have investigated factors that are important for IESCs proliferation and also for crypt homeostasis in particular in the small intestine (Greicius and Virshup, 2019; Kurokawa et al., 2020). At the bottom of the small intestine crypts, Leu-rich repeat-containing G protein-coupled receptor 5 (LGR5)$^{+}$ cells, also referred to as crypt base columnar (CBC) cells, can be found intermixed with Paneth cells. CBC cells differentiate in transit-amplifying (TA) cells that give origin to the different cell types belonging to the absorptive (enterocytes) or secretory (enteroendocrine, goblet, tuft and Paneth cells) lineages (Fig. 3A and C). As for the small intestine, LGR5^{+} CBC stem cells are located at the bottom of the crypt even in the colon where differentiate in TA cells that are the source of all the others cells in the epithelium (Fig. 3B and D). Other cell types, located in close proximity to the bottom of the crypts (endothelial cells, mesenchymal cells,

neural cells, smooth muscle cells, lymphocytes and monocytes) contribute to stem cell homeostasis and activity producing factors that regulate the proliferation of the IECs (Kurokawa et al., 2020).

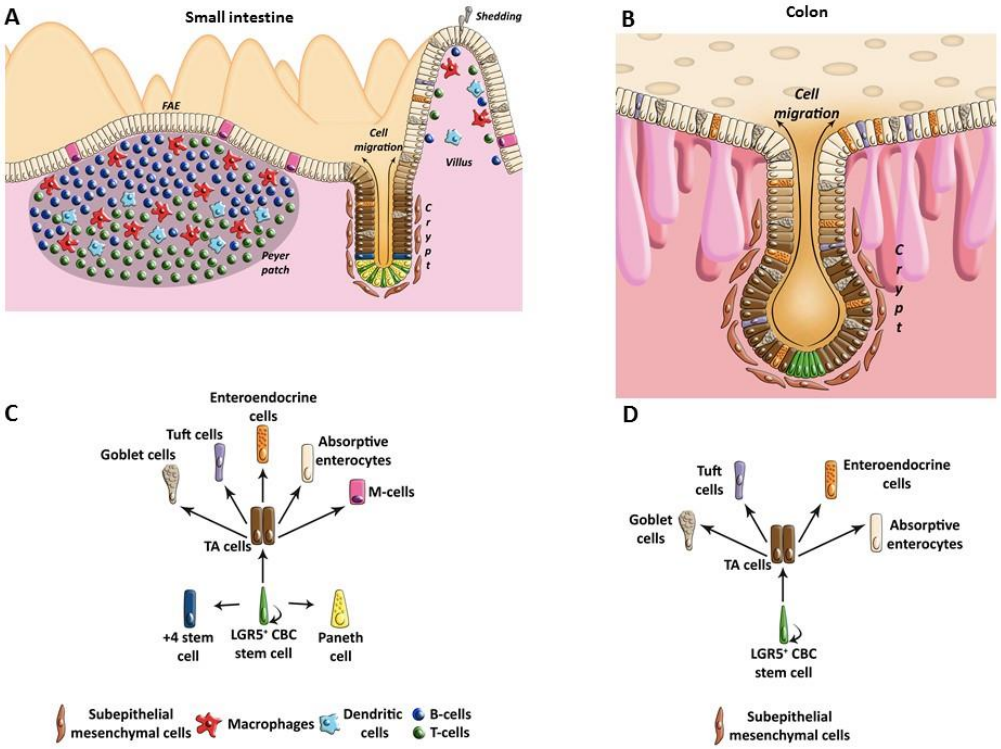

Figure 3. Intestinal crypt arrangement in the small (A, C) and large intestine (B, D). (From Branca et al., 2019).

1.1.2. Intestinal epithelial stem cells (IESCs) in ageing

A better understanding of the impact of ageing on the IESCs has been achieved thanks to the experiments in *Drosophila* midgut (Nászai et al., 2015; Gervais and Bardin 2017) and also thanks to the recognition of the unique marker LGR5 in mice (Barker et al., 2007). Experiments using *Drosophila* midgut showed that there is an increment in the number of IESCs in ageing. However, this numeric increase corresponds to a decrease in function (Lucchetta and Ohlstein, 2012). It has been proposed that the increase in the number of IESCs may be due to the presence of defective differentiated cells that retain IESCs specific markers. It is likely that some factors (for example bacterial infections) might be important for the accumulation of mis-differentiated cells in ageing *Drosophilae*. In particular, IESCs show an increased activity of the c-Jun N-terminal kinase (JNK) pathway in ageing. JNK signaling is an environment-mediated stress response signaling and the interaction between JNK and Notch signaling is necessary to prevent the accumulation of defective differentiated cells (Buchon et al., 2009). Further experiments using flies have also demonstrated that the high levels of IESCs proliferation are also correlated with the presence of damaged proteins and DNA. In particular, the hypothesis that has been put forward is that DNA damage is due to age-related defects in DNA damage repair (DDR) response. The generation of knock-out flies for genes related to the DDR pathway led to a premature ageing characterized by IESCs over-proliferation, centrosome amplification but also reduced survival (Park et al., 2018). One of the latest experiments in flies showed the role played by white (an ATP-binding cassette transporter subfamily G) in ageing-induced IESC proliferation in midgut. In particular, white is important in the transfer of tetrahydrofolate into IESCs. In turn, accumulating tetrahydrofolate induced increased IESCs proliferation in ageing (Sasaki et al., 2021). Sex is another factor that impacts IESCs functions in ageing. In particular, the intestine of female *Drosophilae* shows an excessive proliferation of IESCs in ageing that results in the damage of the epithelium. Eventually, morphological alterations end in the development of tumors. On the other hand, male flies have less proliferative IESCs that has been linked to a delayed development of epithelial alterations. Still, male

Drosophilae appear more susceptible to gut infections (Regan et al., 2016). The function and regenerative ability of IESCs are also altered in ageing mammalians. In particular, IESCs from older mice leads to the development of fewer and less complex organoids compared to younger animals (Moorefield et al., 2017). This phenomenon has been related to a decrease of Wnt signaling in IESCs, Paneth cells and the mesenchymal cells associated to the niche in ageing. The importance of Wnt signaling depletion is supported by the restoration of a young-like organoid regenerative potential by adding Wnt3a (Nalapareddy et al., 2017). In this context, it has been reported that Paneth cells have a critical role in enhancing IESCs function in response to exogenous L-arginine (Hou et al., 2020). Other experiments in aged mice have also demonstrated a higher rate of apoptosis as indirectly verified by the increased expression of apoptosis-promoting genes in IESCs (Moorefield et al., 2017). All these changes have an impact on the gut epithelium, on the general structure of the gut and also for the homeostasis of the crypts. For example, aged mice show an increase in villus height while villi in aged rats result shorter (Wang Q. et al., 2021). Experiments in transgenic mice have demonstrated that in the gut, cell proliferation in the crypt is the driving force for IECs migration along villi. In fact, chemical blockage of IESCs proliferation prevented the movement of IECs along the crypt/villus axis (Parker et al., 2017). Another important feature in ageing is the reduced capacity to fix a damage in the gut crypt due to a partially impaired moving ability of IESCs within the crypt. In particular, in young mice there is a rapid repositioning of the IESCs within the crypt after the application of an insult. This movement is finalized to keep the best organization and distribution of IESCs in the crypt (Choi et al., 2018). Another hallmark of ageing is telomerase attrition that is also responsible for the reduced regenerative capacity of the IESCs. In particular, the generation of adult tissues with longer telomeres demonstrated that it is possible for IESCs to keep juvenile regenerative ability for an extended life-span (Varela et al., 2016). Experiments in telomerase-deficient mice (G3Terc$^{-/-}$) showed that the knock-out of the growth arrest and DNA damage-inducible protein 45 alpha, a pivotal molecule for repair-mediated DNA demethylation, significantly decreased the DDR and progressed the function and the regenerative potential of IESCs. In this way, the life-span of G3Terc$^{-/-}$ mice resulted extended (Diao et al., 2018). Last but not least, another important

player on IESCs proliferation is host-microbe interaction. In particular, studies in mice have demonstrated that microbes stimulate monocytes to interact with cells in the crypt promoting both IESCs proliferation and homeostasis maintenance (Jeffery et al., 2017).

1.1.3. The gut epithelium

The gut epithelium consists of a single layer of columnar epithelial cells arising from the stem cells located in the crypts (Funk et al., 2020). The gut epithelium has to carry on a double task preventing, on one side, the penetration of harmful microorganisms and ensuring, on the other side, nutrients, ions and water absorption. In order to carry out both tasks, intestinal cells are rather non-permeable to water and water-soluble molecules and are provided with composite intercellular junctional complexes (tight, adherens and gap junctions) (Fig. 4) (Branca et al., 2019). At the top of the basolateral domain, epithelial cells are interconnected by tight junctions (TJs). About 40 different proteins contributing to the TJs can be grouped into transmembrane proteins, scaffolding proteins and signaling proteins. Among the proteins found in the TJs, we recall claudins, zonula occludens 1 and 2, occludin and F-actin (Furuse, 2010). Moving along the basolateral membrane from top to base, the second junctional complex observed is the zonula adherens. This is an adherens junction that is important in the assembling of the adjacent TJs and stabilizes cell membranes just below the TJs. Some of the main proteins forming the zonula adherens are E-cadherin, α-catenin 1, β-catenin and catenin δ1. Below the zonula adherens, still along the lateral membrane, a variable number of desmosomes can be spotted (Hartsock and Nelson, 2008). Desmosomes are macula adherens junctions and tie the paracellular space up. Desmosomes are also important protein complexes which include desmoglein, desmocollin, desmoplakin and cytokeratin filaments (Delva et al., 2009).

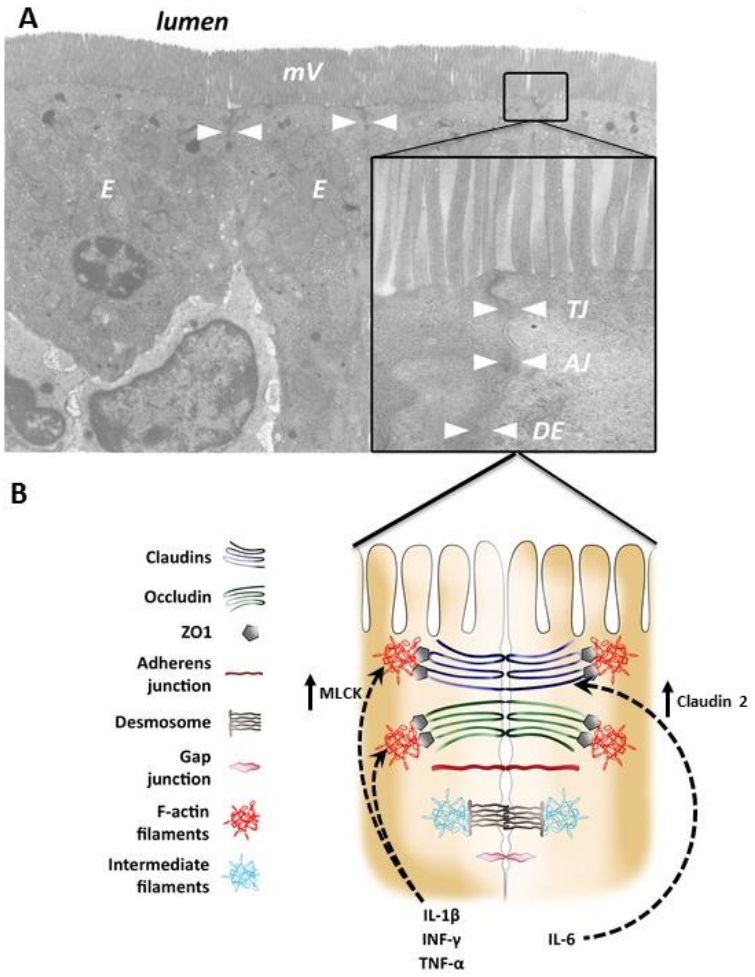

Figure 4. Intercellular junction of the intestinal epithelium. A) Transmission electron microscopy of the main junctional complexes of IECs. B) Sketch of the general arrangement of the junctional complexes and of some molecular mechanisms that affect TJ protein composition or the actomyosin cytoskeleton associated to the junctions. (From Branca et al., 2019).

The junctions are critical in keeping the gut barrier integrity and the disruption of these complexes leads to increased gut permeability and to the occurrence of inflammatory diseases (Funk et al., 2020). For instance, mice lacking the junctional adhesion molecule-A, a TJ protein, have a more permeable gut and up-regulated inflammatory cytokines (Khounlotham et al., 2012). Ageing is an irreversible, complex and multifactorial process that leads to changes in several systems and is an additional challenge for the organization and function of the gut epithelium (Funk et

al., 2020). A recent investigation has addressed the changes occurring to the gut barrier through life (Man et al., 2015). In particular, biopsies of the terminal ileum of people aged 7 to 77 years-old demonstrated an increase in the expression of interleukin 6 (IL-6) in the elderly whereas other proinflammatory cytokines tested in the investigation (INF-γ, TNF-α and IL-1β) did not change with ageing (Man et al., 2015). Analysing the different cell populations, it appeared that $CD11c^+$ dendritic cells (DCs) were responsible for the increased production of IL-6. The increase of IL-6 appeared correlated with an over-expression of claudin-2, a protein involved in the TJs formation. Upregulation of claudin-2 in terminal ileum led to a decline in transepithelial electric resistance (TEER) and was explained by the known ability of the protein to form cation-selective and water permeable paracellular channels (Venugopal et al., 2019). An altered expression of proteins important for the formation of TJs has been reported in baboons too. Aged baboons show a decrease in the expression of ZO-1, occludin and other junctional molecules. This altered pattern of protein expression leads to an increased permeability of the gut epithelium. Interestingly, aged baboons also have increased levels of claudin-2 expression in colonic biopsies (Tran et al., 2013) corroborating the same findings observed a couple of years later in humans (Man et al., 2015). Another study in female vervet monkeys have ascertained the absence of structural alterations in ageing colon but also a decreased capability to act as a fully functioning epithelial barrier as assessed by the translocation of microbial molecules. Unfortunately, however, the latter investigation did not evaluate the level of expression of the TJs components (Wilson et al., 2018).

1.1.4. The mucus layer

The gut epithelium is protected by a coating of mucus. The cells responsible for mucus production are goblet cells whose number is the highest in the colon (Pelaseyed et al., 2014). Mucins are the main protein constituents of the mucus and are characterized by heavily O-glycosylated mucin domains. The mucus coating consists of two layers. The outer layer is in close contact with the IECs and is characterized by the absence of microbes, whereas the inner layer is less firm compared to the outer one, allows the food progression and is also a source of nutrients for some bacteria (Kim and Ho, 2010). The mucus plays a pivotal role in the preservation of the intestinal epithelium. In fact, it has been seen that mucus deficient mice (Muc2 $^{-/-}$) developed severe colitis around four weeks of age (Van der Sluis et al., 2006). Although the mucus is an essential component of the gut barrier, little is known about the changes occurring in ageing. It has been reported that the thickness of the layer does not change in the stomach and duodenum in healthy ageing humans (Newton et al., 2000). Controversial results have been reported by investigating the ileum of aged mice. Tremblay and colleagues reported a rise in the number of goblet cells/villus as well as bigger mucin granules in the ileum of aged mice (Tremblay et al., 2017). In contrast, other researchers did not observe any change in the number of goblet cells located in ileal Peyer's Patches (PPs) of aged mice (Kobayashi et al., 2013). More marked differences have been reported in the thickness of the mucus layer in the colon of ageing animals. In particular, a thinning of the mucus coating has been observed in both wild-type and a transgenic mice model of accelerated ageing compared to young controls. Interestingly, the same set of experiments it showed that it is possible to restore the thickness of the mucus layer in ageing by supplementation of some probiotic bacteria (van Beek et al., 2016). Also, it has been reported that the supplementation of prebiotic galacto-oligosaccharides ameliorates the age-associated gut permeability and also increases the levels of MUC2 and mucus coating in old mice (Arnold et al., 2021). An additional variable that affects the thickness of the mucus layer appears to be the sex as it has been reported that the reduced thickness of the mucus layer is more pronounced in male mice

compared to females (Elderman et al., 2017). Another important aspect that has been unveiled about the mucus coating of ageing animals is the change in its chemical composition. This is important because some bacteria that live in the gut are known to use glycans as metabolic substrates (Bell and Juge, 2021) whereas other bacteria exploit O-glycan domains to adhere to the mucus, a propensity that has been reported to decline with ageing (Bergstrom et al., 2020).

1.1.5. Anti-microbial peptides (AMPs)

Antimicrobial peptides (AMPs) are a large number of molecules secreted by the epithelium that contribute to maintain the integrity of the gut barrier and to fight possible infections. AMPs are small molecules (from 6 to 100 amino acids) that are active against bacteria, parasites, fungi and even viruses. Their role is also crucial in regulating the gut microbiota profile. However, the level of expression of these molecules has to be finely regulated because some AMPs have a harmful effect on mammalian cells too (Mahlapuu et al., 2016). Ageing also affects the levels of AMPs. In particular, aged mice show a diminished concentration of α-defensins and lysozyme (produced by Paneth cells) and an increase in other AMPs (regenerating islet-derived protein 3 beta and gamma, β-defensins 1, angiogenin-4 and resistin-like molecule β) (Tremblay et al., 2017). Experiments to evaluate the levels of AMPs in ageing have been performed also in *Drosophila*. In particular, in this model both Toll-like receptors and immune deficiency pathways regulate the expression of seven families of inducible AMPs. In this context, it is worthwhile to note an up-regulation of AMPs in aged flies. For instance, the over-expression of drosomycin in ageing has been linked to the damage of the gut barrier integrity (Loch et al., 2017; Badinloo et al., 2018; Lin et al., 2018).

1.1.6. Secretory Immunoglobulin A (sIgA)

The secretion of sIgAs is of critical importance at the mucosal surface in order to prevent the infiltration of antigens and pathogens. sIgAs have also a crucial role in forging and preserving the gut microbiota community. Cells producing IgAs are generated in PPs where precursor antigen-specific B-cells are exposed to signals (transforming growth factor-β (TGF-β), $CD103^+$ DC-secreted retinoic acid and IL-6) that allow IgA isotype switching (Agace et al., 2012). Data regarding the effect of ageing on gut elements that are important for IgA response are still very limited. There is no consensus even on the intensity of IgA-mediated responses in ageing. For example, experiments in rodents and nonhuman primates showed reduced levels of gut IgA after the exposure to an oral antigen (i.e., cholera toxin (CT)) (Schmucker, 2002; McDonald et al., 2011; Nagafusa and Sayama, 2020). Other studies, on the other hand, have reported that IgA antibody response in aged mice and humans is unaltered or even increased (Santiago et al., 2008). Interestingly, however, the transfer of antibodies from aged "high responder" mice to young mice was not protective against *Streptococcus pneumoniae*. This lack of protection can be explained as aged mice have an antibody repertoire with a higher heterogeneity of the variable domain of both light and heavy chains. Such higher heterogeneity, for instance, is responsible for a decreased affinity to the bacterial antigen phosphorylcholine (Nicoletti et al., 1991; Nicoletti et al., 1993). Moreover, the demonstration of a reduced expression of molecules important in B cell homing, including mucosal addressin cell adhesion molecule 1 in the lamina propria and sub-mucosa venules, and α_4b_7 integrin on peripheral myeloid blood cells, points to an impairment in IgA-producing cell homing rather than a reduction of their number (Schmucker et al., 2003).

1.1.7. Monitoring the luminal content *via* antigen sampling

The intestinal epithelium is not only a mere barrier. It also mediates a continuous monitoring of the luminal content *via* the antigen sampling operated by specialized membranous (M) cells. M cells are scattered among absorptive IECs within the follicle associated epithelium (FAEs) of PPs. Thanks to their localization, M cells deliver samples of the luminal content in areas where immune cells are concentrated. Then, immune cells can check the delivered luminal content making a discrimination between pathogenic and commensal microbes (Nicoletti, 2000; Ohno, 2016). Contrasting results have been reported regarding M cell up-take and transport of particles in ageing. In particular, some experiments have shown no change or even increased M cell activity in ageing. In contrast, recent results by Kobayashi et al. (2013) unequivocally demonstrated that M cell number, maturation and activity deteriorate in ageing. In particular, they showed that aged animals had a reduced transcytosis of particles through the FAE, a decreased number of cells expressing the M cell specific marker GP2 and, finally, a reduction of cells that play key roles in M cells maturation and differentiation (Kobayashi et al., 2013). Moreover, M cell-mediated sampling activity changes in ageing was also affected by the reduction of the FAE area (Kobayashi et al., 2013) though the number of PPs does not change with ageing (Kawanishi and Kiely, 1989). Other factors, like cytokine macrophage inhibitory factor (Man et al., 2008) and receptor activator of NF-kB ligand (Knoop et al., 2009), are also important for a full activation of M cells. Finally, the antigen-sampling activity is not restricted to FAE M cells. Other cells implicated in this function are villous-associated M cells, lamina propria (LP)-CX3CR1^{+} macrophages, and goblet cells that can deliver antigens to LP-CD103^{+} DCs (Mann and Li, 2014).

1.1.8. The intestinal barrier: inflammation and inflammageing

Inflammation is the first response that takes place to face pathogenic agents, clear cellular debris, and repair lesions (Bosco and Noti, 2021). Inflammation is one of the central factors in ageing and age-related diseases. Ageing is characterized by an imbalance between the levels of pro- and anti-inflammatory cytokines. The chronic, low-grade inflammation that develops during ageing and plays a role in age-related diseases is referred to as "inflammageing" (Franceschi et al., 2018). Diet, infections, obesity, stress, sleep deprivation can commence and sustain inflammageing. The increase in the levels of pro-inflammatory cytokines in gut during ageing has an impact on the intestinal barrier function resulting in a greater permeability. It has been reported that IL-1β, INF-γ, TNF-α and IL-6 levels are increased in ageing. These cytokines affect TJs proteins expression and in turn gut permeability. In particular, the perijunctional actomyosin cytoskeleton is affected by several pro-inflammatory cytokines (IL-1β, INF-γ, TNF-α) in inflammatory bowel disease (IBD). This was connected to an increase of myosin light chain kinase gene and protein expression (Kaminsky et al., 2021; Al-Sadi et al., 2014; Al-Sadi et al., 2016) (Fig. 4B). Another example is IL-6. IL-6 increases gut permeability by activating JNK signaling cascade. This signaling is linked to the increase in claudin-2 gene transcription and protein production (Al-Sadi et al., 2014) (Fig. 4B). In aged humans, the activation of claudin-2 expression enables the paracellular movement of molecules with radii less than 4 Å and a parallel decrease in TEER. *In vitro* and *ex-vivo* experiments in healthy humans demonstrated that the increase in gut permeability in ageing, mediated by claudin-2, is abolished by adding IL-6 blocking antibodies (Man et al., 2015).

Data on the cellular source of cytokines are still few and we do not know what is the contribution of IECs on inflammatory cytokine production in ageing yet. There is a regular cross-talk between microbiota, IECs and immune cells. IECs express pattern-recognition receptors (PRRs) that make IECs able to distinguish between harmful and commensal bacteria (Kelly et al., 2004; Artis, 2008). Commensal bacteria trigger the production of anti-inflammatory molecules by IECs (Iliev et al., 2009). On the contrary, the presence of pathogenic bacteria induces the production of pro-

inflammatory molecules such as CCL20, IL-8 and IL-6 (Mowat, 2003). Little is known on the cytokines that IECs produce in ageing. Recent studies showed that in aged humans the pattern of cytokines produced by IECs differs based on the type of microbial challenge. Studies in healthy humans using small intestine biopsies showed that the production of IL-8, in response to flagellin, is reduced in the elderly compared to young individuals (Man et al., 2015). However, it has also been reported that the use of a probiotic mix on human biopsies from young and aged humans led to the production of similar levels of TNFα. These experiments using human biopsies demonstrated that the cytokine response by IECs in ageing can be less or more altered depending on the challenge and the specific cytokine (Man et al., 2015). Moreover, IECs highly express components of the inflammasome. The environment in which the IECs are located is highly enriched with molecules (such as microbes/pathogen associated molecular patterns and damage associated molecular patterns) that are linked to the activation of inflammasome and that increase in ageing (Kapetanovic et al., 2015). Finally, it is worth to remember that the microbiota composition changes with age and these changes can support the imbalance between pro- and anti-inflammatory cytokines in the gut activating the complex process of inflammageing (Franceschi et al., 2018).

1.1.9. Host-microbe interface in the gut

The study of the gut microbiota and its interaction with the host has gained a great relevance in the last decade. Studies in mice exposed to the same environmental conditions showed an age-dependent change in gut microbiota composition (Miyoshi et al., 2018). The changes occurring to the microbial community has been attributed to altered cytokine balance, immunological profile, different expression of PRRs, impaired nutrient absorption and hormonal status (Langille et al., 2014). On the other hand, the matter is still controversial as other investigations reported that changes in gut microbiota precede age-related alterations of the intestinal epithelial barrier. For example, the transfer of the gut microbiota from aged mice into young germ-free mice by itself is capable of initiating local and systemic inflammation (Fransen et al., 2017). Even studies in *Drosophila* models reported that changes in the microbe composition precede alterations in the gut (Clark and Walker, 2018). A very active and regulated cross-talk between microbes and host is considered important in preserving intestinal homeostasis. An important example in this context is the cross-talk occurring between microbial molecules (histamine, taurine, spermine) and the IEC-associated NLRP6 inflammasome, the latter being important in the regulation of IL18 expression (Elinav et al., 2011; Levy et al., 2015). Another relevant example is the influence exerted by microbe-derived short-chain fatty acids (SCFAs) on IECs. SCFAs act as an important source of energy for IECs and also for the secretion of factors important for barrier function (Fachi et al., 2019; Wang RX. et al., 2021). Recent observations suggest that the interaction between host and microbes in keeping barrier integrity in ageing is crucial to increase the life-span and possibly the quality of life. Experiments on the gut barrier in *C. elegans* and *Drosophila* have shown that the integrity of the gut barrier is important in extending the life-span of flies and worms (Libina et al., 2003, Galenza and Foley, 2021). Studies in humans have reported that age-related neurodegenerative diseases are linked to dysfunctions of the gut epithelial barrier (Pellegrini et al., 2021). Taken together, these findings have

opened the possibility of using probiotic and prebiotics in the attempt to restore barrier integrity and reduce inflammageing (Franceschi et al., 2018) (Fig.5).

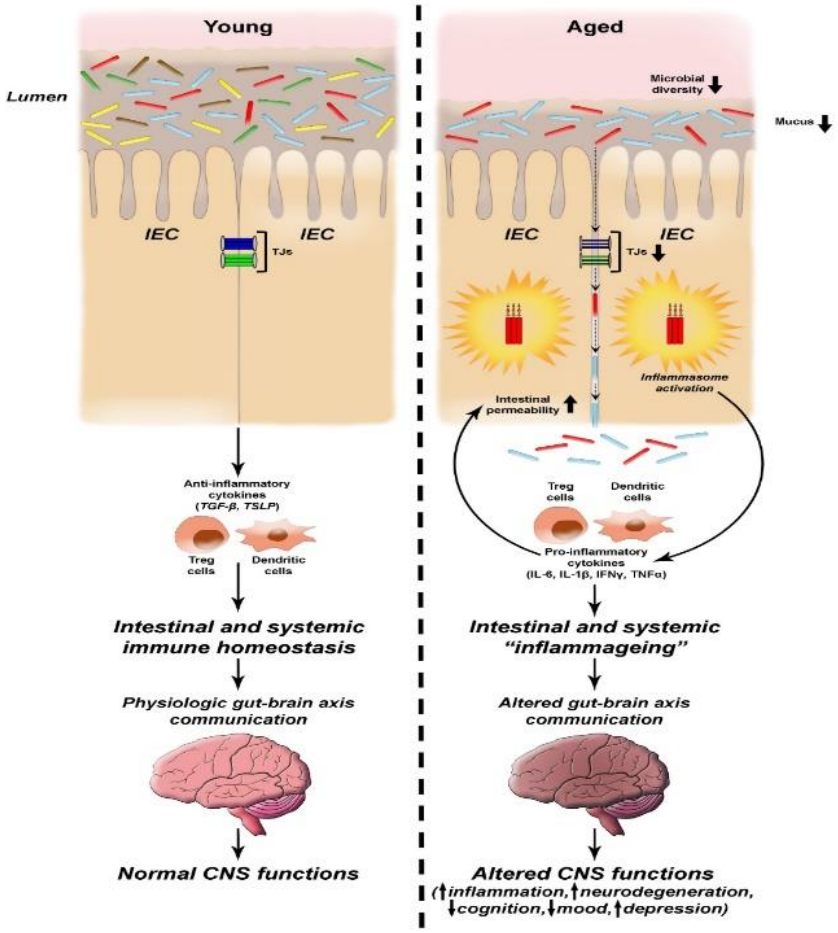

Figure 5. <u>Host-microbe interface in ageing and impact on local and systemic inflammageing.</u> (from Branca et al., 2019).

1.1.10. Gut microbiota and microbiota-gut-brain axis

The “human microbiota” is an expression used to indicate the microorganisms that live in and on us (Cryan et al., 2019). Trillions of bacterial cells colonise different anatomical sites (mouth, skin, genito-urinary and intestinal tracts) and co-evolve with the host (Santoro et al., 2020). With the advancing of sequencing techniques, it has been estimated that there is a ratio of 1.3 microbial cells:1 human cell (Cryan et al., 2019). The human digestive tract is populated by a microbial community consisting of bacteria, viruses, fungi and archaea (Conway and Duggal, 2021). Bacterial colonization of the gut starts after birth and is influenced by mode of delivery, medications, geographical localization, diet, stress, host genetic, physical activity, smoking, sleep quality and also ageing (Thursby and Juge, 2017; Ragonnaud and Biragyn, 2021; Conway and Duggal, 2021). The composition of gut microbiota is subjected to modifications in infants whereas in adulthood it tends to be more stable. In particular, in healthy adults, the gut microbiota is characterized by members of *Actinobacteria (Bifidobacterium), Bacteroidetes (Bacteroides, Prevotella), Firmicutes (Clostridium, Faecalibacterium, Lactobacilli, Ruminococcus), Proteobacteria (Escherichia, Helicobacter, Shigella)* and *Verrucomicrobia (Akkermansia)* phyla (Fig. 6) (Ragonnaud and Biragyn, 2021).

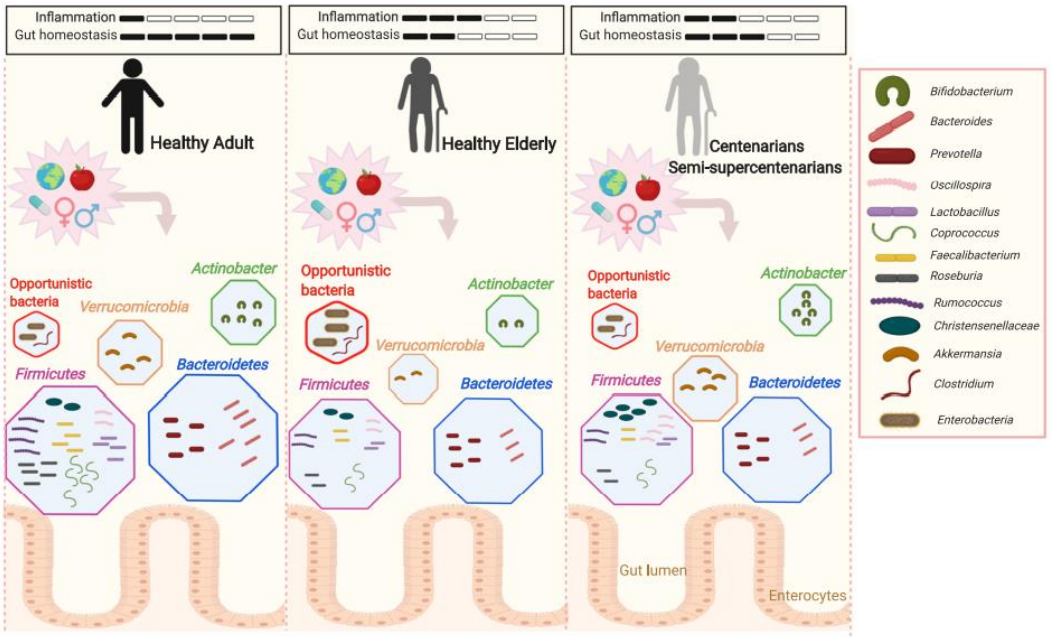

Figure 6. <u>The composition of gut microbiota in ageing.</u> (From Ragonnaud and Biragyn, 2021).

The gut-associated microbiota (i.e., gut microbiota) is currently the most investigated component of the human microbiota and has key functions in metabolism, biosynthesis of vitamins, and in enhancing energy extraction from food. It has also a major role in defending the host from pathogens invasion and in keeping the gut barrier integrity (Santoro et al., 2020). The gut microbiome goes through functional and compositional modifications with ageing, a process referred to as microbial dysbiosis. In particular, studies in human population have reported a decrease in the genera *Faecalibacterium* and *Roseburia* (butyrate producing bacteria) in ageing. On the other hand, there is an increase in members of the families *Enterobacteriaceae*, *Streptococcaceae* and *Staphylococcaceae* (low abundant and potentially noxious bacteria, also called pathobionts). The increase in those aforementioned pathobionts could be the result of the low-grade inflammation in the intestinal mucosa in ageing (Santoro et al., 2020). The increase of pathobionts in age-associated microbial dysbiosis could alter the gut barrier integrity, increase inflammation and enhance the risk of infections (e.a. *Clostridium difficile, Helicobacter pylor* infections*)* (Conway and Duggal, 2021). Studies in mice have highlighted that the ageing process in itself could

be a driving force for the changes in the composition of the gut microbiota. In particular, an age-dependent change in the gut microbiota is observed in mice populations exposed to the same environmental conditions (Miyoshi et al., 2018; Langille et al., 2014). On the other hand, experiments on *Drosophila* showed different results with changes in the microbiota that anticipate alterations in barrier function (Clark and Walker, 2018). However, the impact of gut microbiota and microbial dysbiosis in the ageing process go beyond the gastro-intestinal tract. Actually, it has been reported that events taking place in the gut have an impact on brain too. The reciprocal communication between gut microbiota and brain, the so called "microbiota-gut-brain axis", is one of the hottest scientific topics and the focus has been recently shifted to the effects of this axis on CNS functions (Cryan et al., 2019) (Fig. 7). One of the first study looking at the communication pathway between gut and brain found that germ-free mice had less anxiety-related behaviours and increased serotonin (5-HT) production in the thalamus compared to specific-pathogen free mice (Diaz Heijtz et al., 2011). Recent studies in amyloid precursor protein (APP/PS1) transgenic mice have demonstrated that FMT from conventional APP/PS1 transgenic mice to germ free APP/PS1 mice has an impact on cerebral amyloid deposition (Harach et al., 2017). Although in the last decade there has been an increasing interest in the microbiota-gut-brain axis, the way these two systems communicate is still unclear. Different routes and/or systems involved have been hypothesized: the neural pathway that comprehends the autonomic nervous system, vagus nerve and enteric nervous system; the neuroendocrine-hypothalamic-pituitary-adrenal axis; the immune system; and the release of microbiota-derived neuroactive molecules (Fig. 7) (Gwak and Chang, 2021).

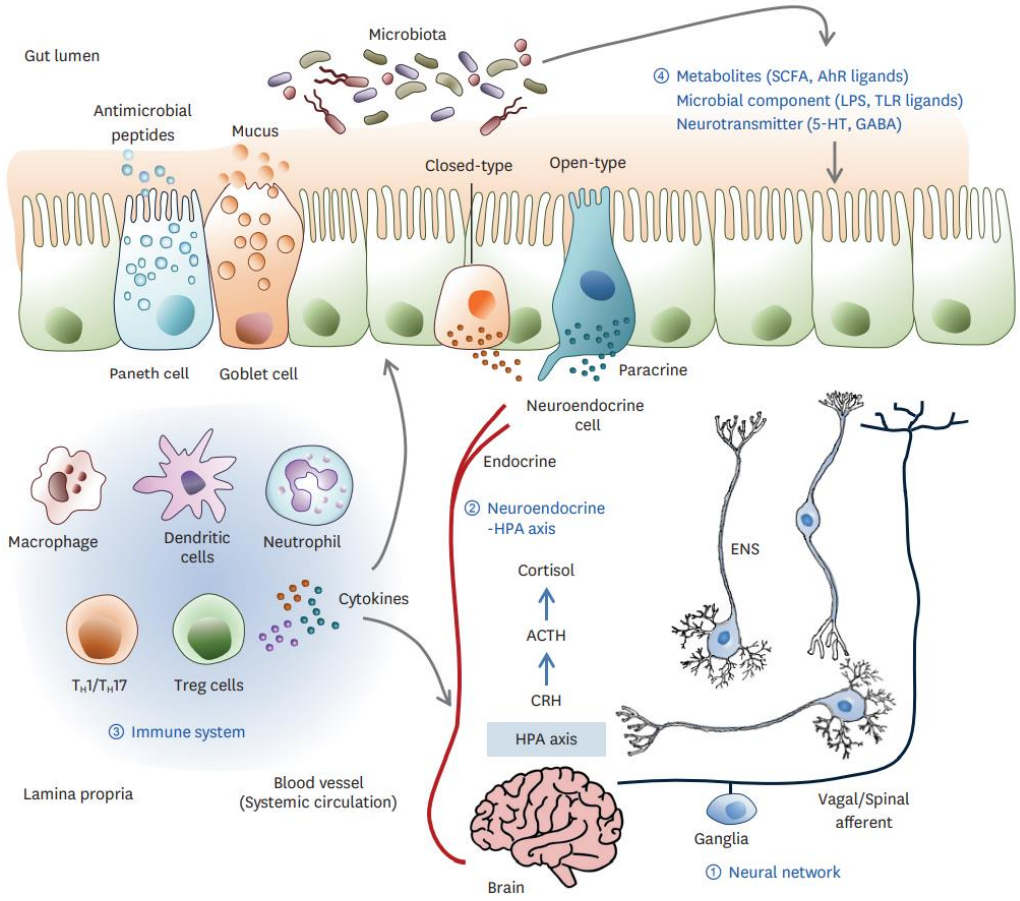

Figure 7. <u>The dynamic communication of the gut microbiota-brain axis.</u> (From Gwak and Chang, 2021).

1.1.11. Faecal microbial transplant (FMT)

It has become more and more evident that the gut microbiota is a promising target to slow down the onset of age-related diseases. A novel therapeutic strategy is represented by FMT. FMT is a technique that entails the transfer of gut microbiota from a donor to a recipient (*via* oral gavage in rodents or colonoscopy in humans). This technique is aimed to establish a donor-like microbiome in the gastro-intestinal tract of the recipient. One of the most notable uses of the FMT is for the treatment of *Clostridium difficile* infection (CDI) in humans (Cryan et al., 2019). It has been evaluated that the efficacy of FMT in patients with recurrent CDI is up to 90% (Mikolasevic et al., 2021). The most common type of FMT in rodents consists of a preliminary treatment with a cocktail of antibiotics (usually broad-spectrum antibiotics) *via* drinking water followed by a single or multiple oral gavages of donor faecal material for several days. In a recent study comparing three different methods of eradication of the pre-existing microbiota (pre-treatment with antibiotics, cleansing of the bowel and no pre-treatment), all followed by FMT through oral gavage, it was observed that antibiotic pre-treatment gave the highest FMT efficacy (Cryan et al., 2019). Apart from the use of FMT for CDI and the studies of its efficacy in other intestinal diseases (e.a. irritable bowel syndrome, IBD) there is a growing interest in the use of FMT for treating extraintestinal diseases. An increasing body of evidence suggests that microbial dysbiosis could be a key factor for mental health and psychiatric diseases (Mikolašević et al., 2021). FMT has been even attempted in children affected by autism spectrum disorder with encouraging results (Kang et al., 2019). Also, another promising area of research is the restoration of a young-like microbiota in aged hosts in the attempt of delaying or balance behavioural changes observed in the elderly. Some results have been achieved in mice with FMT from young donors to aged mice. The treatment showed the reverse of some age-associated variations in brain and peripheral immunity but also the metabolome and transcriptomic profile. An improvement of spatial memory was also reported (Boehme et al., 2021).

1.2. Click chemistry

One important achievement to study microbiota-host interactions would be to gain the possibility to follow small bacterial molecules from microbes to host cells, tracking down their path. To achieve this goal, click chemistry is a possible experimental strategy.

Click chemistry is an expression forged by Sharpless and colleagues in 2001. Click chemistry describes a wide group of chemical reactions that, under the right conditions, form stable products with high selectivity. As defined by Sharpless et al. (2002), click chemistry reactions are "modular, wide in scope, high yielding, create only inoffensive by-products (that can be removed without chromatography), are stereospecific, simple to perform and require benign or easily removed solvent''. The application field of click chemistry has greatly expanded from organic synthesis to drug discovery. One example of click reactions is copper-catalysed version of the Huisgen 1,3-dipolar cycloaddition of azides to terminal alkynes. Azide and alkyne moieties are complementary groups widely used in click chemistry (Moses and Moorhouse, 2007). However, the azide-alkyne reaction rate is not that high. One of the factors that could be modified to improve the efficiency rate of the reaction is the temperature. However, in living models it is not possible to increase the reaction temperature because the biological material is sensitive to heat. Two independent groups of researchers (Sharpless' and Meldal's groups) have separately discovered that there is an improved reaction rate and enhanced selectivity of the products obtained under copper(I) (Cu(I)) catalysis. Among the available sources of Cu(I), the most cost-effective and air-stable is $CuSO_4$ (Breinbauer et al., 2003). Copper-catalyzed azide-alkyne cycloaddition (CuAAC) click chemistry is a bioorthogonal reaction of broad use from medicinal chemistry to chemical biology (Jiang et al., 2019). In presence of Cu(I), the reaction of an azide with a terminal alkyne generates the corresponding stable triazole with excellent selectivity and high yield (Kitteringham et al., 2018). The azide and alkyne moieties can be utilized indiscriminately. In click chemistry experiments, one moiety (alkyne) is used to mark the molecule of interest (i.e. palmitic acid) and the other one (azide) is employed to

detect it. Kits employed for click chemistry experiments allows a fluorescently detection of the molecule of interest using an azide modified fluorophore that reacts with the alkyne moiety tagged to the molecule of interest. In aqueous solution and in presence of copper these to molecules reacts to form a stable triazole conjugate (Fig. 8).

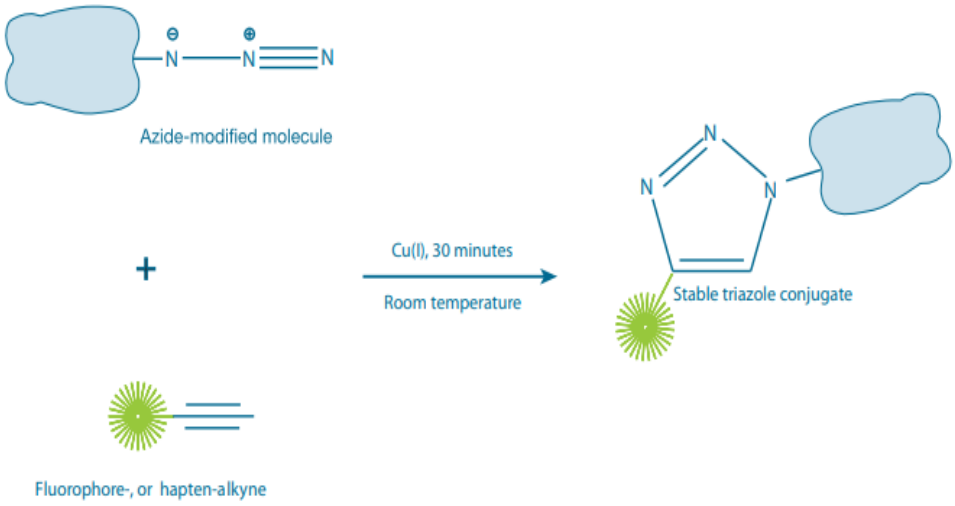

Figure 8. Copper catalyzed azide/alkyne reaction.

2. Material and Methods

2.1. Faecal microbial transplant experiment

2.1.1. Animals

Adult (3 months-old) and aged (24 months-old) male C57BL/6 mice were used in this study. Mice (Envigo, Varese, Italy or Charles River, UK) were provided with food and water *ad libitum*. Environmental temperature was kept at 23 ± 1 °C with a 12-h light/dark cycle. All efforts were made to minimize animal suffering and to reduce the number of mice used.

2.1.2. Faecal material preparation and faecal microbial transplant regime

Faecal material was collected from adult and aged mice and placed into Eppendorf tubes containing 500 mL of freezing solution (sterile saline solution with 12.5% glycerol) and homogenized. The suspended faecal materials were then stored at − 80 °C until utilized. For FMT, mice were randomized into the following groups (n = 12/group): control (no antibiotic treatment, no FMT), FMT-adult (antibiotic treatment followed by FMT from adult age-matched donors) and FMT-aged (antibiotic treatment followed by FMT from aged donors). Antibiotic mix was administered by oral gavage. The antibiotic/anti-fungal regime (scheme 1) was as follows: days 1–3 mice were gavaged daily with amphotericin B 1 mg/kg, days 4– 17 mice received a daily gavage of metronidazole 100 mg/kg while the antibiotic mix (ampicillin 1 g/L, vancomycin 0.5 g/L and neomicin 1 g/L) was added to drinking water, days 18-24 daily oral gavage with the antibiotic mix plus metronidazole and amphotericin B at the same dosage employed in the previous days. FMT was carried out via oral gavage with 150 mL of a 100 mg/mL faecal suspension. FMT was performed daily from day 24 to day 28 and on day 35.

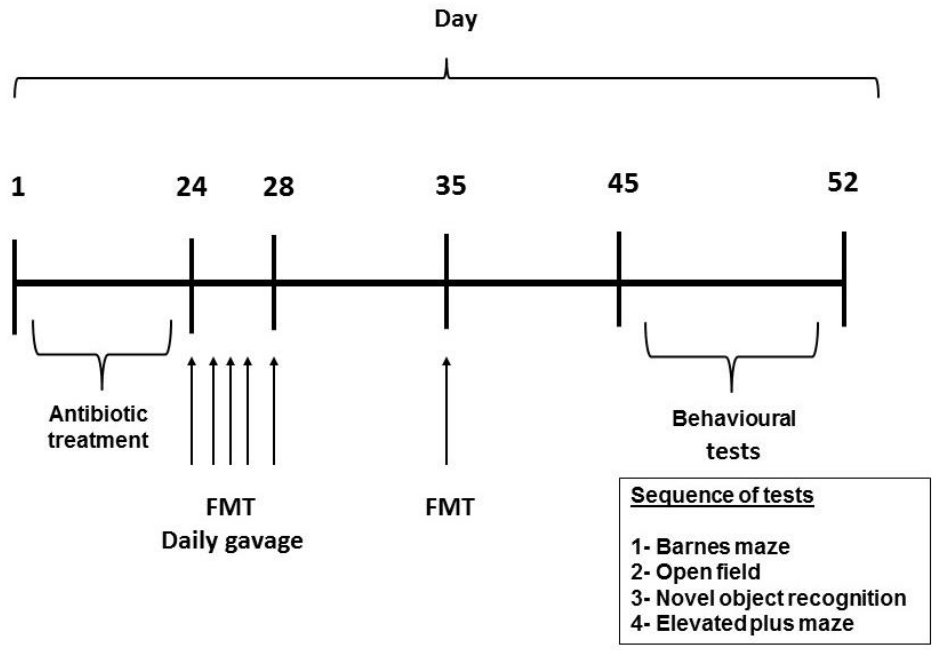

Scheme 1. Summary of pre-treatment and FMT procedure.

2.1.3. DNA extraction, amplicon sequencing, analyses of 16S rRNA gene sequence data and metabolomics analysis

Pre- and post-FMT faecal material was used for microbiota profiling. DNA was extracted from faecal samples using the FastDNA SPIN Kit for Soil (MP Biomedicals) with three bead-beating periods of 1 min as previously described (Fernandes et al., 2014). DNA concentration was normalized to 1 ng/µL by dilution with DNA elution solution (MP Biomedicals, UK) to produce a final volume of 20 µL. Normalized DNA samples were sent to the Earlham Institute (Norwich, UK) for PCR amplification of 16S rRNA genes and paired-end Illumina sequencing (2 × 250 bp) on the MiSeq platform. The V4 hypervariable region of the 16S rRNA genes was amplified using the 515F and 806R primers with built-in degeneracy as previously reported (Caporaso et al., 2011). Sequence data were provided in fastq format. All processing and analyses were done in R/Bioconductor making use of the following packages: GEOquery 2.50.0 (Davis and Meltzer,2007), dada2 1.10.0 (Callahan et al., 2016), phyloseq 1.26.0 (McMurdie et al., 2013), tidyverse 1.2.1 (https://www.tidyverse.org), vegan 2.5.3, viridis 0.5.1, msa 1.14.0 (Bodenhofer et al., 2015), phangorn 2.4.0, ALDEx2 1.14.0 (Fernandes et al., 2014) and gplots 3.0.1. Taxonomy was assigned to chimera-free Exact Sequence Variants (Callahan et al., 2017) using Silva 132 (downloaded from https://zenodo.org/record/1172783#.W-B0iS2cZBw on 5 November 2018). Data were filtered to remove undefined phyla and taxa present in fewer than two animals. Significance of differences between different diversity measures was determined using Wilcoxon rank sum test. ALDEx2 was used to determine statistically significant differences (Welch's t test, Wilcoxon) between mouse groups. The 16S rRNA gene sequence data have been deposited in the NCBI BioProject database (https://www.ncbi.nlm.nih.gov/bioproject/) under accession number PRJNA524024. Metabolites were analysed and quantified by 1H-NMR analysis as previously described (Crost et al., 2018). Briefly, 20 mg of frozen faeces was thoroughly mixed on a vortex with 1 mL of saline phosphate buffer followed by centrifugation (18,000 g, 1 min). High-resolution 1H-NMR spectra were recorded on a 600-MHz Bruker

Avance spectrometer fitted with a 5-mm TCI proton-optimized triple resonance NMR "inverse" cryoprobe and a 60-slot autosampler (Bruker, Rheinstetten, Germany). Metabolites were identified using information found in the literature or on the Human Metabolome Database, http://www.hmdb.ca/ and by use of the 2D-NMR methods, (e.g. COSY, HSQC and HMBC (Le Gall et al., 2011)) and quantified using the software Chenomx® NMR Suite 7.0TM.

2.1.4. Behavioural tests

The tests were performed between 08:00 am and 03:00 pm and in the following order:

- **Barnes Maze test**. This test was conducted according to previously described methods (Pitts et al., 2018). All sessions were performed on a wet platform under a room lighting of 400 lux to increase the mouse aversion for the platform. Sessions were recorded using a video-tracking system (ANYmaze, Ugo Basile, Varese, Italy). The platform and the escape box were cleaned thoroughly between each mouse session and the surface of the platform was moistened again to avoid mice using olfactory clues to solve the task. Before performing the test, mice were trained to find the escape tunnel for 4 days with 2 sessions per day.
- **Open field test (OFT)**. OFT was conducted as previously described (Hölter et al., 2015). Briefly, mice were placed in the centre of the OFT and the total distance the mice travelled as well as the time they spent in the centre of the field within 5 min was recorded with a video tracking system. The OFT was cleaned between each mouse with 20% ethanol to eliminate any scent.
- **Novel object recognition test.** This test was carried out as previously described (Antunes and Biala, 2014). For each mouse, the time spent interacting with each object during the acquisition and recognition phases was video recorded and analysed blindly. The corrected mnesic index (or discrimination index) was calculated as follows: (time spent exploring the

novel object − time spent exploring the well-known object)/total time spent exploring both objects.

- **Elevated plus-maze test.** To evaluate anxiety-related behaviour, the elevated plus-maze test was conducted as previously described (Shoji et al., 2016). Briefly, the apparatus used for the elevated plus maze test is in the configuration of a + and comprises two open arms perpendicular to two closed arms with a centre platform. The open arms have a very low (0.5 cm) wall to decrease the number of falls, whereas the closed arms have a high (16 cm) wall to enclose the arm. The entire apparatus is placed 50 cm above the floor. One mouse at the time is placed in the center area of the maze. The elevated plus maze test is recorded using a video camera attached to a computer, which is controlled by a remote device. Time spent in each kind of arm (s) was recorded for 5 min Percentage of entries into the open arms and that of time spent in the open arms were determined. Data acquisition and analysis were performed automatically using ANY-maze software.

2.1.5. Liquid Chromatography-MS analysis

Microdissections of hippocampus and colon tissues were homogenized by tissue homogenizer (Bertin, France) using zirconium beads for two cycles of 1 minute at 4°C. The lysis was performed in lysis buffer (8M urea in 50mM Tris-HCl pH 8.0, 50mM NaCl, protease inhibitors) at 4°C for 30 minutes. Proteins were reduced by 10mM DTT at 56°C for 30 minutes and alkylated by 55mM iodacetamide at room temperature for 20 minutes. The proteins were then digested by LysC (1/100 w/w) for 4h at 37°C and by trypsin (1/20 w/w) over night at 37°C. The peptide mixtures were desalted by C18 StageTips (Millipore, USA). Each sample was analysed by nLC MS/MS Orbitrap Fusion trihybrid mass spectrometer coupled with a nano flow UHPLC system (Thermo Fischer Scientific, USA), via a nano electrospray source with an ID 0.01mm fused silica PicoTip emitter (New Objective). The peptides were separated, after trapped on a C18 pre-column, using a gradient of 3-40% acetonitrile in 0.1% formic acid, over 50 minutes at flow rate of 300 nL/min, at 40°C. The MS method consisted of a full scan in Orbitrap analyser (120000 resolution), followed by the combination of CID and HCD

collisions. The peptides were fragmented in the linear ion trap by a data-dependent acquisition method, selecting the 40 most intense ions. Dynamic exclusion of sequenced peptides was set to 30s. Data were acquired using Xcalibur software (Thermo Scientific, USA). All analyses were performed in triplicate. MS raw data were analysed by MaxQuant (version 1.6.2.3), using Andromeda search engine in MaxQuant and consulting the Homo Sapiens UniProtKB database; the tolerance on parents was 10 ppm and on fragments was 0.02 ppm. The variable modifications allowed were oxidation on methionine and acetylation on N terminus and carbamidomethylation on cysteine as fixed modification. The false discovery rate was below 1%, using a decoy and reverse database, and a minimum number of seven amino acids were required for peptide identification. Proteins and protein isoforms were grouped into protein groups. Label-free quantitative analyses were also performed by MaxQuant software, using the MaxLFQ algorithm. The quantitation values were obtained on high-resolution three-dimensional peptide profiles in mass-to-charge, retention time and intensity space. The mass spectrometry proteomics data have been deposited to the ProteomeXchange Consortium via the PRIDE (Perez-Riverol et al., 2019) partner repository with the dataset identifier PXD016432.

2.1.6. Western blot

Hippocampal protein samples were prepared as described in Liquid Chromatography-MS analysis. Equal amounts of proteins (15 µg) mixed with sample buffer were separated on a polyacrylamide gradient gel (Invitrogen, Milan, Italy) by electrophoreses and transferred onto nitrocellulose membrane (Porablot NPC, MACHEREY-NAGEL, Milan, Italy). After 1 h blocking with 3% bovine serum albumin (BSA) in Tris-buffered saline containing 0.1% Tween 20 (Tween-TBS) at room temperature (RT), the blots were incubated in Tween-TBS/3% BSA overnight at 4°C with the following primary antibodies; mouse anti-Map-tau or rabbit anti-RNA-splicing ligase RtcB homolog (rtcb) (ThermoFisher Scientific, Milan, Italy), at a 1:500 dilution. After washing with Tween-TBS, the corresponding secondary antibodies HRP conjugated (Santa Cruz Biotechnology) was added at 1:5,000 dilution in Tween-TBS for 1 h at RT and washed again. Proteins were detected by ImageQuant TL (v2003,

Amersham Biosciences, Piscataway, NJ, USA). Protein expression levels were then quantified by the ImageJ analysis software (ImageJ, National Institute of Health, USA, http://imagej.nih.gov/ij, 1.47t). GAPDH (1:10,000 dilution, Cell Signaling Technology) (Santa Cruz Biotechnology, Santa Cruz, CA, United States) normalization was performed for each sample. Each experiment was performed three times.

2.1.7. Intestinal permeability, plasma, brain and gut cytokines

Plasma levels of cytokines were assessed by Enzyme-linked immunosorbent assays (ELISA). Assays were carried out according to the manufacturer's instructions (all kits from eBioscience). Hippocampal and colon levels of cytokines were assessed using ProcartaPlex multiplex protein assays (Thermo Fisher Scientific) according to the manufacturer's instructions. Intestinal permeability was assessed using a slightly modified previously described method (Arques et al., 2009). Animals were orally delivered with 0.5 ml of PBS containing 25 mg of FITC-labelled dextran (FD4; Sigma-Aldrich) and blood samples were collected after 45 minutes. Plasma concentration of FD4 concentration was assessed using fluorescence spectrometer (LS 55 conducted with FL WinLab software, PerkinElmer, USA) at an excitation wavelength of 490 nm and emission wavelength of 520 nm. Standard curves to calculate FD4 concentration in the samples were prepared from dilutions of FD4 in PBS.

2.1.8. Immunofluorescence and confocal microscopy

Seven to eight µm-thick frozen coronal sections of a hemibrain were cut and placed on superfrost slides. Sections were fixed with 10% buffered formalin for 30 minutes and subsequently incubated with rabbit anti-glial fibrillary acidic protein (GFAP) antibody (code 18-0063, Zymed, San Francisco, CA) or with rat anti-F4/80 antibody (code MCA497GA, AbD Serotec) for two hours. Sections were then incubated with the appropriate FITC or Cy3-conjugated secondary antibody (Jackson Immunoresearch Europe, Cambridgeshire, UK) for one hour and nuclei were

counterstained with TO-PRO-3 (Invitrogen, Carlsbad, CA). Sections were analysed by confocal microscope (LSM 510, Carl Zeiss microscopy, Jena, Germany) and fluorescence intensity evaluated with ImageJ software (NIH, Bethesda, MD).

2.1.9. Statistical analysis

Microbiome data (genus level) were correlated (Pearson) with metabolomic and proteomic data using aldex.corr() within the Bioconductor package ALDEx2 (Fernandes et al., 2014). For the MS study, all data were evaluated by Perseus statistical software. The protein expression fold change variation between two groups was analysed by two sides t test, setting FDR less than 0.015 and s0 of 0.1. The differentially expressed proteins, with a significant ratio FMT-aged/FMT-adult (P value < 0.05), were analysed by Ingenuity Pathway Analyses (IPA) (Qiagen), and only the differentially regulated pathway with a significant z-score, after Bonferroni test, was considered. The symbols shown in the network are explained at http://www.qiagenbioinformatics.com/products/ingenuity-pathway-analysis.

Behavioural measurements were performed for each treatment in two different experiments (n = 10–12 mice/group). All assessments were performed in blind of the treatment received by the mouse groups. Results were expressed as means ± S.E.M. and the analysis of variance was performed by two-way ANOVA. A Bonferroni's significant difference procedure was used as post hoc comparison. P values of less than 0.05 or 0.01 were considered significant. Data were analysed using the "Origin 9" software (OriginLab, Northampton, USA).

2.2. Click chemistry

2.2.1. Bacterial culturing

Bacteroides thetaiotamicron (BT) strain VPI 5482 was used in click chemistry experiments. BT was grown under anaerobic conditions at 37° C in either brain heart infusion media (BHIS) or in a minimal medium supplemented with glucose (MMG) as the sole carbon source. The minimal medium composition per L is: 3.6 g KH_2PO_4, 0.875 g NaCl, 1.125 g $(NH_4)_2SO_4$, 5 g glucose, (pH adjusted to 7.2 with 1M NaOH), 1 mL hemin solution (500 mg dissolved in 10 mL of 1 M NaOH then diluted to a final volume of 500 mL with H_2O), 1 mL of 0.1M $MgCl_2$, 1 mL of 0.01% (w/v) $FeSO_4 \times 7H_2O$, 1 mL of 1 mg/mL vitamin K3 dissolved in absolute ethanol, 1 mL of 0.8% (w/v) $CaCl_2$, 250 µL of 0.02 mg/mL vitamin B12 solution. Optical density was measured using Benchmark Plus Microplate Reader (BIO-RAD).

2.2.2. Caco-2 cell culture

Human epithelial colorectal adenocarcinoma cells (Caco-2, ATCC) were cultured in Dulbecco's modified Eagle's medium (DMEM, Thermo Fisher Scientific) supplemented with 10% fetal bovine serum (FBS, Gibco) and 1% penicillin/streptomycin. Ten cm plates were seeded at 5×10^5 cells and incubated at 37 °C with 5% CO_2. Sub-confluent cultures (70-80%) were split 1:3 to 1:6 using 0.25% trypsin-EDTA solution. Cells were counted using Countess™ cell counting chamber slides (INVITROGEN) using Countess II Automated Cell Counter (INVITROGEN).

2.2.3. SK-N-SH cell culture

Human neuroblastoma cell line (SH-N-SK, Merk) were cultured in minimal essential medium (MEM, Sigma Aldrich) supplemented with 10% FBS (Gibco) and 1% penicillin/streptomycin. Cells were seeded in T25 flasks at 1.5×10^6 cells and incubated at 37 °C with 5% CO_2. Sub-confluent cultures (70-80%) were split 1:3 to 1:10 in T25 using 0.25% trypsin-EDTA solution. Cells were counted as described above.

2.2.4. Eukaryotic cell lines co-culture with *Bacteroides thetaiotaomicron*

To assess the metabolite transfer from BT to eukaryotic cell lines, Caco-2 or SH-N-SK cells were incubated with BT in tissue culture dishes (Corning Inc.). Eukaryotic cells were plated on UV-sterilized #1.5 glass coverslips in tissue culture dishes. Caco-2 were seeded at 4×10^5 cells/well and SH-N-SK were seeded at the same density. Eukaryotic cells were seeded 24 hr before co-culture experiments. Bacterial cells were placed on a 0.4 µM cell culture insert (cellQART) situated 1 mm above the eukaryotic cells. In order to perform coculture experiments, BT was grown in minimal medium supplemented with 25 µM PAA (Cayman Chemical) or with DMSO (Sigma-aldrich) as negative control. 50 mL of BT culture (OD600=0.4) were collected and washed three times in PBS and resuspended in 6 mL of appropriate cell culture media (with 10% FBS, without antibiotics). One mL of bacterial suspension was added to upper-well inserts of the 6-well transwell culture dishes and incubated at 37 °C with 5% CO_2. Contents of the upper bacterial insert and the lower well were collected 4 h after the addition of the bacteria. Alkyne containing metabolites in bacterial cells and in eukaryotic cell lines were labelled with Alexa Fluor 647 azide (final concentration 5µM) (Thermo Fisher Scientific) using the Click iT cell reaction buffer kit (Thermo Fisher Scientific) following the manufacture instructions. Cells that were grown in transwell without bacterial cells were also incubated with the Click reaction buffer containing Alexa Fluor 647 as a control of non-specific fluorescence. Eukaryotic cells and bacterial cells were mounted onto glass slides adding DAPI and Fluoroshield

(Sigma-aldrich) and imaged on a LSM 880 confocal microscope (Zeiss) using Zeiss Zen software (Zeiss Zen 2012 SP1black edition).

3. Results

3.1. Faecal microbial transplant

3.1.1. Microbiota of adult mice acquires an aged phenotype following FMT from aged donors

Before proceeding to FMT, we analysed the faecal microbiota of two groups of mice (adult and aged animals). The group of adult mice included 3 months-old mice whereas the group of aged animals consisted of 24 months-old mice. We evaluated alpha and beta diversity and also the relative abundance of different taxa (Fig. 1). The alpha diversity between the aged and adult groups demonstrated a significant (P=0.0107) difference only in species diversity. In particular, aged mice had more different amplicon sequence variants (ASVs) compared to adult mice. No significant differences could be found when looking at the Shannon Index and inverse Simpson (Fig. 1a). A definite separation between the two groups of mice was evident when assessing the beta diversity (Fig. 1b). Beta diversity was analysed using Bray-Curtis dissimilarity (that examines the abundances of microbes shared between two samples, and the number of microbes found in each sample). The comparison of the abundance of different taxa showed interesting significant differences between the two groups of animals. Compared to the aged group, the adult group had more ASVs associated with *Ruminiclostridium*, *Butyricicoccus*, *Lachnoclostridium*, *Lachnospiraceae* spp., *Shuttleworthia* and *Marvinbryantia*, and significantly fewer associated with *Staphylococcus*, *Jeotgalicoccus*, *Facklamia*, *Parvibacter*, *Enterorhabdus*, *Muribaculum*, *Parabacteroides* and *Anaerostipes* (Fig. 1c).

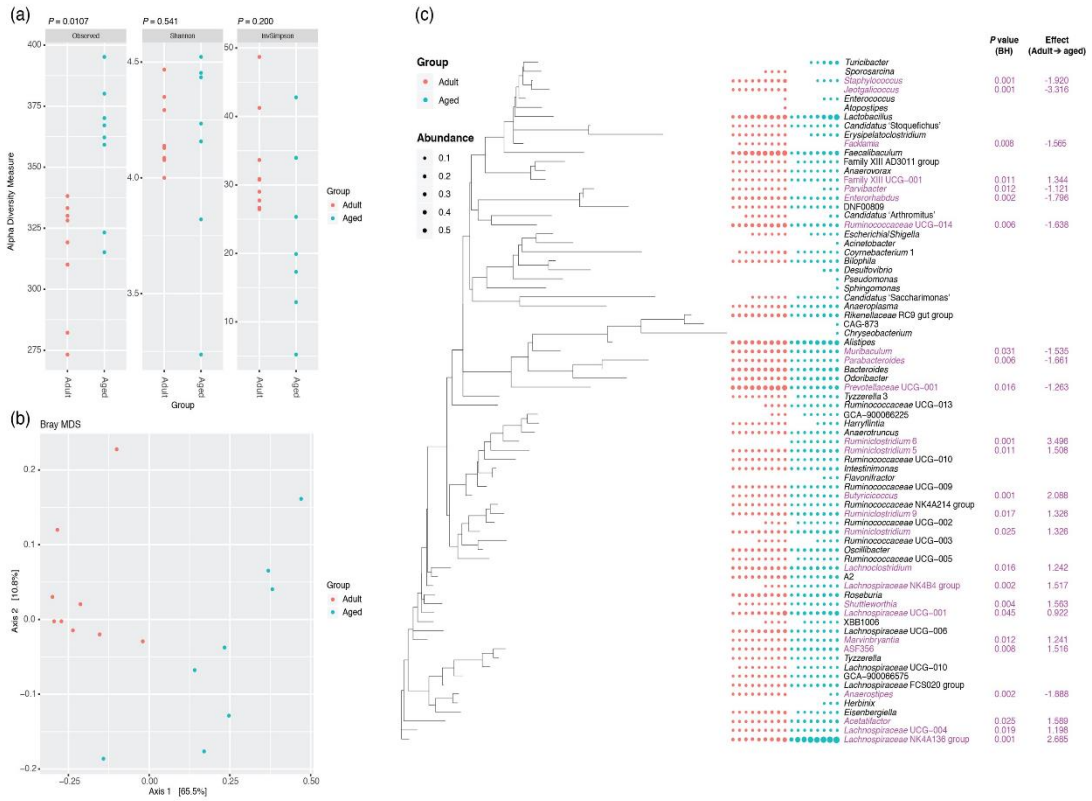

Figure 1. <u>Analysis of the faecal microbiota of adult (3-months old) and aged (24-months old) mice.</u> (a) Alpha diversity measure. Significance of differences between the two groups was assessed by Wilcoxon rank sum test. (b) Multidimensional scaling (MDS) plot of Bray-Curtis analysis of beta-diversity between adult and aged mice. Data presented are for ASVs present in more than two animals and prevalence threshold of 1% at the genus level. (c) Comparison of the relative abundance of different genera present in the faecal microbiota of the two groups. Purple text, significantly different genera (Welch's t test and Wilcoxon; $P < 0.05$, Benjamini-Hochberg) based on ALDEx2 analyses.

On the ground of these results, faeces from three adult donors and from two aged mice representative of the two groups were gathered to create two distinct pools to be used for the FMT treatment. In the present study we did not use germ-free (GF) animals. Although many researchers use GF models to assess the impact of gut microbiota on different aspects of host physiology, for our purpose this model was not suitable because GF mice bear abnormalities in blood-brain barrier structure and integrity (Braniste et al., 2014) and also changes in microglia morphology and number

(Erny et al., 2015). For these reasons, using GF mice could have added confounding factors and could have altered our results or made troublesome their correct interpretation. Hence, depletion of the gut microbiota before FMT was achieved by antibiotic treatment. Although antibiotic treatment does not lead to the complete eradication of the gut microbiota, it has the advantage to avoid the interference of other factors resulting from a development in a GF environment. For FMT treatment, adult mice were transplanted with faeces from either aged mice (FMT-aged) or age-matched donors (FMT-adult). The microbiota profile was assessed before FMT for both donor pools and for recipient mice. In the latter case, microbiota profile was ascertained at the end of the antibiotic treatment and was repeated after FMT (Fig. 2). Measure of alpha diversity between post FMT-aged and post FMT-adult mice showed no significant difference (Fig. 2a). In contrast, analysis of beta diversity using Bray-Curtis indicated a clear separation of the groups (Fig. 2b). In particular, both post FMT aged and post FMT adult groups clustered with the respective donors. The antibiotic treatment was not completely successful for all the recipient mice. In particular mouse 1 (MS1) and 2 (MS2) clustered with the adult donor and post FMT-adult group. However, even these two mice clustered with the aged group after the transplant with faeces from the aged group (Fig. 2b). We were not able to detect significant differences in the microbiota of the different groups after FMT (as the differences showed in the initial part of the study) as such a less stringent Benjamini-Hochberg cut-off ($P < 0.1$) was used when analysing these data (Fig. 1). However, this is not surprising because mice analysed in the first part of the study did not undergo to any intervention (such as antibiotic treatment and FMT). When looking at the different genera found in the faeces only four were differentially regulated. In particular, *Prevotellaceae*, *Faecalibaculum*, *Lachnospiraceae* and *Ruminococcaceae* were found to be significantly less abundant in the faeces of FMT-aged mice compared to faeces of FMT-adult animals (Fig. 2c). When analysing the correlation between the microbiomic and metabolomic data we found only few significant associations. In particular, O-phosphocholine is positively correlated with *Lachnospiraceae* NK4A136 group, hypoxanthine and succinate are negatively correlated *Faecalibaculum*. Trimethylamine and isobutyrate are negatively correlated with *Tyzzerella* 3 and *Marvinbryantia* respectively. Guanosine derivate is

positively correlated with *Lachnospiraceae* FCS020 group. Finally, tartrate is negatively correlated with *Tyzzerella* 3, *Bilophila* and *Faecalibaculum* and is positively correlated with DNF00809, *Lachnospiraceae* NK4A136 group, *Lachnospiraceae* FCS020 group (Fig. 2d).

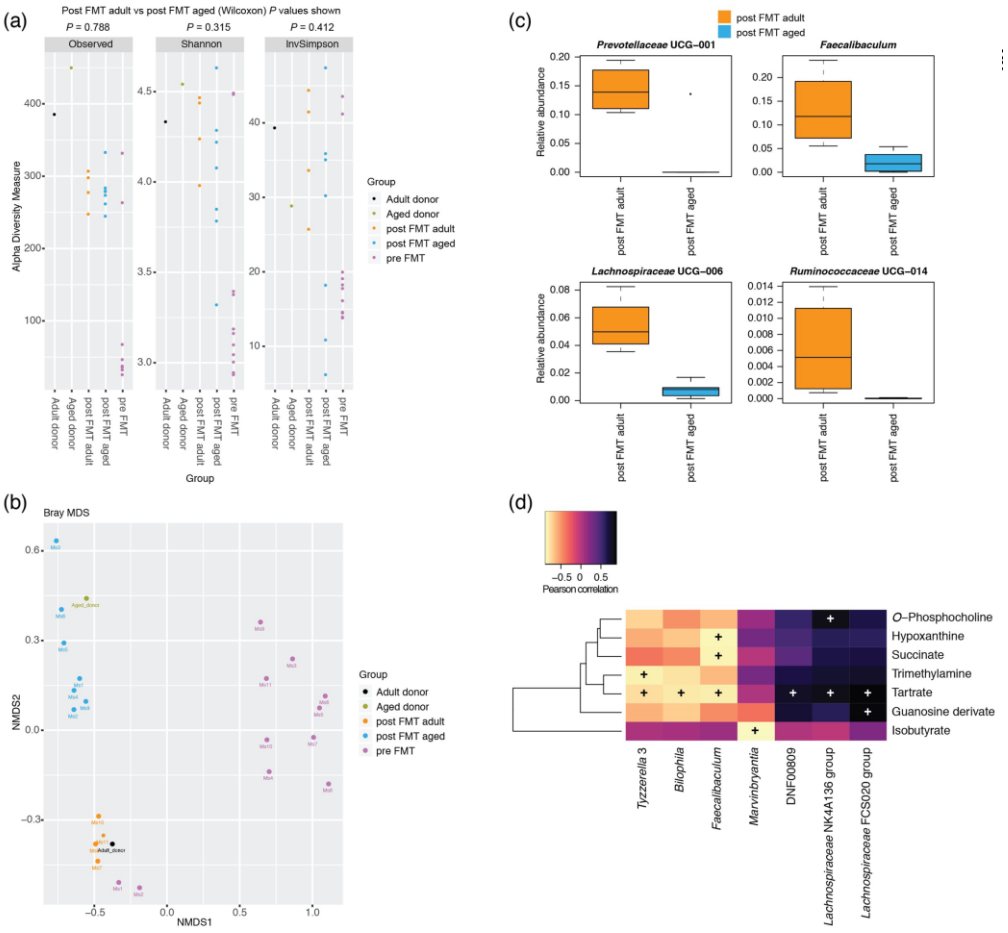

Figure 2. **<u>Effect of FMT on the faecal microbiotas of adult mice.</u>** (a) Alpha diversity measure among the grouped adut (n = 1) and aged (n = 1) samples, the adult mice pre FMT (n = 11) and the adult mice after FMT with adult (n = 4) and aged (n = 7) faeces. (b) MSD plot of Bray Curtis measure of beta diversity. Data presented are for ASVs present in more than two animals and prevalence threshold of 1% at the genus level. (c) Box plots shows the significantly different genera (Welch's t test and Wilcoxon; P < 0.1, Benjamini-Hochberg) between post FMT adult (n = 4) and post FMT (n = 4) aged groups. based on ALDEx2 analyses. Pearson correlation of faecal microbiomic and metabolomic data. Only rows/ columns that contained significant data (P < 0.1, Benjamini-Hochberg) are shown.

3.1.2. Impact of faecal microbial transplant on memory, behaviour and motor activity

To assess the effect of FMT from aged donors to adult mice, we performed a series of tests (spatial learning, memory, motor activity and anxiety-like behaviour) (Figs. 3 and 4). Memory and spatial learning were evaluated using *Barnes maze test*. After the initial training, a retention test was carried out. In this test the escape tunnel was taken away and the lapse of time needed to reach the point where the former escape tunnel was located for the first time was recorded. The average primary latency was significantly higher for adult recipients of microbiota from aged mice compared to control groups (untreated or colonized with microbiota from age-matched donors) (41.7 ± 3.5 s; 30.5 ± 3.9 s and 23.5 ± 6.7 s, respectively; $P < 0.05$) (Fig. 3a). Also, during retention test, FMT-aged mice spent less time in the quadrant that previously had the escape tunnel (28.9 ± 2.6 s in comparison to untreated 46.5 ± 6.3 s, and FMT adult 51.8 ± 10.2 s; $P < 0.05$) (Fig. 3b; heat map in Fig. 3c). This test supported an involvement of the gut microbiota in processes of memory and spatial learning. Another test that we employed to assess memory and learning was the *novel object recognition test*: on day 1, mice were exposed to two similar objects and on day 2 mice were exposed to the same test area with one object substituted by a novel one. The time spent exploring the novel and the familiar object was recorded. Control groups would rather explore the novel object than the familiar one whereas FMT aged mice spent significantly less time in exploring the novel object compared to control (0.23 ± 0.04 and 0.46 ± 0.05, respectively; $P < 0.01$) (Fig. 3d-e) suggesting a reduced discrimination due to impaired memory.

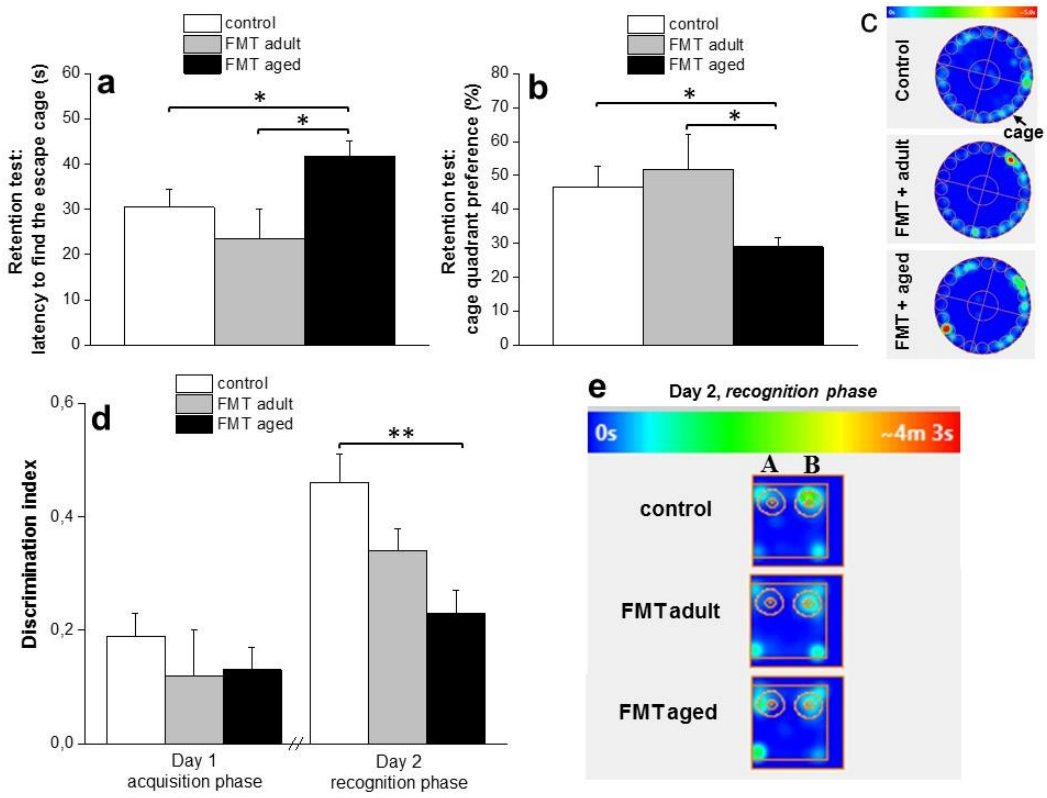

Figure 3. **Impact of FMT from old donor into adult mice on spatial learning and memory.** **Barnes maze test** (Fig. 3a–c): in the initial practice mice were trained to find the escape tunnel for 4 successive days (twice per day). The average primary latency (Fig. 3a) was significantly higher for adult mice transplanted with faeces from aged donors (FMT aged) compared to mice either left untreated (control) or transplanted with faeces from adult donors (FMT adult). During this test FMT aged mice spent significantly less time in the quadrant that contained the escape tunnel compared to the two control groups (Fig. 3b; heat map in Fig. 3c). The values represent the mean ± SEM for each group (n = 10–12 mice/group). *P < 0.05 vs control animals and FMT-adult. The **novel object recognition test** (Fig. 3d–e): on the acquisition phase (day 1) mice were exposed to two similar objects; on the recognition phase mice were exposed to the same area containing one familiar object and a novel object. No differences have been recorded in the discrimination index between the different groups in the acquisition phase (Fig 3d). In the recognition phase control groups, either untreated or FMT-adult mice, preferred the novel object more than the familiar one, whereas FMT-aged mice showed a significant reduction in the time spent exploring the novel object (Fig. 3d and heat map in 3e). The values represent the mean ± SEM for each group (n = 10–12 mice/group). **P < 0.01 vs control animals.

Moreover, as microbiota has been reported to have an impact on locomotion and anxiety (Diaz Heijtz et al., 2011; De Palma et al., 2017), we next assessed the effect of FMT on these activities utilizing the *open field* and the *elevated plus maze tests*. In the open field test, FMT-aged mice showed no difference in the distance travelled compared to other groups (Fig. 4a) suggesting that FMT from aged mice in adult recipients has no impact on motor capacity. However, in the same test, untreated or FMT-adult mice spent a longer time in the centre of the arena compared to FMT-aged mice who preferred the periphery (Fig. 4b-e). In the *elevated plus maze*, there was no differences in the time spent in opened or closed arms, even though most of the mice spent a longer time in closed arms regardless of the treatment (Fig. 4f-g).

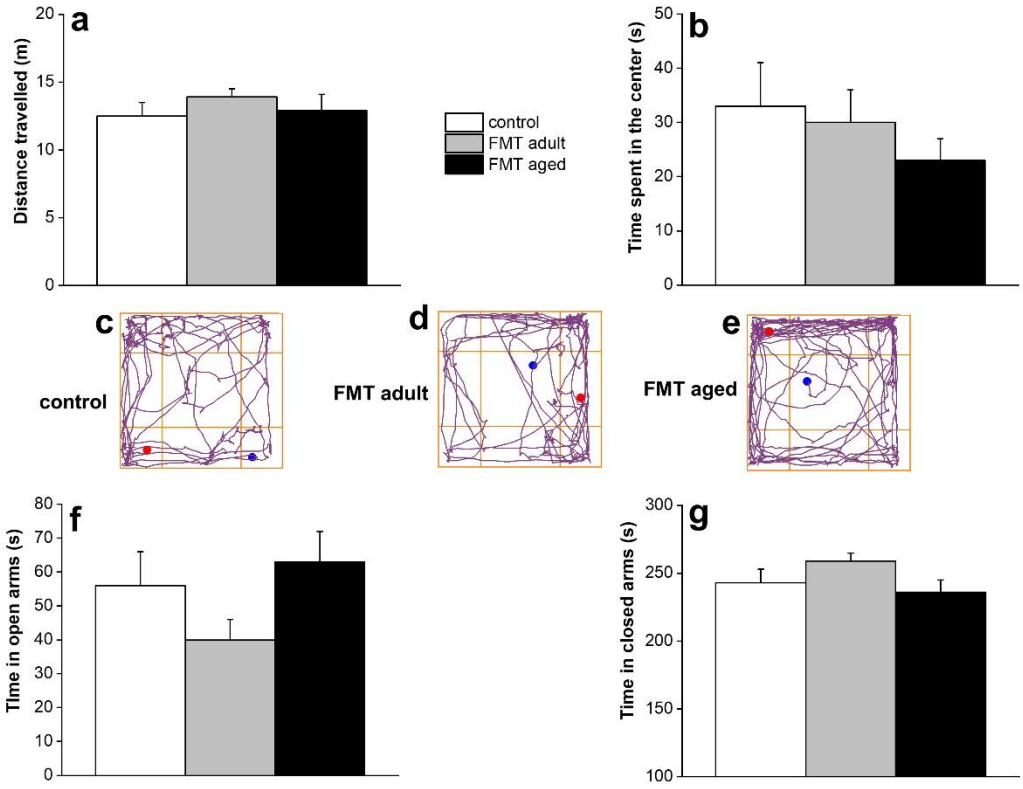

Figure 4. Effect of FMT from old mice on locomotion, explorative and anxiety-related behaviour. In the **open field test** mice transplanted with faeces from aged donors did not show significant difference in the distance travelled compared to control groups (Fig 4 a). No significant differences have been observed in the time spent in the center of the arena (Fig. 4b). However, FMT-aged mice displayed a tendency to prefer the periphery of the arena instead of the center (Fig. 4b and Fig 4e). The representative tracks of movement patterns are depicted in Fig. 4c–e (ANY-maze software). In the **elevated plus maze**, FMT-aged mice did not display significant differences in time spent in open or closed arms of the maze compared to control groups (Fig. 4f, g). However, mice spent more time in closed arms regardless of the treatment. The values represent the mean ± SEM for each group (n = 10–12 mice/group).

3.1.3. Effect of faecal microbial transplant on protein expression in hippocampus of adult mice

The results obtained with behavioural tests led us to look into the molecular mechanisms that could be important in explaining FMT-induced different behaviours. For this purpose, we used one-shot label-free quantitative proteomics method. The hippocampus was the primary target of this analysis because it has a crucial role in memory and learning (Bettio et al 2017). The whole protein extracted from hippocampus yielded 2180 quantified proteins and 16,083 peptides (data not shown). The volcano plot was obtained comparing by two-sided *t* test FMT-aged mice with FMT-adult mice (Fig. 5).

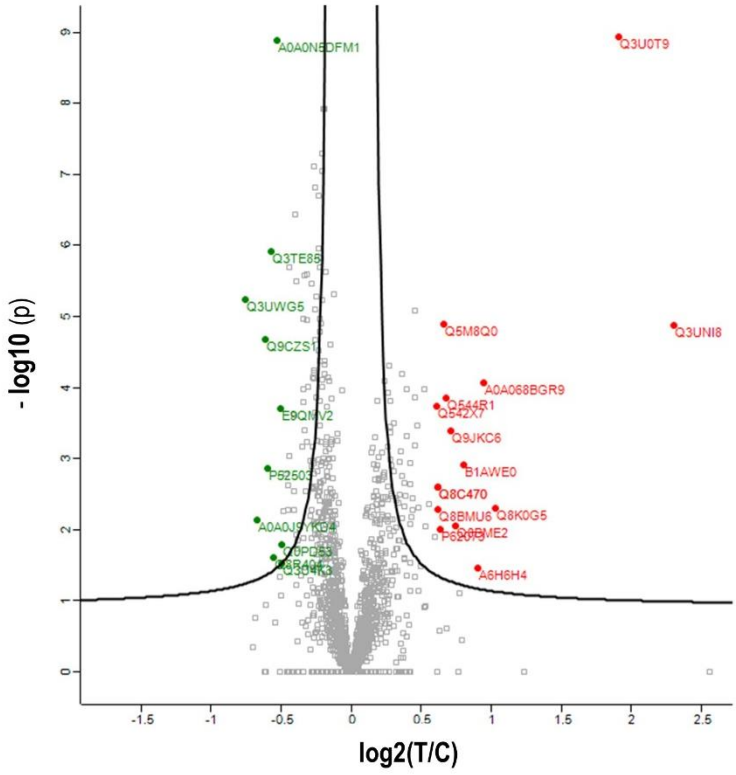

Figure 5. **Volcano plot.** Quantitative analysis of proteins in the hippocampus. Plot of quantified proteins in hippocampus tissue (A). Differentially regulated proteins after transplant of aged faeces into adult mice (T) versus faeces from adult mice transplanted into adult age-matched mice (C) are showed (T/C). The proteins in red are up regulated and in green down regulated.

One hundred forty proteins were differentially expressed as 52 of them were up-regulated and 88 were down-regulated. Forty-seven proteins were differentially regulated with a fold change rate higher than 1.5 (Table 1). To further confirm these data, western blot analysis was performed on two selected proteins that were found differentially regulated by proteomics (Figs. 6, 7). In particular, protein expression of the tRNA-splicing ligase RtcB homolog (Rtcb) in FMT-aged mice was found reduced compared to controls (Fig. 6d), whereas the microtubule-associated protein (MAPT) was overexpressed after the same treatment (Fig. 7d). RtcB decreased by less than half (FMT-aged versus FMT-adult ratio: 0.46) and MAPT doubled its rate of expression (FMT aged versus FMT adult ratio: 2.38) (data not shown).

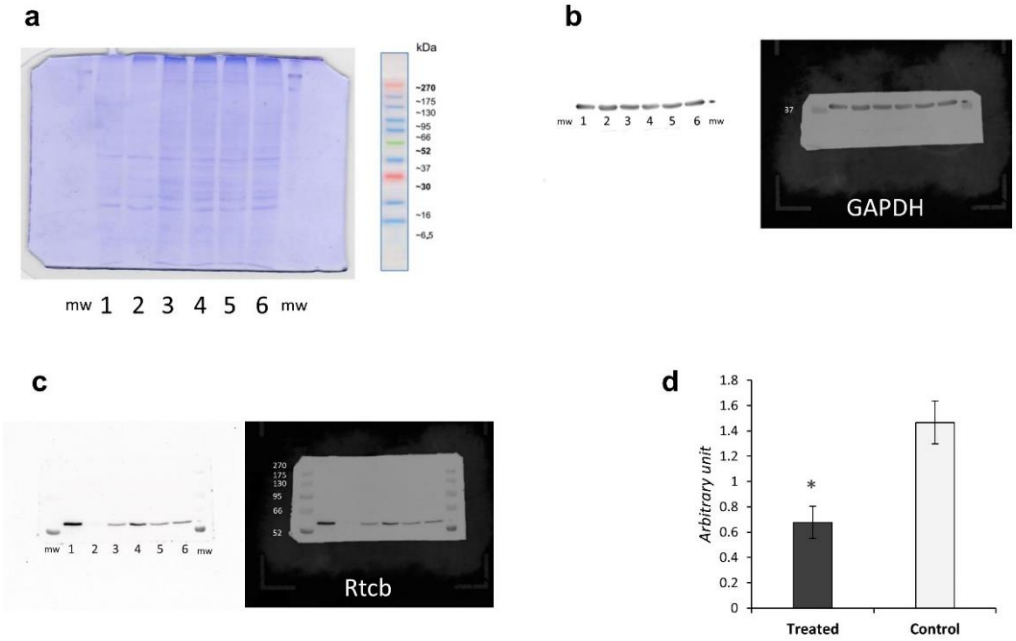

Figure 6. <u>Western Blot analysis</u>. Western blot for Rtcb in the hippocampus of mice transplanted with aged faeces (treated) or with adult faeces (control). Polyacrylamide (12%) gel stained with blue Coomassie with a representative image of molecular weight marker with kDa (a). GAPDH bands (panel b, left) and merged with nitrocellulose membrane (panel b, right). Rtcb bands (panel c, left) and merged with nitrocellulose membrane (panel c, right). In (d) histogram shows levels of analysed protein both in treated and control animals. Lane 1 (positive control, SH-SY5Y cell line); lane 2 (negative control, mouse adipose tissue); lane 3 (aged mouse hippocampal proteins); lane 4 (adult mouse hippocampal protein); lane 5 (FMT-aged hippocampal proteins); lane 6 (FMT-adult hippocampal proteins). Rtcb protein was detected approximately at 56 kDa (right blots). GAPDH (37 kDa) was used as housekeeping (left panel). Molecular weight (mw) used was SHARPMASS VII.

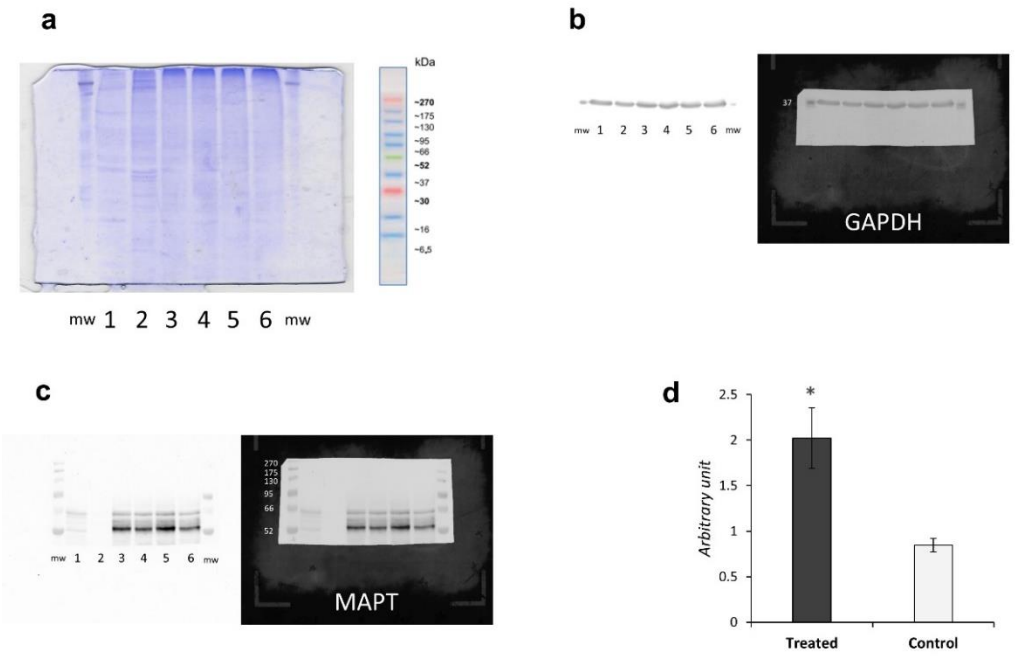

Figure 7. **<u>Western Blot analysis</u>**. Western blot for MAPT in the hippocampus of mice transplanted with aged faeces (treated) or with adult faeces (control). Polyacrylamide (12%) gel stained with blue Coomassie with a representative image of molecular weight marker with kDa (a). GAPDH bands (panel b, left) and merged with nitrocellulose membrane (panel b, right). Rtcb bands (panel c, left) and merged with nitrocellulose membrane (panel c, right). In (d) histogram shows levels of analysed protein both in treated and control animals. Lane 1 (positive control, SH-SY5Y cell line); lane 2 (negative control, mouse adipose tissue); lane 3 (aged mouse hippocampal proteins); lane 4 (adult mouse hippocampal protein); lane 5 (FMT-aged hippocampal proteins); lane 6 (FMT-adult hippocampal proteins). Rtcb protein was detected approximately at 56 kDa (right blots). Mapt protein was detected approximately at 50 kDa (right blots). Molecular weight (mw) used was SHARPMASS VII.

The IPA of the significantly up- and down-regulated proteins revealed modifications in proteins related to different pathways such as synaptic transmission, cognition, neurotransmission, axonal elongation, locomotion (Table 1) in the hippocampus of adult mice transplanted with faeces from aged donors compared to adult mice transplanted with faeces from age-matched donors. All the aforementioned pathways were down-regulated in the hippocampus of adult mice transplanted with aged faeces. In particular, there were 35 molecules differentially regulated in synaptic transmission, 46 in cognition, 41 in neurotransmission, 12 in elongation of neurites and 28 in locomotion (Table 1).

	Functions Annotation	p-Value	Activation z-score	Molecules	# Molecules
Cell-To-Cell Signaling and Interaction, Nervous System Development and Function	synaptic transmission	2.83E-11	-1.763	AMPH,ANKS1B,CAMK2A,CNP,CPNE6,DLG2,DLG4,DPYSL2 ,ERC2,FBXO2,GNAI2,HNRNPK,MAPT,NAPA,NPTX1,NRCAM, NSF,PAFAH1B1,PARK7,PPP3CA,PPP3R1,PRKCG,PSMC5,RAB3A, S100B,SH3GL2,SLC12A5,SLC1A3,SNAP25,SNPH,SYN1,SYN2, SYNGAP1,UNC13A,VDAC1	35
Behavior	learning	2.72E-14	-1.697	ACTG1,AMPH,ATP1A3,CAMK2A,CFL1,CKB,CKMT1A/CKMT1B ,CPT1C,CRMP1,CTNND2,DLG3,DLG4,ELAVL4,FBXO2,GMFB, GSK3B,HAPLN1,KCNAB2,MAPT,NCAM1,NCDN,NRAS,NRCAM, NTRK2,PAFAH1B1,PARK7,PDE1B,PEX5L,PPP3CA,PPP3R1, PRKAR1A,PRKAR2B,PRKCG,RTN4,S100B,SHANK1,SLC12A5, SNAP25,SOD2,SRCIN1,SYNGAP1,SYNJ1,SYNPO,TRIM3,TSN,VDAC1	46
Cell-To-Cell Signaling and Interaction, Nervous System Development and Function	neurotransmission	4.44E-12	-1.656	AMPH,ANKS1B,CAMK2A,CNP,CPNE6,DLG2,DLG4,DNM1,DPYSL2, ERC2,FBXO2,GDAP1,GNAI2,HNRNPK,KCTD12,MAPT,NAPA,Nefm, NPTX1,NRCAM,NSF,NTRK2,PAFAH1B1,PARK7,PPP3CA,PPP3R1, PRKCG,PSMC5,RAB3A,S100B,SH3GL2,SLC12A5,SLC1A3,SNAP25, SNPH,SRCIN1,SYN1,SYN2,SYNGAP1,UNC13A,VDAC1	41
Cell Morphology, Cellular Assembly and Organization, Nervous System Development and Function	elongation of neurites	4.27E-08	-0.228	ALCAM,CAMK2A,DPYSL2,GNAS,MAPT,NTRK2,OMG,PACSIN1, PAFAH1B1,PFN1,PFN2,RAB35	12
Behavior	locomotion	6.83E-07	-0.087	ABAT,AGAP2,ATP1A1,ATP1A3,CAMK2A,CNP,DLG3,DLG4,DNM1, ELAVL4,GMFB,HINT1,MAPT,NCAM1,NEFL,NRCAM,NTRK2,OMG, OXR1,PAFAH1B1,PARK7,PDE1B,RTN4,SNAP25,SOD1,SOD2, SPTBN4,TSN	28

Table 1. <u>IPA in the hippocampus.</u> IPA analysis of the significantly up- and down regulated proteins (after Bonferroni correction) in the hippocampus of FMT-aged mice versus FMT-adult mice. The enriched categories, related to specific function annotations, the P value, the z-score of the software and the involved proteins are displayed.

The wheel charts graphically underline these movements of protein expression with up- (in red) and down-regulated (in green) proteins (external side of the wheel) involved in cognition (Fig. 8) synaptic transmission (Fig. 9) and neurotransmission (Fig. 10) pathways (centre of the wheel). As regards cognition (Fig. 8), 59 proteins were associated to this pathway. In particular, the most up-regulated proteins were CPT1C, MAPT, PEX5L (dark red). Though to a lesser extent, other proteins, like GRN, KIF1A, PRKAR1A, SHANK1, TSN, UBQLN2 (light red), were also up-regulated. All the other proteins in the graph were down-regulated (green). Among the down-regulated proteins that are important for their functions we recall: FBXO2 (ubiquitin ligase substrate adaptor), HOMER1 (postsynaptic density scaffolding protein), RTN4 (a developmental neurite growth regulatory factor and a facilitator of neurite branching), GMFB (an important protein that causes differentiation of brain cells and stimulation of neural regeneration), and S100b. The cognition pathway resulted overall down-regulated. As regards the synaptic transmission pathway (Fig. 9) 43 proteins were associated to this pathway. The majority of the proteins (40 proteins) were down-regulated (green) and only three proteins (MAPT, SNPH, UNC13A) were up-regulated (red). As for the latter pathway, also the synaptic transmission pathway was overall down-regulated in the hippocampus of FMT-aged mice. Fifty-two differentially expressed proteins were associated to the neurotransmission pathway (Fig. 10). Those that were the most up-regulated were GDAP1, MAPT and UNC13A. Other up-regulated proteins, though to minor extent, were KCTD12 and SNPH. All the other differentially expressed proteins of the neurotransmission pathway were down-regulated. FBOX2, HOMER1, s100b are some of the proteins down-regulated in the neurotransmission pathway and are also shared with the cognition and the synaptic transmission pathways. Taken together, these results show that the intestinal microbiota characterizing aged animals is capable of inducing behavioural modifications and changes in the expression of brain proteins regardless the actual age of the animals. Interestingly, all these modifications pointed to an overall diminished brain function which is also associated with the physiological ageing process.

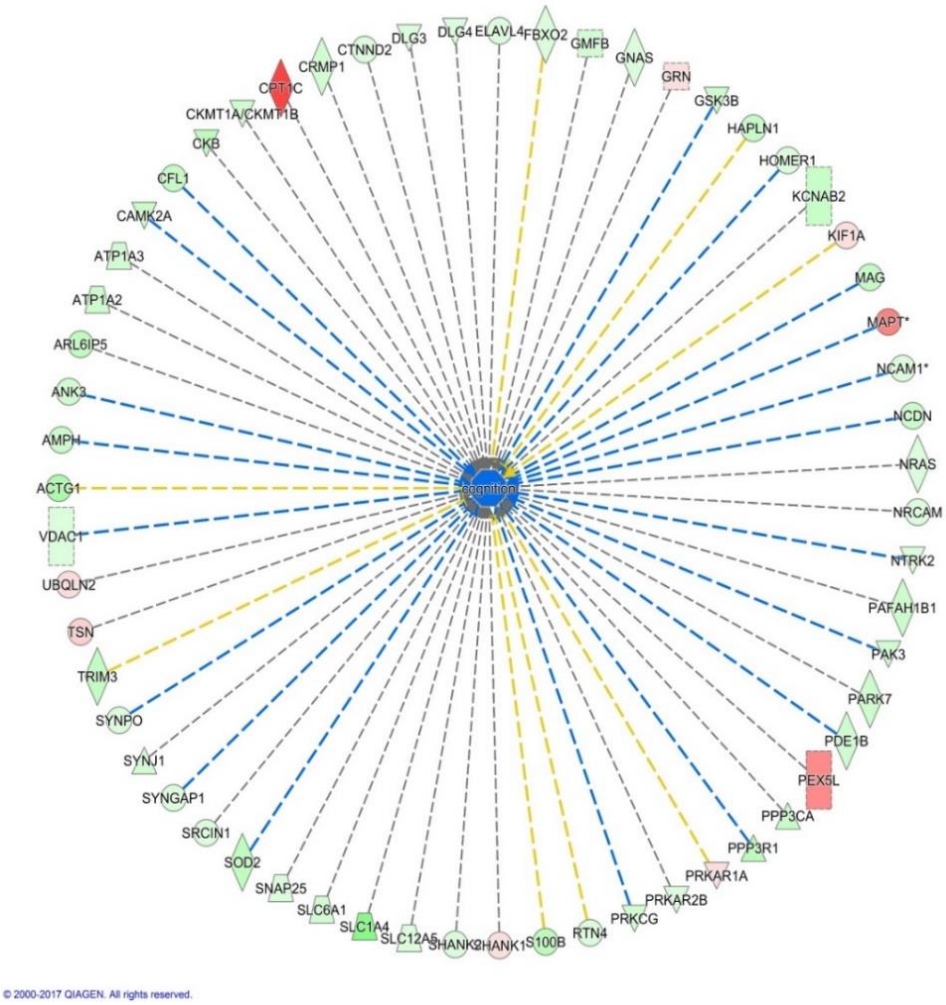

Figure 8. <u>Wheel chart of the cognition pathway.</u> IPA of the significantly up- and down-regulated proteins (after Bonferroni analysis) in the hippocampus tissue of FMT-aged mice versus FMT-adult mice. The up-regulated proteins are marked in red, while those that that were down-regulated are marked in green. The blue colour indicates that the pathway is down regulated.

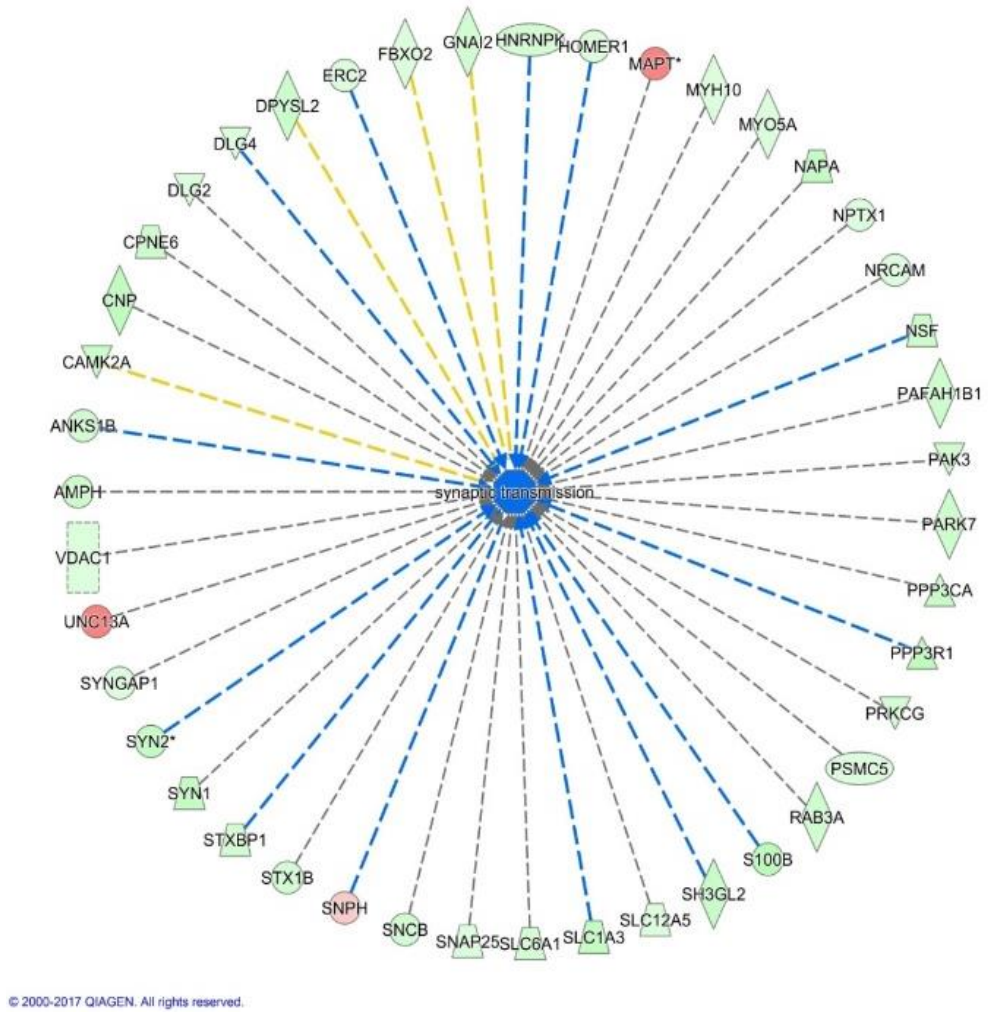

Figure 9. <u>Wheel chart of the synaptic transmission pathway.</u> IPA of the significantly up- and down-regulated proteins (after Bonferroni analysis) in the hippocampus tissue of FMT-aged mice versus FMT-adult mice. The up-regulated proteins are marked in red, while those that that were down-regulated are marked in green. The blue colour indicates that the pathway is down regulated.

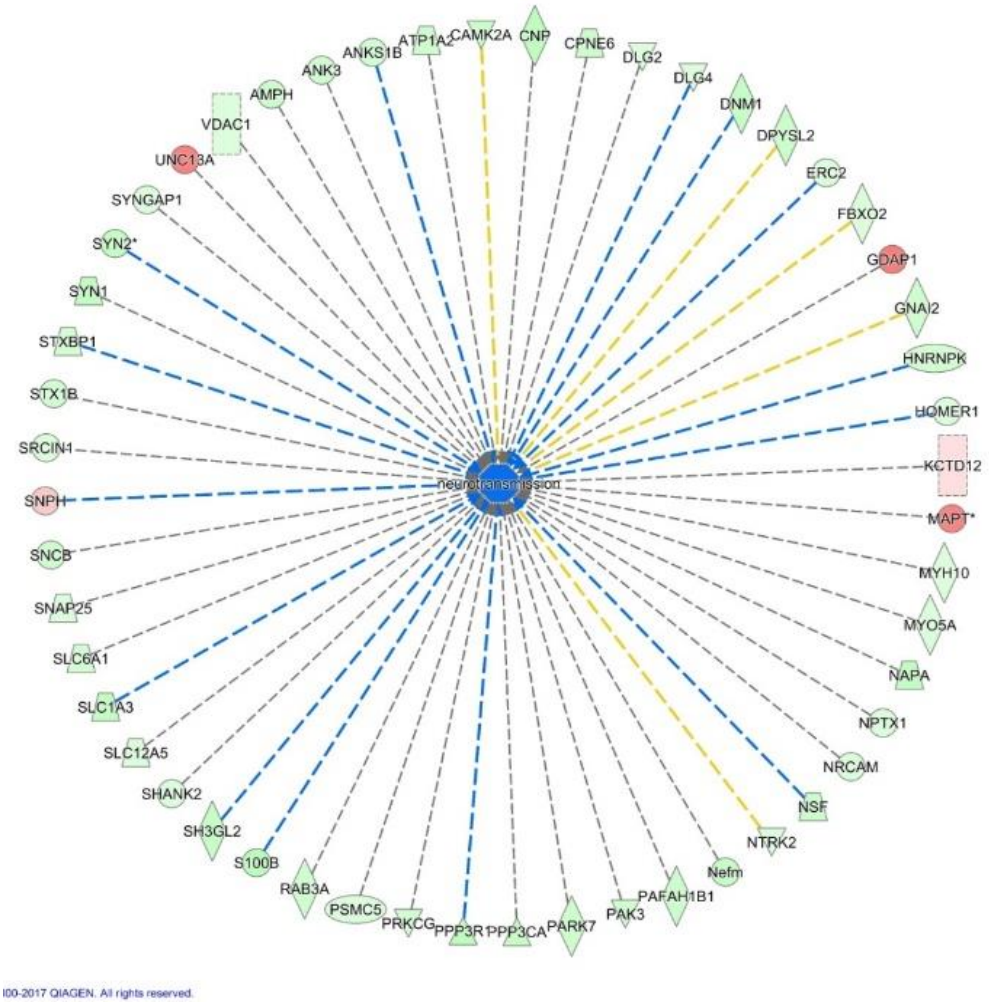

Figure 10. <u>Wheel chart of the neurotransmission pathway.</u> IPA of the significantly up- and down-regulated proteins (after Bonferroni analysis) in the hippocampus tissue of FMT-aged mice versus FMT-adult mice. The up-regulated proteins are marked in red, while those that that were down-regulated are marked in green. The blue colour indicates that the pathway is down regulated.

3.1.4 Glial cells of the hippocampus fimbria of adult mice undergo phenotypic changes after faecal microbial transplant from aged mice but no differences in the level of cytokines in the hippocampus of adult mice transplanted with aged faeces

To further substantiate the results obtained with the proteomic approach, we analysed the expression of GFAP by immunofluorescence in astrocytes in different hippocampal regions (dentate gyrus, CA4 and CA3). In this case, we did not find any significant difference in the expression of GFAP in the hippocampus of FMT-aged mice compared to adult recipients receiving faeces from age-matched animals (Fig. 11a-i). This result pointed to the absence of an evident neuroinflammatory state. We also evaluated, by immunofluorescence, the expression of F4/80 in the microglia of the hippocampus fimbria (Fig. 11 j-l). Contrary to GFAP, in this case we did find a significant (P= 0.0168) increase in the expression of F4/80 in the fimbria of adult mice transplanted with faeces from aged donors (Fig. 11 j-l). The levels of expression of F4/80 were subsequently further confirmed by western blot analysis (data not shown).

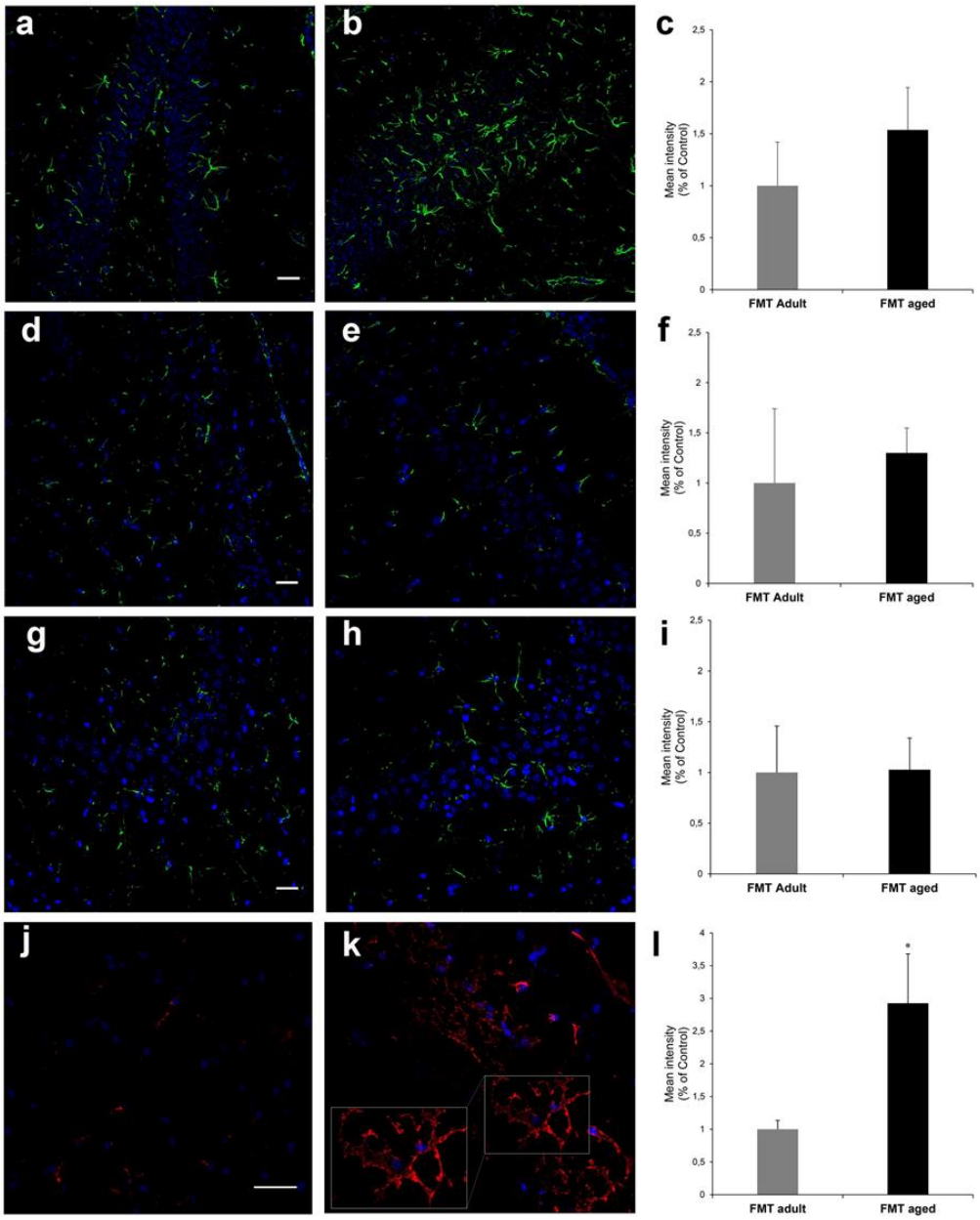

Figure 11. Levels of <u>GFAP and F4/80 in hippocampal areas</u>. Representative images acquired at the confocal microscope with anti-GFAP antibody (green) and the mean fluorescent intensity in different areas of the hippocampus (a–i). No difference was observed between FMT-adult (left panels a, d and g) and FMT-aged (middle panels b, e and h) in the expression of GFAP. The analysis was carried out in the dentate gyrus region (a, b, fluorescent intensity shown in c), CA4 region (d, e, fluorescent intensity shown in f) and CA3 region (g–I, fluorescent intensity shown in i). On the contrary, a significant increase of the expression of F4/80 (red) (j, k, fluorescent intensity shown in l) was observed in the white matter of the hippocampus fimbria between FMT-adult (j) and FMT-aged mice (k). Fluorescence intensity bars represent the mean ± SEM from 3 mice/group and asterisk indicates P = 0.0168. Nuclei have been counterstained with ToPro-3 (in blue). (Scale bars=30 µm).

We also analysed cytokines levels in the hippocampus of mice after FMT experiments (Fig. 12). In particular, we evaluated five cytokines (IL-12p70, IL-4, TNFα, IL-23, IL-9)in the hippocampus of FMT-aged and FMT-adult mice without any significant difference in their level of expression. All these results supported the absence of an overt FMT-induced neuroinflammation in adult mice at least at the time point tested.

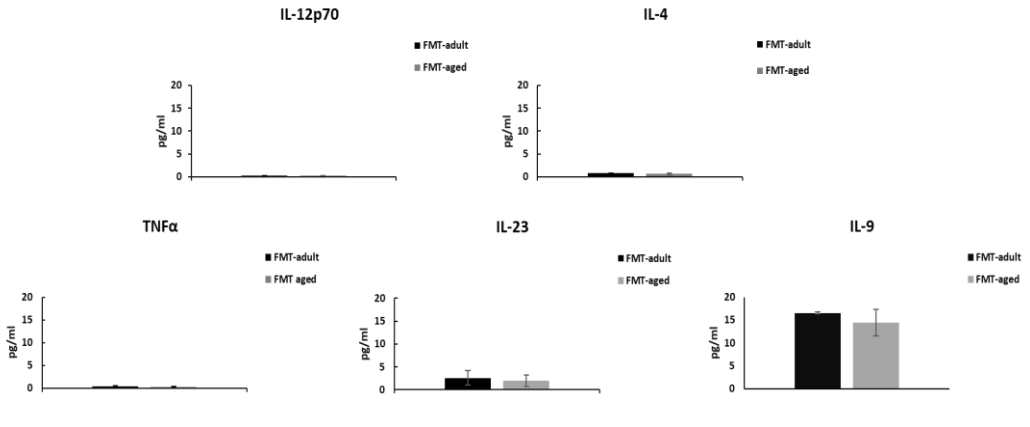

Figure 12. **<u>Cytokines levels in the hippocampi.</u>** Cytokines levels were evaluated in the hippocampi of FMT-aged mice and FMT-adult mice. We detected no difference in the levels of the cytokines tested. Bars represent the mean ± SEM (n = 8 mice/group).

3.1.5. Effect of faecal microbial transplant on protein expression in colon of adult mice

In order to get a better insight in the molecular mechanisms behind the changes observed in both behavioural tests and in proteomics of the hippocampus, we applied the one-shot label-free quantitative proteomics method on colon samples. Since mice were subjected to FMT, it is crucial to understand changes in the colon that could precede the modifications observed in the brain. The obtained whole protein extract resulted in 2389 quantified proteins. The volcano plot was obtained by two-sided *t* test of the two groups: FMT-aged versus FMT-adult mice (Fig. 13).

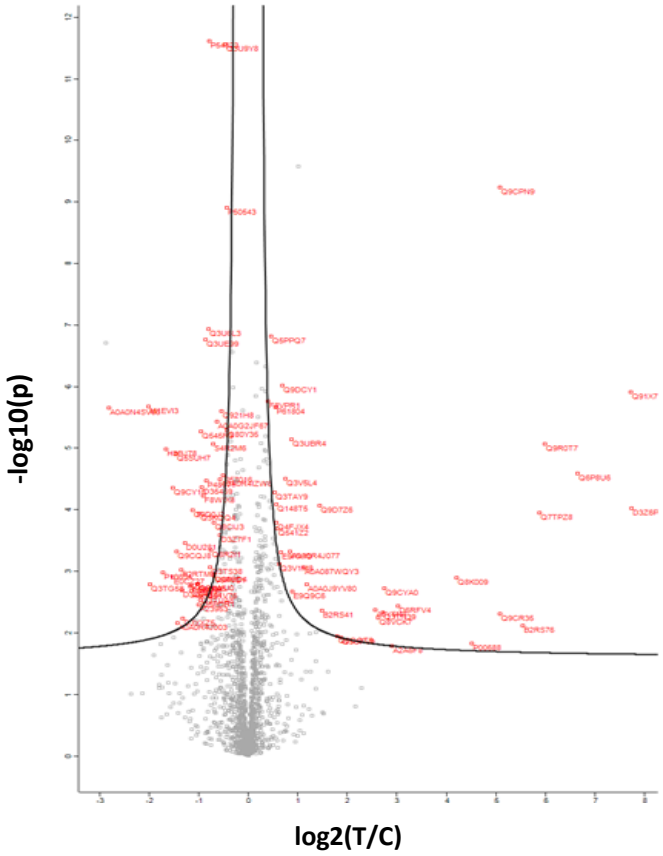

Figure 13. **Volcano plot in colon.** Quantitative analysis of proteins in the colon. Plot of quantified proteins in colon tissue. Differentially regulated proteins after transplant of aged faeces into adult mice (T) versus faeces from adult mice transplanted into adult age-matched mice (C) are showed (T/C).

Among the top ten up-regulated proteins (Table 2) the one showing the highest rate of protein expression increase was protein disulphide-isomerase (PDI) A2 (PDIA2). PDIA2 was 10.5-fold more expressed in the colon of mice transplanted with faeces from aged animals compared to controls. PDIA2 is a disulphide isomerase involved cell redox homeostasis, protein folding and retention in endoplasmic reticulum lumen. Carboxypeptidase B1 (CPB1) and A1 (CPA1) were also over-expressed (8.1 and 7.3-fold respectively) in FMT-aged mice. These proteins are well-known proteolytic enzymes. Chymotrypsin-like elastase family member 1 (CELA1) is 8.1-fold more expressed in colon of FMT-aged mice compared to FMT-adult animals. CELA1 has different functions such as hydrolase activity, metal ion binding, and peptidase activity. It is implicated in digestive system development, elastin catabolic processes, inflammatory response. Among the down-regulated proteins (Table 3) Prostaglandin E synthase 2 (PTGES2) was the one with the highest rate of decrease in expression levels (3.7-fold down-regulated) in the colon of FMT-aged mice. Map2k1, in turn, was 3.3-fold down-regulated and it is involved in several different functions including apoptosis, cell cycle progression and proliferation. Vasoactive intestinal peptide (VIP), on the other hand, was 3.2-fold down-regulated in mice transplanted with aged faeces. VIP is produced and released by some enteroendocrine cells and it is also expressed in fibres of the autonomous nervous system.

Expr Log Ratio up-regulated

Molecules	Expr. Value
PDIA2	↑ 10.512
CPB1	↑ 8.147
CELA1	↑ 8.112
CPA1	↑ 7.391
CTRB2	↑ 6.731
PRSS3	↑ 6.339
ALDH1L2	↑ 4.887
SEC11C	↑ 4.868
CRELD2	↑ 4.329
2210010C04Rik	↑ 4.178

Table 2. <u>The top ten up-regulated proteins in colon.</u> Expression protein levels in colon of mice transplanted with faeces from aged animals compared to mice transplanted with adult faeces.

Expr Log Ratio down-regulated	
Molecules	Expr. Value
PTGES2	-3.729
MAP2K1	-3.300
VIP	-3.219
CARHSP1	-3.125
DCPS	-3.074
RBM47	-2.920
DYNLL1	-2.479
NDUFB9	-2.432
ARF5	-2.352
CHGB	-2.304

Table 3. The top ten down-regulated proteins in colon. Expression protein levels in colon of mice transplanted with faeces from aged animals compared to mice transplanted with adult faeces.

The IPA showed a different regulation of some pathways in the colon of FMT-aged mice compared to the colon of FMT-adult mice. The IPA showed that some of the pathways were up-regulated, including LPS/IL-1 mediated inhibition of RXR function, EIF2 signaling, integrin signaling, paxillin signaling, actin cytoskeleton signaling and integrin-linked kinase (ILK) signalling. Other pathways were down-regulated like remodelling of epithelial adherens junctions, peroxisome proliferator-activated receptor (PPAR)α (PPARα)/retinoid X receptor a (RXRa) activation and fMLP signaling (Fig. 14).

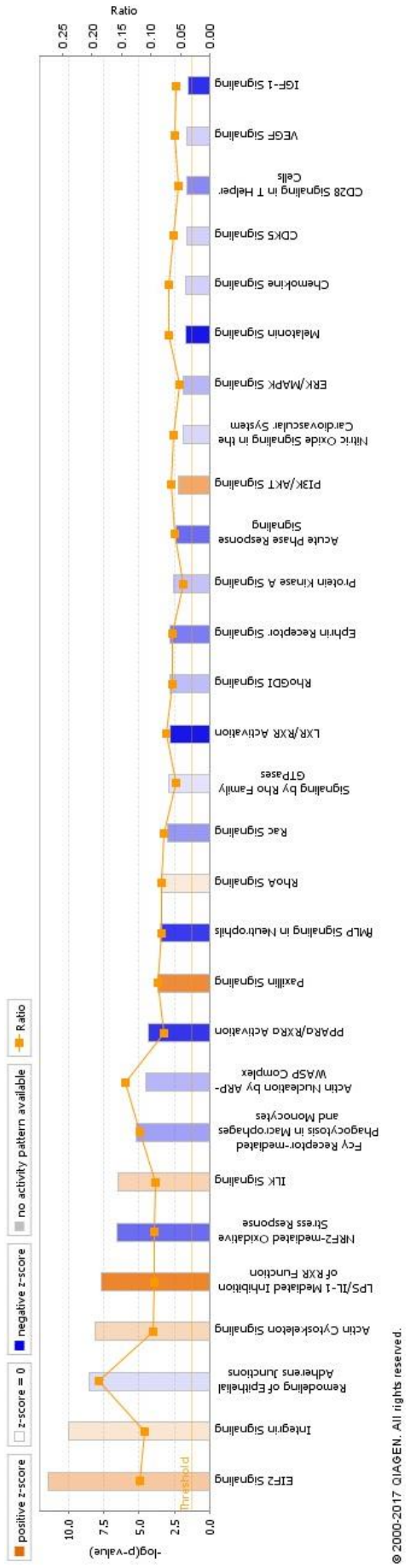

Figure 14. <u>Canonical pathways.</u> Analysis of differentially regulated pathways in colon.

Twenty-six molecules were associated with the EIF2 signaling (Table 4). The majority of these molecules were cytoplasmatic whereas five molecules were nuclear proteins. Twenty-three molecules were up-regulated and three were down-regulated. Though heat shock protein family A member 5 and tryptophanyl-t RNA synthetase were expected to be down-regulated, they were actually found up-regulated. In contrast, mitogen activated protein kinase 1 and 3, expected to be up-regulated, were actually found down-regulated. Overall, the EIF2 signaling was up-regulated.

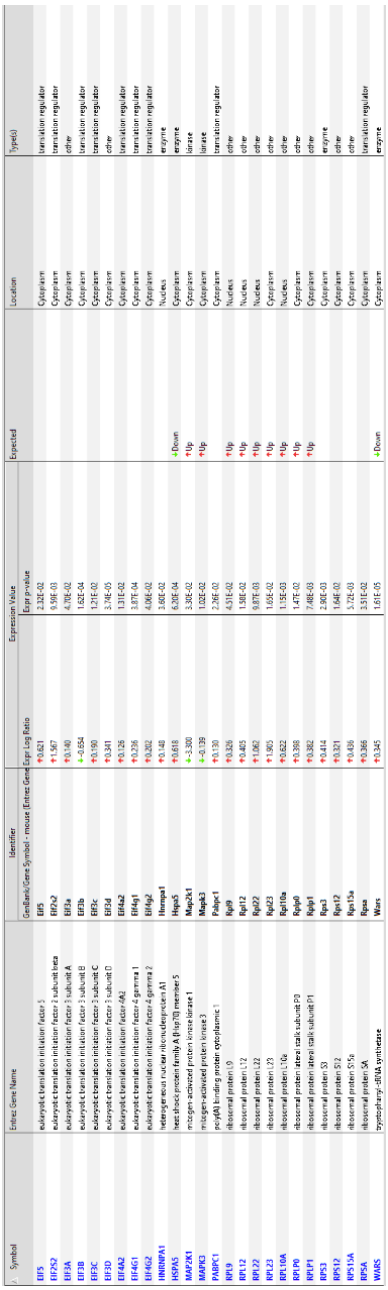

Symbol	Identifier: Entrez Gene Name	Identifier: GenBank/Gene Symbol - mouse (Entrez Gene)	Expression Value: Expr Log Ratio	Expression Value: Expr p-value	Expected	Location	Type(s)
EIF5	eukaryotic translation initiation factor 5	Eif5	+0.621	2.32E-02		Cytoplasm	translation regulator
EIF2S2	eukaryotic translation initiation factor 2 subunit beta	Eif2s2	+1.567	9.59E-03		Cytoplasm	translation regulator
EIF3A	eukaryotic translation initiation factor 3 subunit A	Eif3a	+0.140	4.70E-02		Cytoplasm	other
EIF3B	eukaryotic translation initiation factor 3 subunit B	Eif3b	+-0.654	1.62E-04		Cytoplasm	translation regulator
EIF3C	eukaryotic translation initiation factor 3 subunit C	Eif3c	+0.190	1.21E-02		Cytoplasm	translation regulator
EIF3D	eukaryotic translation initiation factor 3 subunit D	Eif3d	+0.341	3.74E-05		Cytoplasm	other
EIF4A2	eukaryotic translation initiation factor 4A2	Eif4a2	+0.126	1.31E-02		Cytoplasm	translation regulator
EIF4G1	eukaryotic translation initiation factor 4 gamma 1	Eif4g1	+0.236	1.87E-04		Cytoplasm	translation regulator
EIF4G2	eukaryotic translation initiation factor 4 gamma 2	Eif4g2	+0.202	4.06E-02		Cytoplasm	translation regulator
HNRNPA1	heterogeneous nuclear ribonucleoprotein A1	Hnrnpa1	+0.148	3.66E-02		Nucleus	enzyme
HSPA5	heat shock protein family A (Hsp70) member 5	Hspa5	+0.818	6.20E-04	+Down	Cytoplasm	enzyme
MAP2K1	mitogen-activated protein kinase kinase 1	Map2k1	+-3.300	3.30E-02	+Up	Cytoplasm	kinase
MAPK3	mitogen-activated protein kinase 3	Mapk3	+-0.139	1.02E-02	+Up	Cytoplasm	kinase
PABPC1	polyA(A) binding protein cytoplasmic 1	Pabpc1	+0.130	2.76E-02		Cytoplasm	translation regulator
RPL9	ribosomal protein L9	Rpl9	+0.326	4.51E-02	+Up	Nucleus	other
RPL12	ribosomal protein L12	Rpl12	+0.405	1.58E-02	+Up	Nucleus	other
RPL22	ribosomal protein L22	Rpl22	+1.062	9.87E-03	+Up	Nucleus	other
RPL23	ribosomal protein L23	Rpl23	+1.065	1.65E-02	+Up	Cytoplasm	other
RPL10A	ribosomal protein L10a	Rpl10a	+0.622	1.15E-03	+Up	Nucleus	other
RPLP0	ribosomal protein lateral stalk subunit P0	Rplp0	+0.388	1.47E-02	+Up	Cytoplasm	other
RPLP1	ribosomal protein lateral stalk subunit P1	Rplp1	+0.382	2.46E-03	+Up	Cytoplasm	other
RPS3	ribosomal protein S3	Rps3	+0.414	2.30E-03		Cytoplasm	enzyme
RPS12	ribosomal protein S12	Rps12	+0.331	1.64E-02		Cytoplasm	other
RPS15A	ribosomal protein S15a	Rps15a	+0.436	1.72E-03		Cytoplasm	other
RPSA	ribosomal protein SA	Rpsa	+0.366	3.31E-02		Cytoplasm	translation regulator
WARS	tryptophanyl-tRNA synthetase	Wars	+0.345	1.61E-05	+Down	Cytoplasm	enzyme

Table 4. <u>EIF2 signaling.</u> Analysis of molecules involved in the EIF2 signaling.

As for the EIF2 signaling, also the integrin signaling (Table 5) was up-regulated in the colon of adult mice transplanted with aged faeces. Twenty-four proteins were associated with the integrin signaling. Fourteen of them had a cytoplasmic localization, eight were plasma membrane-associated proteins, one had a nuclear localization and one was referred to the extracellular space. Eleven molecules were up-regulated and thirteen were down-regulated.

Symbol	Entrez Gene Name	Identifier		Expression Value		Expected	Location	Type(s)
		GenBank/Gene Symbol - mouse (Entrez Gene)	Expr Log Ratio	Expr p-value				
ACTN1	actinin alpha 1	Actn1	+0.237	4.48E-03	+Up	Cytoplasm	transcription regulator
ACTN4	actinin alpha 4	Actn4	+0.204	9.89E-03	+Up	Cytoplasm	transcription regulator
ACTR2	ARP2 actin related protein 2 homolog	Actr2	+0.165	5.86E-03	+Up	Plasma Membrane	other
ACTR3	ARP3 actin related protein 3 homolog	Actr3	-0.092	4.91E-03	+Up	Plasma Membrane	other
ARF1	ADP ribosylation factor 1	Arf1	-0.061	4.54E-02	-Down	Cytoplasm	enzyme
ARF5	ADP ribosylation factor 5	Arf5	-2.352	1.53E-02	-Down	Cytoplasm	enzyme
ARF6	ADP ribosylation factor 6	Arf6	+0.093	3.55E-02	-Down	Plasma Membrane	transporter
ARPC2	actin related protein 2/3 complex subunit 2	Arpc2	-0.221	1.19E-03	+Up	Cytoplasm	other
ARPC4	actin related protein 2/3 complex subunit 4	Arpc4	-0.192	8.63E-05	+Up	Cytoplasm	other
ARPC5	actin related protein 2/3 complex subunit 5	Arpc5	+0.221	5.60E-04	+Up	Cytoplasm	other
ARPC1B	actin related protein 2/3 complex subunit 1B	Arpc1b	-0.254	1.58E-05	+Up	Cytoplasm	other
CAPNS1	calpain small subunit 1	Capns1	-0.555	3.23E-05	+Up	Cytoplasm	peptidase
GSN	gelsolin	Gsn	+0.161	4.48E-02		Extracellular Space	other
ITGB1	integrin subunit beta 1	Itgb1	+0.125	4.03E-02	+Up	Plasma Membrane	transmembrane receptor
ITGB4	integrin subunit beta 4	Itgb4	-0.442	5.18E-03	+Up	Plasma Membrane	transmembrane receptor
MAP2K1	mitogen-activated protein kinase kinase 1	Map2k1	-3.300	3.30E-02	+Up	Cytoplasm	kinase
MAPK3	mitogen-activated protein kinase 3	Mapk3	-0.139	1.02E-02	+Up	Cytoplasm	kinase
MYLK	myosin light chain kinase	Mylk	+0.174	4.26E-02	+Up	Cytoplasm	kinase
PARVA	parvin alpha	Parva	+0.347	6.41E-06	+Up	Cytoplasm	other
Ppp1r12b	protein phosphatase 1, regulatory (inhibitor) subunit 12B	Ppp1r12b	-0.825	2.08E-03		Cytoplasm	other
TLN1	talin 1	Tln1	+0.287	9.70E-04	+Up	Plasma Membrane	other
TLN2	talin 2	Tln2	-0.206	2.50E-05	+Up	Nucleus	other
VASP	vasodilator-stimulated phosphoprotein	Vasp	-0.173	2.92E-03	-Down	Plasma Membrane	other
VCL	vinculin	Vcl	+0.198	1.33E-03	+Up	Plasma Membrane	enzyme

Table 5. <u>Integrin signaling.</u> Analysis of molecules involved in the integrin signaling.

The paxillin signaling (Table 6) and the actin cytoskeleton signaling (Table 7) were both up-regulated pathways. Ten molecules were associated with the paxillin signaling and 22 proteins with the actin cytoskeleton signaling. Five proteins of the paxillin signaling pathway were associated with plasma membrane, four had a cytoplasmic localization and one had a nuclear localization. Seven proteins out of ten were up regulated. Twelve proteins of the actin cytoskeleton signaling pathway had a cytoplasmic localization, six were plasma membrane proteins, three were referred to the extracellular space and one was a nuclear protein. Twelve molecules out of 22 were up-regulated.

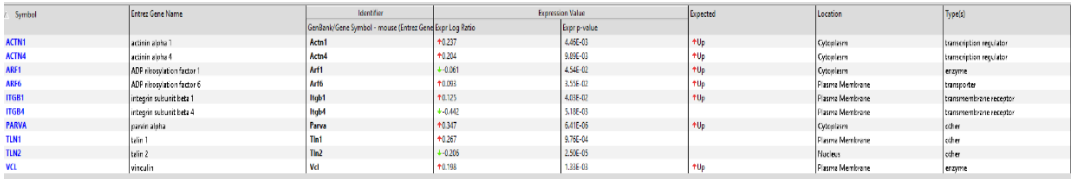

Symbol	Entrez Gene Name	Identifier	Expression Value		Expected	Location	Type(s)
		GenBank/Gene Symbol - mouse (Entrez Gene)	Expr Log Ratio	Expr p-value			
ACTN1	actinin alpha 1	Actn1	↑0.237	4.46E-03	↑Up	Cytoplasm	transcription regulator
ACTN4	actinin alpha 4	Actn4	↑0.204	9.89E-03	↑Up	Cytoplasm	transcription regulator
ARF1	ADP ribosylation factor 1	Arf1	↓-0.061	4.54E-02	↑Up	Cytoplasm	enzyme
ARF6	ADP ribosylation factor 6	Arf6	↑0.093	3.55E-02	↑Up	Plasma Membrane	transporter
ITGB1	integrin subunit beta 1	Itgb1	↑0.125	4.03E-02	↑Up	Plasma Membrane	transmembrane receptor
ITGB4	integrin subunit beta 4	Itgb4	↓-0.442	5.10E-03		Plasma Membrane	transmembrane receptor
PARVA	parvin alpha	Parva	↑0.347	6.41E-06	↑Up	Cytoplasm	other
TLN1	talin 1	Tln1	↑0.267	9.79E-04		Plasma Membrane	other
TLN2	talin 2	Tln2	↓-0.206	2.59E-05		Nucleus	other
VCL	vinculin	Vcl	↑0.198	1.33E-03	↑Up	Plasma Membrane	enzyme

Table 6. <u>Paxillin signaling.</u> Analysis of molecules involved in the paxillin signaling.

Symbol	Entrez Gene Name	Identifier	Expression Value		Expected	Location	Type(s)
		GenBank/Gene Symbol - mouse (Entrez Gene	Expr Log Ratio	Expr p-value			
ACTN1	actinin alpha 1	Actn1	↑0.237	4.46E-03	↑Up	Cytoplasm	transcription regulator
ACTN4	actinin alpha 4	Actn4	↑0.204	9.89E-03	↑Up	Cytoplasm	transcription regulator
ACTR2	ARP2 actin related protein 2 homolog	Actr2	↑0.165	5.60E-03	↑Up	Plasma Membrane	other
ACTR3	ARP3 actin related protein 3 homolog	Actr3	↓-0.092	4.91E-03	↑Up	Plasma Membrane	other
ARPC2	actin related protein 2/3 complex subunit 2	Arpc2	↓-0.221	1.19E-03	↑Up	Cytoplasm	other
ARPC4	actin related protein 2/3 complex subunit 4	Arpc4	↓-0.192	8.63E-05	↑Up	Cytoplasm	other
ARPC5	actin related protein 2/3 complex subunit 5	Arpc5	↑0.221	5.60E-04	↑Up	Cytoplasm	other
ARPC1B	actin related protein 2/3 complex subunit 1B	Arpc1b	↓-0.254	1.56E-05	↑Up	Cytoplasm	other
FLNA	filamin A	Flna	↑0.356	3.12E-04	↑Up	Cytoplasm	other
FN1	fibronectin 1	Fn1	↑0.281	6.69E-04	↑Up	Extracellular Space	enzyme
GSN	gelsolin	Gsn	↑0.161	4.48E-02	↓Down	Extracellular Space	other
ITGB1	integrin subunit beta 1	Itgb1	↑0.125	4.03E-02	↑Up	Plasma Membrane	transmembrane receptor
MAP2K1	mitogen-activated protein kinase kinase 1	Map2k1	↓-3.300	3.30E-02	↑Up	Cytoplasm	kinase
MAPK3	mitogen-activated protein kinase 3	Mapk3	↓-0.139	1.02E-02	↑Up	Cytoplasm	kinase
MSN	moesin	Msn	↑0.155	1.54E-03	↑Up	Plasma Membrane	other
MYH14	myosin heavy chain 14	Myh14	↓-0.161	3.04E-03	↑Up	Extracellular Space	enzyme
MYL6	myosin light chain 6	Myl6	↑0.196	4.82E-02	↑Up	Cytoplasm	enzyme
MYLK	myosin light chain kinase	Mylk	↑0.174	4.26E-02		Cytoplasm	kinase
Ppp1r12b	protein phosphatase 1, regulatory (inhibitor) subunit 12B	Ppp1r12b	↓-0.825	2.08E-03	↓Down	Cytoplasm	other
TLN1	talin 1	Tln1	↑0.267	9.76E-04	↑Up	Plasma Membrane	other
TLN2	talin 2	Tln2	↓-0.206	2.50E-05	↑Up	Nucleus	other
VCL	vinculin	Vcl	↑0.198	1.33E-03	↑Up	Plasma Membrane	enzyme

Table 7. <u>Actin cytoskeleton signaling.</u> Analysis of molecules involved in the actin cytoskeleton signaling.

Two other pathways that activate in response to pro inflammatory cytokines were found up-regulated: the LPS/IL-1 mediated inhibition of RXR function (Table 8) and the ILK signaling pathway (Table 9). Twenty-one proteins were associated with the LPS/IL-1 mediated inhibition of RXR function and 18 with the ILK signaling pathway. In the LPS/IL-1 mediated inhibition of RXR function all but one of the identified molecules had a cytoplasmic localization. The only protein which was not cytoplasmic had a nuclear localization. Eleven identified molecules belonging to the ILK signaling had a cytoplasmic localization, 5 were plasma membrane-associated proteins and 2 were referred to the extracellular space.

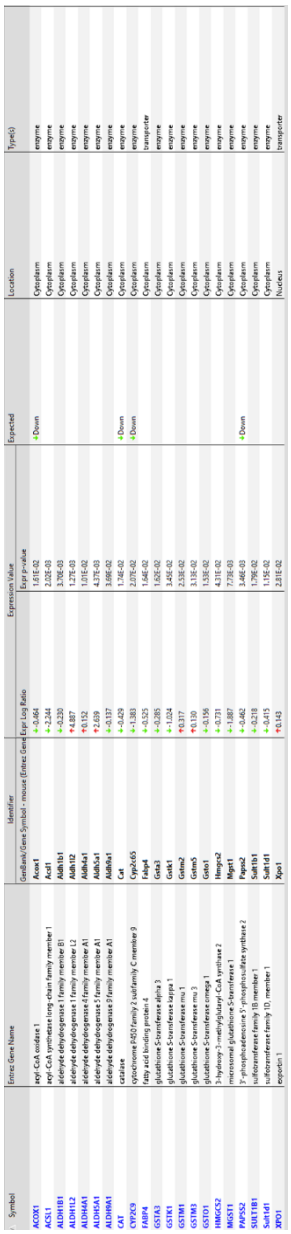

Symbol	Entrez Gene Name	Identifier	Expression Value		Expected	Location	Type(s)
		GenBank|Gene Symbol - mouse (Entrez Gene)	Expr Log Ratio	Expr p-value			
ACOX1	acyl-CoA oxidase 1	Acox1	-0.464	1.61E-02	Down	Cytoplasm	enzyme
ACSL1	acyl-CoA synthetase long-chain family member 1	Acsl1	-2.244	2.02E-03		Cytoplasm	enzyme
ALDH1B1	aldehyde dehydrogenase 1 family member B1	Aldh1b1	-0.230	3.70E-03		Cytoplasm	enzyme
ALDH1L2	aldehyde dehydrogenase 1 family member L2	Aldh1l2	4.887	1.27E-03		Cytoplasm	enzyme
ALDH4A1	aldehyde dehydrogenase 4 family member A1	Aldh4a1	0.152	1.01E-02		Cytoplasm	enzyme
ALDH5A1	aldehyde dehydrogenase 5 family member A1	Aldh5a1	-0.439	4.23E-03		Cytoplasm	enzyme
ALDH6A1	aldehyde dehydrogenase 6 family member A1	Aldh6a1	-0.337	3.98E-02		Cytoplasm	enzyme
CAT	catalase	Cat	-0.429	1.74E-02	Down	Cytoplasm	enzyme
CYP2C9	cytochrome P450 family 2 subfamily C member 9	Cyp2c65	-1.383	2.07E-02	Down	Cytoplasm	enzyme
FABP4	fatty acid binding protein 4	Fabp4	-0.525	1.64E-02		Cytoplasm	transporter
GSTA3	glutathione S-transferase alpha 3	Gsta3	-0.285	1.62E-02		Cytoplasm	enzyme
GSTK1	glutathione S-transferase kappa 1	Gstk1	-1.024	3.49E-02		Cytoplasm	enzyme
GSTM1	glutathione S-transferase mu 1	Gstm2	0.317	2.53E-02		Cytoplasm	enzyme
GSTM3	glutathione S-transferase mu 3	Gstm3	0.103	3.13E-02		Cytoplasm	enzyme
GSTO1	glutathione S-transferase omega 1	Gsto1	-0.156	1.53E-02		Cytoplasm	enzyme
HMGCS2	3-hydroxy-3-methylglutaryl-CoA synthase 2	Hmgcs2	-0.731	4.31E-02		Cytoplasm	enzyme
MGST1	microsomal glutathione S-transferase 1	Mgst1	-1.887	7.73E-03		Cytoplasm	enzyme
PAPSS2	3'-phosphoadenosine 5'-phosphosulfate synthase 2	Papss2	-0.482	3.46E-03	Down	Cytoplasm	enzyme
SULT1B1	sulfotransferase family 1B member 1	Sult1b1	-0.218	1.79E-02		Cytoplasm	enzyme
Sult1d1	sulfotransferase family 1D, member 1	Sult1d1	-0.415	1.15E-02		Cytoplasm	enzyme
XPO1	exportin 1	Xpo1	0.145	2.81E-02		Nucleus	transporter

Table 8. <u>LPS/IL-1 mediated inhibition of RXR Function.</u> Analysis of molecules involved in the LPS/IL-1 mediated inhibition of RXR function signaling.

Symbol	Entrez Gene Name	Identifier	Expression Value		Expected	Location	Type(s)
		GenBank/Gene Symbol - mouse (Entrez Gene	Expr Log Ratio	Expr p-value			
ACTN1	actinin alpha 1	**Actn1**	↑0.237	4.46E-03	↑Up	Cytoplasm	transcription regulator
ACTN4	actinin alpha 4	**Actn4**	↑0.204	9.89E-03	↑Up	Cytoplasm	transcription regulator
CDH1	cadherin 1	**Cdh1**	↑0.135	2.08E-03	↑Up	Plasma Membrane	other
DSP	desmoplakin	**Dsp**	↓-0.125	9.73E-03		Plasma Membrane	other
FERMT2	fermitin family member 2	**Fermt2**	↑0.352	4.73E-07	↑Up	Cytoplasm	other
FLNA	filamin A	**Flna**	↑0.356	3.12E-04	↓Down	Cytoplasm	other
FLNB	filamin B	**Flnb**	↑0.089	3.67E-02	↓Down	Cytoplasm	other
FLNC	filamin C	**Flnc**	↑0.592	7.70E-04	↓Down	Cytoplasm	other
FN1	fibronectin 1	**Fn1**	↑0.281	6.69E-04	↑Up	Extracellular Space	enzyme
ITGB1	integrin subunit beta 1	**Itgb1**	↑0.125	4.03E-02	↑Up	Plasma Membrane	transmembrane receptor
ITGB4	integrin subunit beta 4	**Itgb4**	↓-0.442	5.18E-03	↑Up	Plasma Membrane	transmembrane receptor
MAPK3	mitogen-activated protein kinase 3	**Mapk3**	↓-0.139	1.02E-02	↑Up	Cytoplasm	kinase
MYH14	myosin heavy chain 14	**Myh14**	↓-0.161	3.04E-03	↑Up	Extracellular Space	enzyme
MYL6	myosin light chain 6	**Myl6**	↑0.196	4.62E-02	↑Up	Cytoplasm	enzyme
NACA	nascent polypeptide-associated complex alpha subunit	**Naca**	↑0.221	1.01E-03	↑Up	Cytoplasm	transcription regulator
PARVA	parvin alpha	**Parva**	↑0.347	6.41E-06	↑Up	Cytoplasm	other
PPP2R1A	protein phosphatase 2 scaffold subunit Aalpha	**Ppp2r1a**	↓-0.159	1.18E-04	↓Down	Cytoplasm	phosphatase
VCL	vinculin	**Vcl**	↑0.198	1.33E-03	↓Down	Plasma Membrane	enzyme

Table 9. <u>ILK signaling.</u> Analysis of molecules involved in the ILK signaling.

Some pathways were found down-regulated in the colon of FMT-aged mice. One of these was the remodelling of epithelial adherens junctions (Table 10). Thirteen molecules were associated with this pathway: eight of them were cytoplasmic proteins whereas the other 5 were associated with the plasma membrane. Finally, two other pathways that are activated in response to IL-1 were also down-regulated: the PPARα/RXRa (Table 11) and the fMLP signaling (Table 12). The proteins found associated with these pathways were 14 and 10 respectively. With the exception of one plasma membrane-associated protein and one protein referred to the extracellular space, all molecules associated with the PPARα/RXRa pathway had a cytoplasmic localization. As for the fMLP signaling pathway, 7 molecules were cytoplasmatic and three were plasma membrane-associated. All the proteins associated with this pathway were expected to be up-regulated but only two out of ten were found actually up-regulated.

Symbol	Entrez Gene Name	Identifier	Expression Value		Expected	Location	Type(s)
		GenBank/Gene Symbol - mouse (Entrez Gene	Expr Log Ratio	Expr p-value			
ACTN1	actinin alpha 1	Actn1	↑0.237	4.46E-03		Cytoplasm	transcription regulator
ACTN4	actinin alpha 4	Actn4	↑0.204	9.89E-03		Cytoplasm	transcription regulator
ACTR2	ARP2 actin related protein 2 homolog	Actr2	↑0.165	5.60E-03	↑Up	Plasma Membrane	other
ACTR3	ARP3 actin related protein 3 homolog	Actr3	↓-0.092	4.91E-03	↑Up	Plasma Membrane	other
ARF6	ADP ribosylation factor 6	Arf6	↑0.093	3.55E-02	↑Up	Plasma Membrane	transporter
ARPC2	actin related protein 2/3 complex subunit 2	Arpc2	↓-0.221	1.19E-03	↑Up	Cytoplasm	other
ARPC4	actin related protein 2/3 complex subunit 4	Arpc4	↓-0.192	8.63E-05	↑Up	Cytoplasm	other
ARPC5	actin related protein 2/3 complex subunit 5	Arpc5	↑0.221	5.60E-04	↑Up	Cytoplasm	other
ARPC1B	actin related protein 2/3 complex subunit 1B	Arpc1b	↓-0.254	1.56E-05	↑Up	Cytoplasm	other
CDH1	cadherin 1	Cdh1	↑0.135	2.08E-03	↑Up	Plasma Membrane	other
DNM1L	dynamin 1 like	Dnm1l	↓-0.124	7.31E-03	↑Up	Cytoplasm	enzyme
TUBB	tubulin beta class I	Tubb5	↓-0.251	2.79E-03		Cytoplasm	other
VCL	vinculin	Vcl	↑0.198	1.33E-03		Plasma Membrane	enzyme

Table 10. <u>Remodeling of epithelial adherens junctions.</u> Analysis of molecules involved in the remodeling of epithelial adherens junctions signaling.

Symbol	Entrez Gene Name	Identifier	Expression Value		Expected	Location	Type(s)
		GenBank/Gene Symbol - mouse (Entrez Gene)	Expr Log Ratio	Expr p-value			
ACAA1	acetyl-CoA acyltransferase 1	**Acaa1a**	-0.499	2.53E-06	Up	Cytoplasm	enzyme
ACOX1	acyl-CoA oxidase 1	**Acox1**	-0.464	1.61E-02	Up	Cytoplasm	enzyme
APOA2	apolipoprotein A2	**Apoa2**	-2.216	7.25E-03	Up	Extracellular Space	transporter
CD36	CD36 molecule	**Cd36**	-1.573	1.50E-02	Up	Plasma Membrane	transmembrane receptor
CYP2C9	cytochrome P450 family 2 subfamily C member 9	**Cyp2c65**	-1.383	2.07E-02	Up	Cytoplasm	enzyme
CYP2C18	cytochrome P450 family 2 subfamily C member 18	**Cyp2c55**	-0.685	1.50E-02	Up	Cytoplasm	enzyme
FASN	fatty acid synthase	**Fasn**	-0.428	1.88E-03	Up	Cytoplasm	enzyme
GOT2	glutamic-oxaloacetic transaminase 2	**Got2**	0.187	3.10E-06	Up	Cytoplasm	enzyme
HSP90AA1	heat shock protein 90 alpha family class A member 1	**Hsp90aa1**	0.081	9.42E-03	Down	Cytoplasm	enzyme
HSP90B1	heat shock protein 90 beta family member 1	**Hsp90b1**	0.373	1.51E-05	Down	Cytoplasm	other
MAP2K1	mitogen-activated protein kinase kinase 1	**Map2k1**	-3.300	3.30E-02	Down	Cytoplasm	kinase
MAPK3	mitogen-activated protein kinase 3	**Mapk3**	-0.139	1.02E-02	Down	Cytoplasm	kinase
PLCB3	phospholipase C beta 3	**Plcb3**	-0.217	2.84E-04		Cytoplasm	enzyme
PRKAR2A	protein kinase cAMP-dependent type II regulatory subunit	**Prkar2a**	-0.146	8.80E-03	Up	Cytoplasm	kinase

Table 11. <u>PPARα/RXRa activation.</u> Analysis of molecules involved in the PPARα/RXRa activation signaling.

Symbol	Entrez Gene Name	Identifier	Expression Value		Expected	Location	Type(s)
		GenBank/Gene Symbol - mouse (Entrez Gene	Expr Log Ratio	Expr p-value			
ACTR2	ARP2 actin related protein 2 homolog	Actr2	↑0.165	5.69E-03	↑Up	Plasma Membrane	other
ACTR3	ARP3 actin related protein 3 homolog	Actr3	↓-0.092	4.91E-03	↑Up	Plasma Membrane	other
ARPC2	actin related protein 2/3 complex subunit 2	Arpc2	↓-0.221	1.19E-03	↑Up	Cytoplasm	other
ARPC4	actin related protein 2/3 complex subunit 4	Arpc4	↓-0.192	8.63E-05	↑Up	Cytoplasm	other
ARPC5	actin related protein 2/3 complex subunit 5	Arpc5	↑0.221	5.60E-04	↑Up	Cytoplasm	other
ARPC1B	actin related protein 2/3 complex subunit 1B	Arpc1b	↓-0.254	1.56E-05	↑Up	Cytoplasm	other
GNB1	G protein subunit beta 1	Gnb1	↓-0.546	2.42E-04	↑Up	Plasma Membrane	enzyme
MAP2K1	mitogen-activated protein kinase kinase 1	Map2k1	↓-3.300	3.30E-02	↑Up	Cytoplasm	kinase
MAPK3	mitogen-activated protein kinase 3	Mapk3	↓-0.139	1.02E-02	↑Up	Cytoplasm	kinase
PLCB3	phospholipase C beta 3	Plcb3	↓-0.217	2.64E-04	↑Up	Cytoplasm	enzyme

Table 12. <u>fMLP Signaling.</u> Analysis of molecules involved in the fMLP signaling.

3.1.6. Faecal microbial transplant from aged mice did not induce differences in gut permeability or in levels of local and systemic cytokines

It has been suggested that FMT from aged mice boosts inflammation in young germ-free mice and contribute to the leakage of inflammatory components into the circulation (Fransen et al., 2017). This led us to investigate whether FMT from aged into adult mice could cause an increase in the levels of plasmatic (Fig. 15) and colon (Fig. 16) cytokines and in gut permeability (Fig. 15). Gut permeability was assessed evaluating the plasmatic level of previously orally administered FITC-dextran. We found that FMT from aged mice did not affect gut permeability in adult mice recipients (Fig. 15A). As regards the plasma levels of the cytokines we found no significant differences in the levels of different proinflammatory (IL-1β, IL-6, INF-γ, TNF-α) or anti-inflammatory (IL-10) cytokines (Fig. 15B) in adult mice recipients after FMT from aged mice.

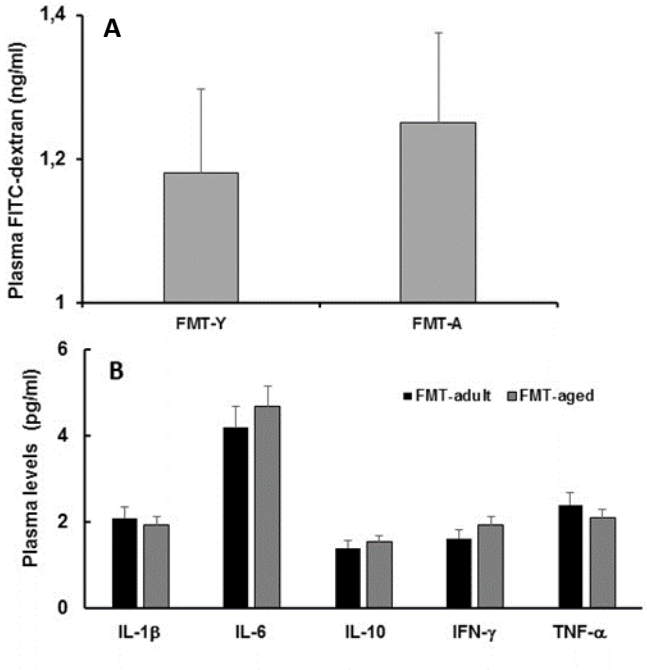

Figure 15. <u>Gut permeability and plasma level of different cytokines</u>. Mice received a FITC-dextran solution and plasma levels of FITC were measured after 3 hours. A) There were no differences in the levels of plasma FITC-dextran between mice transplanted with age-matched faeces (FMT-Y) or with aged faeces (FMT-A). B) No significant differences were observed in the levels of plasma anti- or pro-inflammatory cytokines in both FMT-adult or FMT-aged mice (n = 8 mice/group).

In addition, levels of a large group of cytokines (IL-13, IL-4, IL-22, TNFα, GM-CSF, IL-23, IL-9, MCP-1, MIP-1α) were also tested in protein extracts from colon samples. We found no differences in the concentration of these molecules between the colon of FMT-aged mice and the colon of FMT-adult animals (Fig. 16). All these results supported the absence of an overt FMT-induced inflammation in adult mice after FMT from aged donors at least at the time point tested.

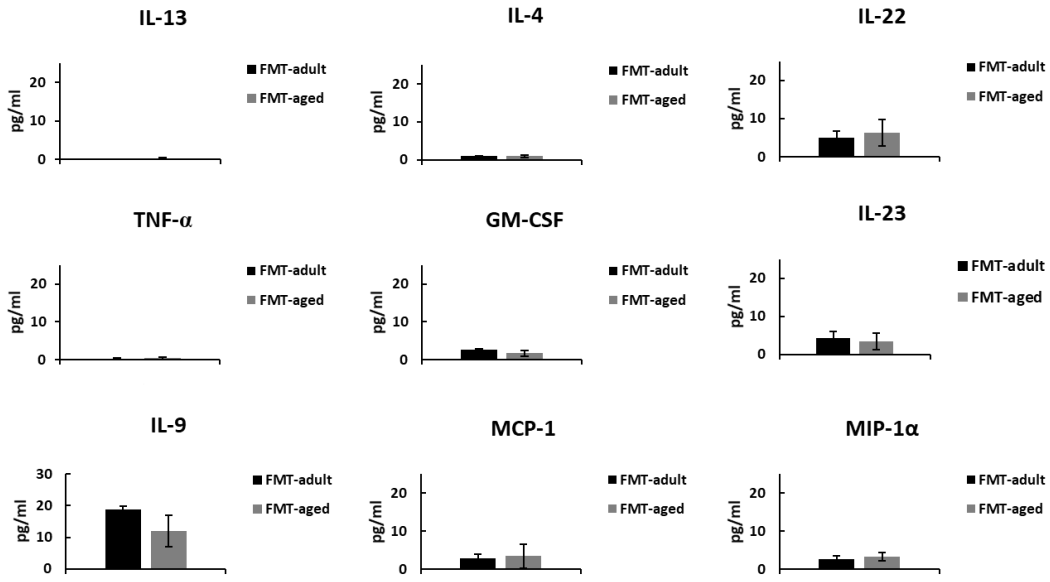

Figure 16. <u>Colon level of different cytokines.</u> Cytokines levels were evaluated in the colon of FMT-aged and FMT-adult mice. We detected no difference in the levels of the cytokines tested. Bars represent the mean ± SEM (n = 8 mice/group).

3.2. Click chemistry

FMT experiments showed that, somehow, a different gut microbiota can induce behavioural changes in mice. In particular, transplant of faeces from aged animals into adult recipients switched the results of some behavioural tests towards those that are typical of older mice. In addition, the same FMT experiments induced a modification in the expression levels of several proteins in the hippocampus. This suggests that some bacterial products could operate as signaling molecules capable of inducing the above-mentioned changes. In order to set up a useful technique to track down bacterial products and to find the paths that they can follow through the host we endeavoured ourselves to chemically modify small bacterial metabolites, to see if they are efficiently incorporated in bacterial cells and, finally, to verify if they can be transferred from bacteria to eukaryotic cells observing their progress within cells.

3.2.1. Optimisation of bacterial growth curve in minimal medium

Click chemistry experiments were performed using *Bacteroidetes thetaiotamicron* (BT) as model organism. First of all, we wanted to optimize BT growth in minimal medium and we tested three different inoculum concentrations in minimal medium (1%, 2% and 5%). To evaluate bacterial growth rate, we measured the optical density (OD) at 600 nm at different time points after the inoculum. As shown in figure 17, we obtained an almost classical growth curve (lag phase, log phase, stationary phase and death phase) for all the concentrations tested. As expected, when bacteria were inoculated in minimal medium at a higher concentration, they grew faster compared to *inocula* at lower concentrations (Fig. 17). For the click chemistry experiments, 1% inoculum was used.

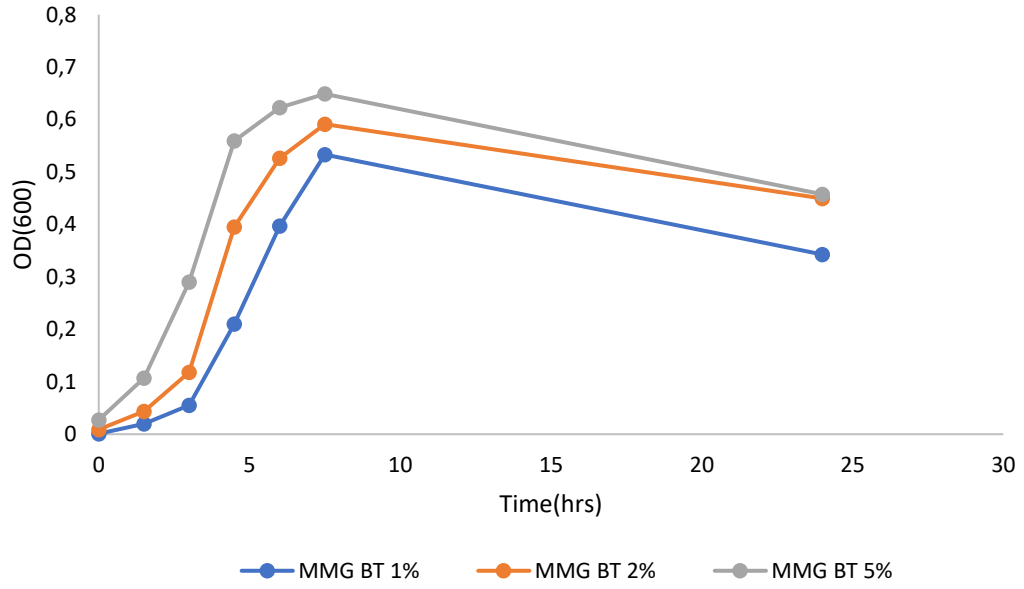

Figure 17. *Bacteroidetes thetaiotamicron* (BT) growth curves in MMG. BT was grown in minimal medium at three different inoculum concentration: 1% (blue), 2% (orange), 5% (grey). Optical density at 600 nm was measured at different time points. BT was able to grow in the minimal medium and at all the concentration tested.

3.2.2. Click chemistry experiments in bacterial cells

After growth curve optimization, we evaluated the incorporation of chemically modified molecules. BT was grown in minimal medium supplemented with PAA or with DMSO as negative control. OD was recorded until bacteria reached a value of 0.4. We chose that level of optical density because it was in the mid-log phase in which the majority of bacteria are metabolically active. Then bacteria were chemically fixed and PAA was fluorescently detected using a commercially available kit (see materials and methods) and an Alexa Fluor 647 azide. Bacterial cells were detected with DAPI. As expected, when bacteria were grown in minimal medium supplemented with DMSO we only detected bacterial cells (Fig. 18A). On the other hand, when they were grown in the presence of PAA, they could be subsequently

labelled by the modified fluorochrome (Fig. 18B). This preliminary experiment demonstrated that bacteria incorporated PAA and that it could be detect in the bacterial cells.

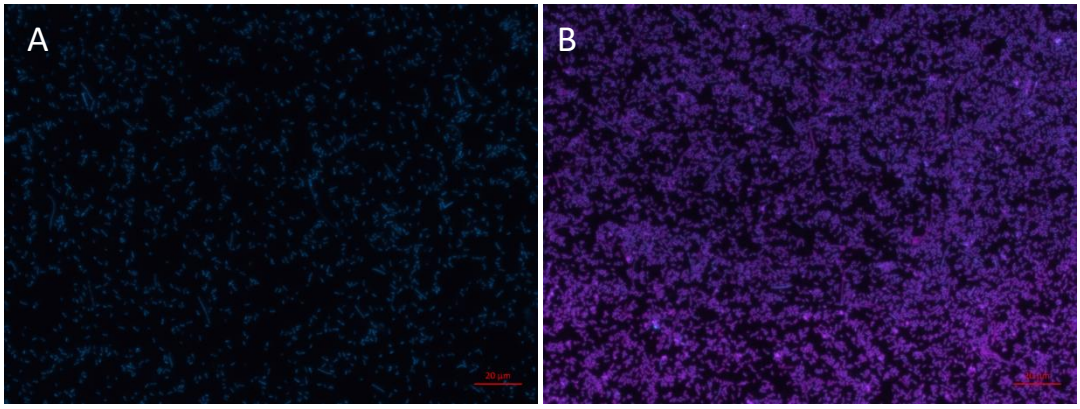

Figure 18. <u>Incorporation of chemically modified molecules in bacterial cells.</u> Fluorescent microscopy images of *Bacteroides thetaiotamicron* grown in minimal medium supplemented with DMSO (A) or with PAA (B). We detected the incorporation of PAA only when bacterial cells were grown in minimal medium supplemented with PAA (B). Bacterial cells were detected with DAPI. (Scale bar 20 µM).

3.2.3. Co-culture experiments

After successfully detecting the presence of PAA in bacterial cells, we tried to co-cultivate bacteria with eukaryotic cell lines. Co-culture experiments were performed to try to evaluate: 1) lipid transfer between bacteria and eukaryotic cells; 2) the ability to detect bacterial molecules in eukaryotic cells. To this aim, BT cells were placed in a transwell system with either Caco-2 intestinal cell line (Fig. 19) or with SK-N-SH neuroblastoma cell line (Figs. 20, 21). In particular, bacteria were placed in the upper chamber and eukaryotic cells in the lower chamber. After 4 hours, cells were fixed and PAA stained using the above-mentioned kit. As expected, when eukaryotic cells were grown without bacteria (Fig. 19A and Fig. 20A) or with bacteria cultivated in minimal medium supplemented with DMSO (Fig. 19B and Fig. 20 B) we didn't detect any fluorescent signal referable to the presence of PAA. When eukaryotic cells lines were co-cultivated with *Bacteroides* grown in minimal medium supplemented with

PAA we successfully detected the presence of PAA in eukaryotic cells (Fig. 19C, Fig. 20C, D and Fig. 21). This experiment demonstrated that a lipid transfer from bacteria to eukaryotic cells is actually possible and that chemically modified lipids can be fluorescently detected in different eukaryotic cell lines.

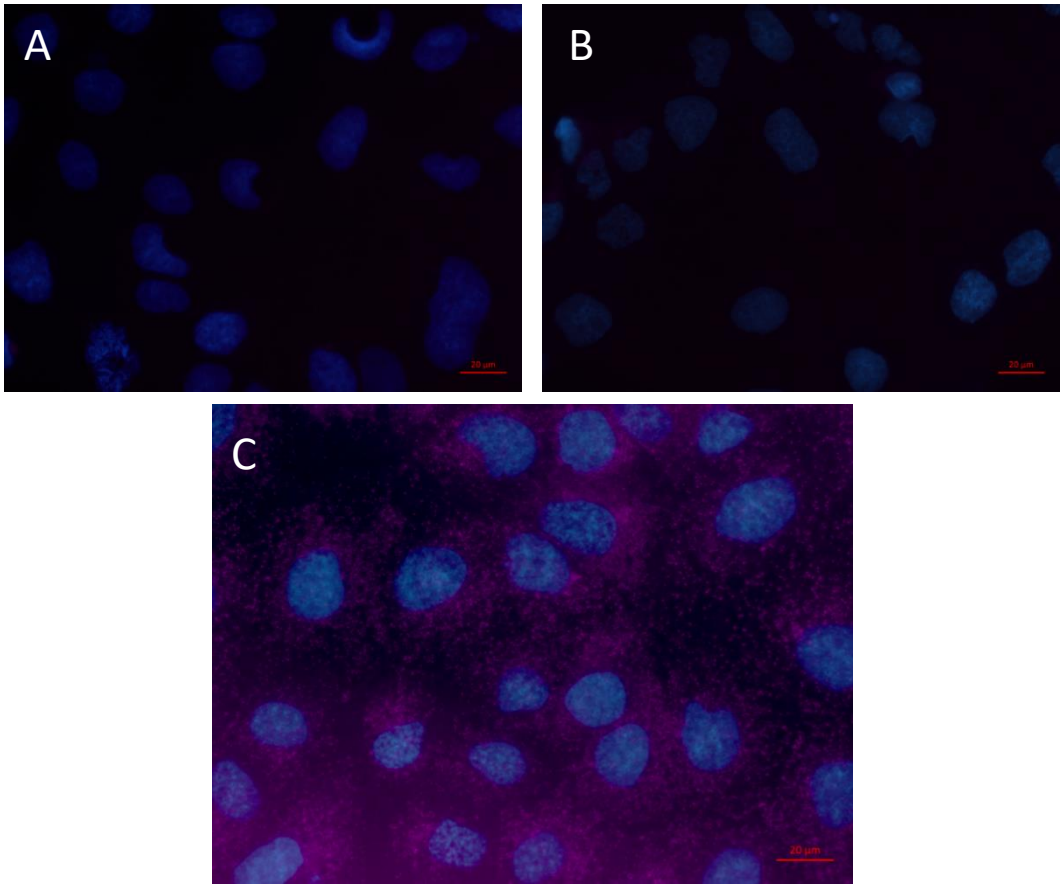

Figure 19. <u>Co-culture experiments.</u> Fluorescent microscopy images of Caco-2 intestinal cell line cultivated without bacteria (A), with bacteria grown in minimal medium either with DMSO (B) or with PAA (C). We detected the presence of PAA only when eukaryotic cells were co-cultivated with bacteria grown in minimal medium supplemented with PAA (C). Cells were detected with DAPI. (Scale bar 20 µM).

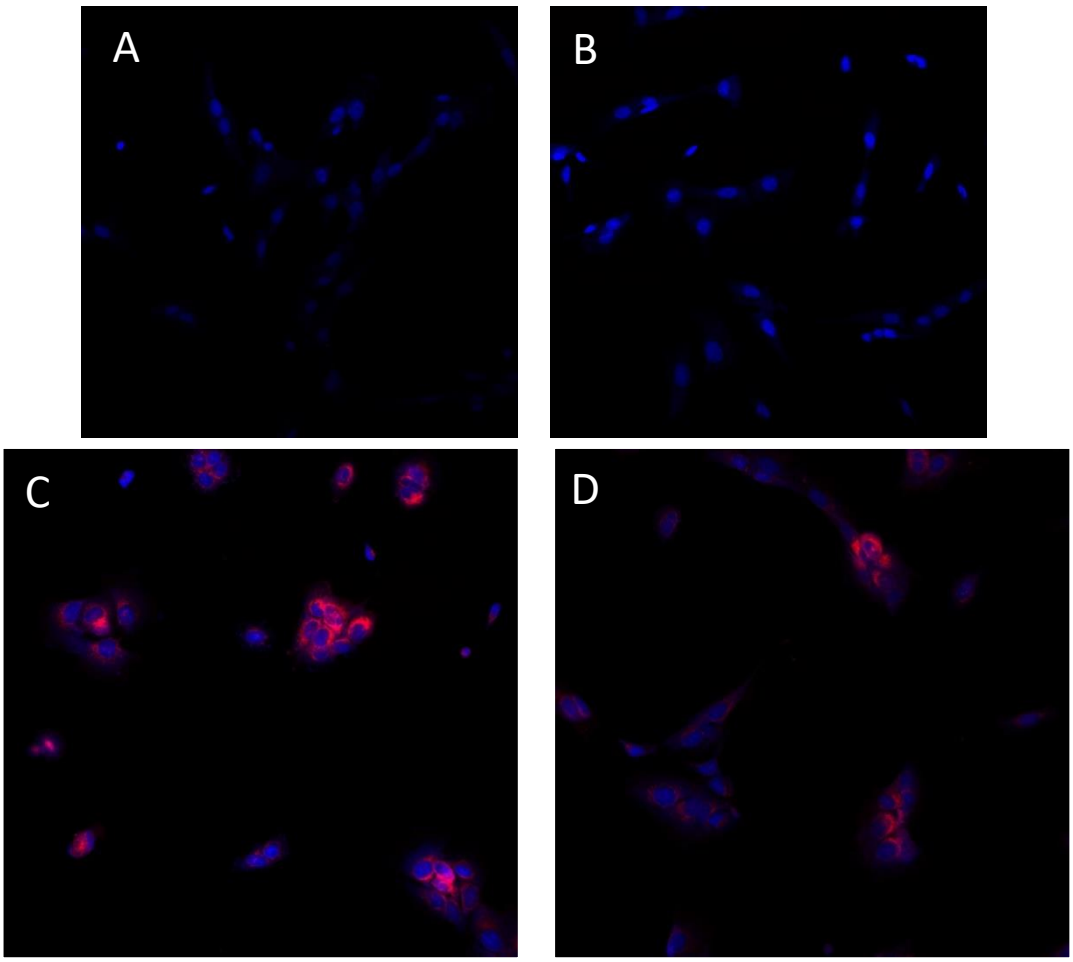

Figure 20. <u>Co-culture experiments.</u> Confocal microscopy images of SK-N-SH neuroblastoma cell line cultivated without bacteria (A), with bacteria grown in minimal medium either with DMSO (B) or with PAA (C and D). We detected the presence of PAA only when eukaryotic cells were co-cultivated with bacteria grown in minimal medium supplemented with PAA (C and D). Cells were detected with DAPI. (Magnification 20x).

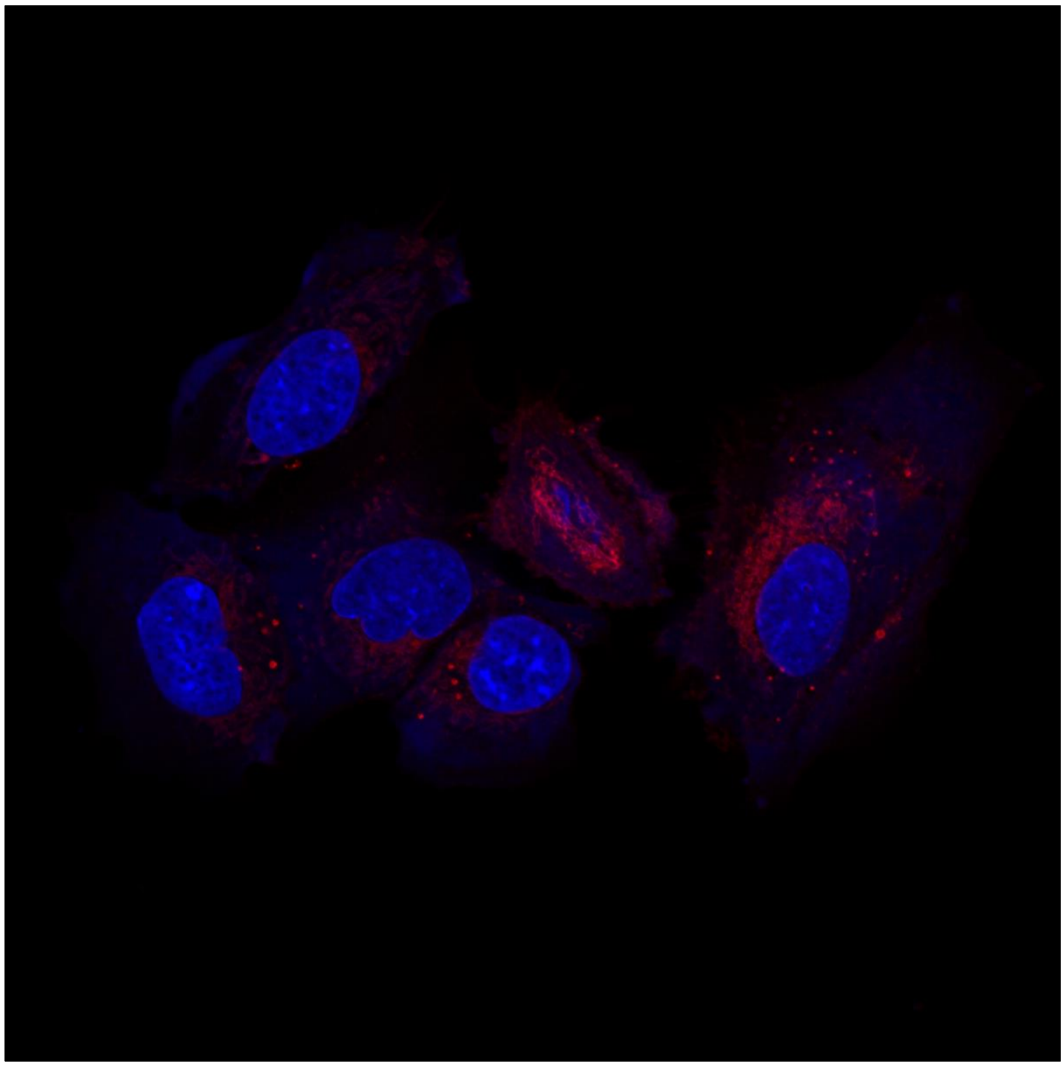

Figure 21. <u>Co-culture experiments.</u> Confocal microscopy image of SK-N-SH neuroblastoma cell line cultivated with bacteria grown in minimal medium supplemented with PAA. Cells were detected with DAPI. (Magnification 63x).

4. Discussion

It is well-known that the gut microbiota has an impact on human health. The interest in the gut microbiome and its possible involvement in different aspects of health and disease has begun approximately since 2010. One factor acting as catalyzer of attention by investigators was possibly the beginning of the Human Microbiome Project in 2008 (Buford, 2020). Actually, in the following decade the gut microbiota became the focus of intense research testified by the increasing number of published articles dealing in general with the correlations health/microbiota but also with ageing/microbiota. Starting from O'Toole and Jeffrey's work (2015) showing age-related changes of gut microbiota, many investigations tried to demonstrate a causative correlation between microbiota changes and age-related health decline. Nevertheless, a better understanding of the role played by gut microbiota on health and in the context of ageing is still needed (Buford, 2020). The work required to accomplish such task appears overwhelming as much as it is overwhelming the variety of the microbial population that dwells within the gut. Recent studies have highlighted a functional connection occurring between the gut and the brain (the so-called gut-brain axis) and, in particular, the important role that the gut microbiota plays in the axis. The explosion of interest for the gut microbiota and its role in the gut-brain axis certainly derives from researches that have established a link between gut microorganisms (in particular bacteria) and memory and learning performances, stress, mood and even neurodevelopment and neurodegenerative diseases (Dinan and Cryan, 2017). Despite the enormous advancement of knowledge accumulated over the last 15 years, much work is still required to understand the mechanistic aspect of the microbiota-gut-brain axis and how the shift of the gut microbiota is capable of affecting gut and CNS functions in ageing (Petrella et al., 2021). Loss of cognitive functions is one of the typical traits of ageing (Juan and Adlard, 2019). In particular, spatial learning and memory are hippocampal-dependent functions that decline with ageing (Bartsch and Wulff, 2015). The present thesis has described the work undertaken to study the impact in adult mice of a sudden shift of the microbiota

from the one regularly residing in the adult intestine to the one characteristic of aged individuals. This study was conducted operating an FMT from aged donor mice to adult recipients. This sudden change in microbiota population, therefore, was aimed to highlight the effects due exclusively to the microbiota rather than to the microbiota-unrelated intrinsic changes occurring to aged subjects. Our interest has been focused on studying behavioral modifications, as well as alterations in protein expression levels and inflammation markers in the hippocampus and in the large intestine. We also started to set up a technique to follow bacterial metabolites within eukaryotic cells.

Our results show that the microbiota dwelling in aged hosts transplanted in adult mice is sufficient to recapitulate memory and cognitive alterations normally seen in aged animals. These results are important in reinforcing the concept that gut microbiota is capable of affecting CNS functions. It has also been reported that in ageing there are changes in anxiety-like behaviors and a decrease in locomotion in aged mice that could be attenuated by the supplementation of prebiotics (Bordner et al., 2011; Shoji et al., 2016; Yang et al., 2020). In contrast, we report that FMT from aged animals did not impact locomotion and anxiety-like behaviors in adult recipients. These observations suggest that, at least in our experimental setting, FMT from aged animals has a targeted impact on cognition and memory rather than on locomotion and anxiety. Results obtained in cognitive and behavioral tests led us to examine the molecular mechanisms that could underlie the observed modifications. To this end, we used one-shot label-free quantitative proteomic method analysing the hippocampus. The IPA showed alterations in pathways related to synaptic transmission, cognition and neurotransmission. Also, we found that MAPT is up-regulated in the hippocampus of mice transplanted with faeces from aged individuals. MAPT encodes for tau protein that is important in microtubule assembly and serves for axonal transport and synaptic plasticity. In accordance to our experimental setting, increased expression levels of MAPT have been previously observed in age-related neurodegeneration (Shunsuke et al., 2020). Ageing and changes in gut microbiota have been linked to the so-called “inflammageing”, the low-grade activation of the innate and adaptive immune system observed in ageing (Li et al., 2021). However, we could not observe changes in the levels of inflammatory

cytokines in the hippocampus of FMT-aged mice, pointing to the age-related inflammageing in the CNS as a phenomenon unrelated to gut microbiota. This latter concept is further reinforced by the observation, carried out by immunofluorescence and western blotting, that levels of GFAP protein do not increase in the hippocampus, indicating the absence of an overt activation of astrocytes. However, cytokines levels have been assessed at the end of the FMT treatment and we cannot rule out the possibility that transient changes might have been occurred at earlier time points. Interestingly, FMT-aged mice show changes in microglia morphology in the fimbria. Microglia are the immunocompetent cells in the CNS and are important in neuronal surveillance in both homeostatic and pathological conditions (Galloway et al., 2019). As observed in ageing (Hart et al., 2012), a significant increase in the expression of F4/80 in the microglia cells in the hippocampus fimbria can be observed even in our experimental setting. If these phenotypic changes and increased expression of F4/80 in microglia are indeed related to the changes observed to the expression levels of other CNS proteins and in memory and cognition remains to be explored. F4/80 is a seven transmembrane G-protein coupled receptor with an extracellular domain containing repeated Epidermal Growth Factor-like calcium binding domains. Even though the enhanced expression of F4/80 has been correlated to oral tolerance, its function still remains to be determined (Gordon et al., 2011).

The results obtained in behavioral tests and the modifications observed in the hippocampus of FMT-aged mice prompted us to investigate if there were earlier alterations in the colon that could explain changes observed in the CNS. It has been reported that in ageing there is an increase in both systemic and gut inflammation that is linked to changes in gut microbiota (dysbiosis) and to a partially impaired barrier function (leaky gut) (Qi et al., 2017; Nagpal et al., 2018). The increase in gut permeability leads to an influx of antigens, pathogens and inflammatory molecules from gut into the systemic circulation that activates systemic inflammation. In turn, inflammation has a negative impact on gut barrier function generating a vicious circle where increased gut permeability generates inflammation which further promotes gut permeability (Nagpal et al., 2018). In this context, microbial dysbiosis is a key player. In fact, it has been reported that GF mice conventionalized with FMT from aged animals induces systemic inflammation. This assertion, based on the greater

level of T cell activation achieved by FMT with faeces from aged mice compared to FMT with faeces from young mice, unfortunately was not paralleled by investigations on behavioral differences in the recipients nor evaluated the levels of local and systemic inflammatory cytokines (Fransen et al., 2017). Also, gut dysbiosis and increased gut permeability in humans, assessed by levels of circulating biomarkers and bacterial inflammatory molecules, have been correlated to depression and anxiety (Stevens et al., 2018). Intriguingly, we did not observe changes in gut permeability as well as in the levels of gut and systemic cytokines. As for the hippocampus, however, both cytokine levels and gut permeability assessments have been weighed at the end of FMT treatment and we cannot exclude that there might have been earlier changes or that significant changes in gut permeability may require longer time to become evident.

As regards changes in gut microbiota composition, we found a decrease in genera *Prevotellaceae, Faecalibaculum, Lachnospiraceae* and *Ruminococcaceae* in FMT-aged mice. Changes in microbiota composition have been observed in several experimental settings investigating CNS disorders and some changes involve the same bacterial populations that were affected in our experiments. For instance, lower levels of *Ruminococcaceae* and *Prevotellaceae* have been reported in human apolipoprotein E4 (APOE4)-targeted replacement mice and APOE4 is the most prevalent genetic risk factor of Alzheimer disease (Tran et al., 2019). On the other hand, sequencing of the microbiota and quantitative analysis of SCFA concentrations in fecal samples from patients with Parkinson's disease revealed reduced populations of *Bacteroidetes* and *Prevotellaceae*, increased populations of *Enterobacteriaceae*, as well as reduced production of SCFAs when compared to faeces from age-matched controls (Unger et al., 2016). Populations of *Ruminococcaceae* have been found decreased even in models of osteoarthritis (OA) which is not a CNS disease but certainly affects aged individuals with a greater frequency. In mice transplanted with faeces from humans suffering of OA, a greater abundance of *Fusobacterium* and *Faecalibacterium*, and a decrease in *Ruminococcaceae* were consistently correlated with OA severity and systemic inflammatory biomarkers (Huang et al., 2020).

The IPA on colon samples revealed modification in several pathways after the transfer of faeces from aged animals into adult mice. Interestingly, one of the up-regulated pathways in the colon of FMT-aged mice is the paxillin signaling. Although there is no evidence for a role of paxillin in the ageing colon yet, this pathway has been extensively studied in the colorectal cancer (CRC), a disease which increases in frequency with ageing, where it was found consistently up-regulated (SEER 2014-2018; Zhao et al., 2015; Zhao et al., 2017; Wen et al., 2020). Paxillin is a cytoplasmic multi-domain focal adhesion adaptor protein important for the recruitment of structural and signaling molecules involved in the regulation of cytoskeletal rearrangements and cell motility. In *vitro* and in *vivo* experiments demonstrated that the downregulation of paxillin reduced migration and invasion ability in CRC. Also, the downregulation of paxillin was paralleled with a reduced expression of epithelial-mesenchymal transition (EMT) markers (like N-cadherin, vimentin and Snail) and with an increase in E-cadherin. Knockdown of paxillin inhibits EMT, an important process required for cell migration and invasion in cancer (Wen et al., 2020). Another pathway that we found up-regulated in the colon of FMT-aged mice is the ILK pathway. The ILK pathway controls different processes such as cell cycle, angiogenesis and cancer. The up-regulation of ILK has been linked to different cancers including prostate cancer, gastric cancer, non-small cell lung cancer and CRC. This is not surprising as ILK binds to paxillin and the two proteins pathways (ILK and paxillin) share many molecules (e.a. vinculin, integrin β1 and integrin β4). In addition, ILK signaling upregulation has been linked to EMT (lowering the expression of E-cadherin) and promotes tumor invasion (Zhuang et al., 2016). Interestingly, our experiments demonstrated that paxillin and ILK upregulation in FMT-aged mice is paralleled by a decrease in the populations of *Lachnospiraceae* and *Ruminococcaceae*, the same families that are found depleted in CRCs (Peters et al. 2016). It is indeed tempting to correlate changes in the microbiota of aged individuals to the upregulation of the paxillin and ILK signaling pathways and to the increased incidence of CRC. Alternatively, paxillin and ILK upregulation might be indicative of a rearrangement of cell focal adhesions and increased motility that could predict a reorganization of the epithelial gut barrier.

Among the down-regulated pathways we found the activation of PPARα/RXRa. PPARs are transcription factors activated by a ligand. Several different isoforms, PPARα, PPARβ/δ and PPARγ, have been characterized. PPARα is expressed in different tissues including liver, hearth, brown adipose tissue, kidney and gut. PPARs trigger the transcription of their target genes when heterodimerized with RXRs. PPARs are important regulators of lipid metabolism but also of cell proliferation, survival and differentiation. PPARγ is highly expressed in colon where it promotes the maturation of colonocytes. In the small intestine, PPARβ/δ is important for the maturation of Paneth cells (Feige et al., 2006). Interestingly, PPARα is important in the context of inflammation. In particular, experiments in PPARα$^{-/-}$ mice are characterized by a protracted inflammatory response (Korbecki et al., 2019). Also, in the context of colon carcinogenesis it has been reported that the loss of PPARα in the gut supports colon tumorigenesis in mice with carcinogen-induced CRC (Luo et al., 2019). Thus, reduced activation of PPARα/RXRa in FMT-aged mice fits well with the upregulation of paxillin and ILK signaling pathways in the context of epithelial modifications in CRCs. Although we did not detect any sign of cancer, for which longer experiments are needed, nor we observed increased levels of inflammatory cytokines or disruption of the epithelial gut barrier in FMT-aged mice, taking together data obtained from the proteomic analysis outline a general frame-work pointing to CRC tumorigenesis in FMT-aged mice. This hypothesis is indirectly supported by the finding that among the up-regulated proteins in the colon of FMT-aged mice we could detect PDIA2 and CPB1 that have been also related to cancer (Lee and Lee, 2017; Kothari et al., 2021). In particular, over-expressed PDI proteins have been frequently correlated with metastasis and invasiveness. PDIA1 is significantly over-expressed in brain, kidney, ovarian, prostate and lung cancer. Interestingly, in the context of cancer, it has been seen that PDI proteins have different functions depending on the cellular localization. For example, when PDI proteins are found on the cell surface they are linked to cell migration through the activation of the signaling of metalloproteases and to cell adhesion through activation of integrin signaling, while when they are located in the nucleus they are involved in the regulation of apoptosis and EMT (Lee and Lee, 2017). On the other hand, CPB1 is highly expressed in some forms of breast cancer (Kothari et al., 2021). Among the proteins down-regulated in

FMT-aged mice we found VIP and RNA binding motif protein 47 (RBM47). Both proteins have been also linked to CRC (Rokavec et al., 2017; Yang et al., 2019). In particular, in a study analysing high-sequenced data, using bioinformatic approach, it has been observed that VIP is down-regulated in CRC tissues compared to normal tissues (Yang et al., 2019). As far as RBM47 is concerned, a bioinformatic analysis of different tumor types allowed to identify a link between RBM47 mRNA downregulation with metastatic tumors and reduced survival rate in patients with CRC. Also, a reduced RBM47 protein expression has been related to the presence of metastasis in individuals with primary CRCs (Rokavec et al., 2017).

Taking together, data obtained from FMT-aged mice seems to point to the possibility that the microbiota switch could be a predisposing factor for cancer of the large intestine. Further targeted studies will be needed to evaluate the involvement of microbiota in CRC development.

5. Future perspectives

Nowadays there is a worldwide increase in the life expectancy in the population. However, life expectancy in the elderly should be paralleled by health expectancy. In this respect, the gut microbiota could be a promising target to work with.

The results obtained in the behavioral tests, the differences in protein expression in the hippocampus and colon of FMT-aged mice might be explained in the context of the microbiota-gut-brain axis. Although the concept of the existence of a communication axis between the gut and the brain is a well-established one, it is not clear yet the way these two systems communicate. Different routes have been proposed: neural pathway, neuroendocrine-hypothalamic-pituitary-adrenal axis, immune system, vagus nerve and the release of microbiota-derived neuroactive molecules (Gwak and Chang, 2021). In particular, it has been showed that different bacterial strains can produce different neurotransmitters such as γ-aminobutyric acid, 5-HT, dopamine and noradrenaline. In turn, these molecules have an impact on microglia activation and other cerebral functions. Other mediators in the microbiota-gut-brain axis include enterochromaffin cells that can be engaged by microbial molecules and secrete 5-HT in the lamina propria, thus increasing the levels of this neurotransmitter locally in the colon and systemically (Silva et al., 2020). Another important player in this axis is the vagus nerve. In particular, thanks to their proximity, bacteria can interact and trigger the activation of the vagus nerve and in this way promoting CNS effects (Bonaz et al., 2018). The importance of the vagus nerve in this axis has been well demonstrated in studies in which mice treated either with probiotics or pathogens have an activation of vagal sensory neurons in the gastrointestinal tract affecting CNS functions. These effects are abolished in vagotomized mice (Wang et al., 2002; Goehler et al., 2005). However, it is still unclear if the activation of the vagus is mediated by a physical interaction with bacteria or *via* bacterial metabolites (Bonaz et al., 2018). Also, bacterial-derived molecules are considered important mediators in the microbiota-gut-brain axis. Among these molecules, SCFAs play an important role and altered SCFAs production has been

reported in neurological disorders (Silva et al., 2020). In our experimental setting, there is a decreased representation of *Lachnospiraceae* and *Ruminococcaceae* that are SCFAs producing bacteria. Our results showed that differences in gut microbiota induce behavioral changes and also altered expression of several proteins in the hippocampus. Although we cannot exclude other mechanisms involved in gut-brain axis communication, one hypothesis that could be put forward is that some bacterial molecules might act as signaling molecules. In order to set up a protocol to visualize bacterial molecules and track their pathway in the host we used chemically modified bacterial molecules. Click chemistry is a group of chemical reactions that, under the right conditions, form stable products with high selectivity (Moses and Moorhouse, 2007). There are different click chemistry reactions and, in this work, we used copper catalyzed azide-alkyne cycloaddition. In particular, we added PAA to the minimal medium of *Bacteroides thetaiotaomicron* to evaluate both the incorporation of this molecule in the bacterial cells and the possibility to stain and track it. We were able to detect this chemically modified molecule in the bacterial cells using an alkyne modified dye and a commercially available kit. Once established, this protocol has been used in co-culture experiments where we could successfully track the presence of bacterial derived molecule in eukaryotic cell lines. We believe that click-chemistry is promising tool that can be exploited to track bacteria-derived molecules in order to shed some light on the pathway that bacterial metabolites follow to interact with the host nervous system.

6. References

- Agace WW, Persson EK. How vitamin A metabolizing dendritic cells are generated in the gut mucosa. Trends Immunol. 2012 Jan;33(1):42-8. doi: 10.1016/j.it.2011.10.001. Epub 2011 Nov 11. PMID: 22079120.
- Al-Sadi R, Guo S, Ye D, Rawat M, Ma TY. TNF-α Modulation of Intestinal Tight Junction Permeability Is Mediated by NIK/IKK-α Axis Activation of the Canonical NF-κB Pathway. Am J Pathol. 2016 May;186(5):1151-65. doi: 10.1016/j.ajpath.2015.12.016. Epub 2016 Mar 4. PMID: 26948423; PMCID: PMC4861759.
- Al-Sadi R, Ye D, Boivin M, Guo S, Hashimi M, Ereifej L, Ma TY. Interleukin-6 modulation of intestinal epithelial tight junction permeability is mediated by JNK pathway activation of claudin-2 gene. PLoS One. 2014 Mar 24;9(3):e85345. doi: 10.1371/journal.pone.0085345. PMID: 24662742; PMCID: PMC3963839.
- Antunes M, Biala G. The novel object recognition memory: neurobiology, test procedure, and its modifications. Cogn Process. 2012;13(2):93-110. doi:10.1007/s10339-011-0430-z
- Arnold JW, Roach J, Fabela S, Moorfield E, Ding S, Blue E, Dagher S, Magness S, Tamayo R, Bruno-Barcena JM, Azcarate-Peril MA. The pleiotropic effects of prebiotic galacto-oligosaccharides on the aging gut. Microbiome. 2021 Jan 28;9(1):31. doi: 10.1186/s40168-020-00980-0. Erratum in: Microbiome. 2021 Feb 26;9(1):56. PMID: 33509277; PMCID: PMC7845053.
- Arques JL, Hautefort I, Ivory K, Bertelli E, Regoli M, Clare S, Hinton JC, Nicoletti C. Salmonella induces flagellin- and MyD88-dependent migration of bacteria-capturing dendritic cells into the gut lumen. Gastroenterology. 2009 Aug;137(2):579-87, 587.e1-2. doi: 10.1053/j.gastro.2009.04.010. Epub 2009 Apr 16. PMID: 19375423.
- Artis D. Epithelial-cell recognition of commensal bacteria and maintenance of immune homeostasis in the gut. Nat Rev Immunol. 2008 Jun;8(6):411-20. doi: 10.1038/nri2316. PMID: 18469830.
- Badinloo M, Nguyen E, Suh W, Alzahrani F, Castellanos J, Klichko VI, Orr WC, Radyuk SN. Overexpression of antimicrobial peptides contributes to aging through cytotoxic effects in Drosophila tissues. Arch Insect Biochem Physiol. 2018 Aug;98(4):e21464. doi: 10.1002/arch.21464. Epub 2018 Apr 10. PMID: 29637607; PMCID: PMC6039247.
- Barker N, van Es JH, Kuipers J, Kujala P, van den Born M, Cozijnsen M, Haegebarth A, Korving J, Begthel H, Peters PJ, Clevers H. Identification of stem cells in small intestine and colon by marker gene Lgr5. Nature. 2007 Oct 25;449(7165):1003-7. doi: 10.1038/nature06196. Epub 2007 Oct 14. PMID: 17934449.

- Bartsch T, Wulff P. The hippocampus in aging and disease: From plasticity to vulnerability, Neuroscience, Volume 309, 2015, Pages 1-16, ISSN 0306-4522, https://doi.org/10.1016/j.neuroscience.2015.07.084.
- Bell A., Juge N. Mucosal glycan degradation of the host by the gut microbiota, Glycobiology, Volume 31, Issue 6, June 2021, Pages 691–696, https://doi.org/10.1093/glycob/cwaa097
- Bergstrom K, Shan X, Casero D, Batushansky A, Lagishetty V, Jacobs JP, Hoover C, Kondo Y, Shao B, Gao L, Zandberg W, Noyovitz B, McDaniel JM, Gibson DL, Pakpour S, Kazemian N, McGee S, Houchen CW, Rao CV, Griffin TM, Sonnenburg JL, McEver RP, Braun J, Xia L. Proximal colon-derived O-glycosylated mucus encapsulates and modulates the microbiota. Science. 2020 Oct 23;370(6515):467-472. doi: 10.1126/science.aay7367. PMID: 33093110; PMCID: PMC8132455.
- Bettio LEB, Rajendran L, Gil-Mohapel J. The effects of aging in the hippocampus and cognitive decline. Neurosci Biobehav Rev. 2017 Aug;79:66-86. doi: 10.1016/j.neubiorev.2017.04.030. Epub 2017 May 2. PMID: 28476525.
- Bodenhofer U, Bonatesta E, Horejš-Kainrath C, Hochreiter S. msa: an R package for multiple sequence alignment. Bioinformatics. 2015 Dec 15;31(24):3997-9. doi: 10.1093/bioinformatics/btv494. Epub 2015 Aug 26. PMID: 26315911.
- Boehme, M., Guzzetta, K.E., Bastiaanssen, T.F.S. et al. Microbiota from young mice counteracts selective age-associated behavioral deficits. Nat Aging 1, 666–676 (2021). https://doi.org/10.1038/s43587-021-00093-9
- Bonaz B, Bazin T, Pellissier S. The Vagus Nerve at the Interface of the Microbiota-Gut-Brain Axis. Front Neurosci. 2018 Feb 7;12:49. doi: 10.3389/fnins.2018.00049. PMID: 29467611; PMCID: PMC5808284.
- Bordner KA, Kitchen RR, Carlyle B, George ED, Mahajan MC, Mane SM, Taylor JR, Simen AA. Parallel declines in cognition, motivation, and locomotion in aging mice: association with immune gene upregulation in the medial prefrontal cortex. Exp Gerontol. 2011 Aug;46(8):643-59. doi: 10.1016/j.exger.2011.03.003. Epub 2011 Mar 29. PMID: 21453768; PMCID: PMC3664302.
- Bosco N, Noti M. The aging gut microbiome and its impact on host immunity. Genes Immun. 2021 Oct;22(5-6):289-303. doi: 10.1038/s41435-021-00126-8. Epub 2021 Apr 19. PMID: 33875817; PMCID: PMC8054695.
- Branca JJV, Gulisano M, Nicoletti C. Intestinal epithelial barrier functions in ageing. Ageing Res Rev. 2019 Sep;54:100938. doi: 10.1016/j.arr.2019.100938. Epub 2019 Jul 29. PMID: 31369869.
- Braniste V, Al-Asmakh M, Kowal C, Anuar F, Abbaspour A, Tóth M, Korecka A, Bakocevic N, Ng LG, Kundu P, Gulyás B, Halldin C, Hultenby K, Nilsson H, Hebert H, Volpe BT, Diamond B, Pettersson S. The gut

microbiota influences blood-brain barrier permeability in mice. Sci Transl Med. 2014 Nov 19;6(263):263ra158. doi: 10.1126/scitranslmed.3009759. Erratum in: Sci Transl Med. 2014 Dec 10;6(266):266er7. Guan, Ng Lai [corrected to Ng, Lai Guan]. PMID: 25411471; PMCID: PMC4396848.

- Breinbauer R, Köhn M. Azide-alkyne coupling: a powerful reaction for bioconjugate chemistry. Chembiochem. 2003 Nov 7;4(11):1147-9. doi: 10.1002/cbic.200300705. PMID: 14613105.
- Buchon N, Broderick NA, Poidevin M, Pradervand S, Lemaitre B. Drosophila intestinal response to bacterial infection: activation of host defense and stem cell proliferation. Cell Host Microbe. 2009 Feb 19;5(2):200-11. doi: 10.1016/j.chom.2009.01.003. PMID: 19218090.
- Buford TW. The Gut Microbiome and Aging. J Gerontol A Biol Sci Med Sci. 2020 Jun 18;75(7):1229-1231. doi: 10.1093/gerona/glaa103. PMID: 32556115
- Callahan BJ, McMurdie PJ, Rosen MJ, Han AW, Johnson AJ, Holmes SP. DADA2: High-resolution sample inference from Illumina amplicon data. Nat Methods. 2016 Jul;13(7):581-3. doi: 10.1038/nmeth.3869. Epub 2016 May 23. PMID: 27214047; PMCID: PMC4927377.
- Callahan, B. J., McMurdie, P. J., & Holmes, S. P. (2017). Exact sequence variants should replace operational taxonomic units in marker-gene data analysis. The ISME journal, 11(12), 2639–2643. https://doi.org/10.1038/ismej.2017.119
- Caporaso JG, Lauber CL, Walters WA, Berg-Lyons D, Lozupone CA, Turnbaugh PJ, Fierer N, Knight R. Global patterns of 16S rRNA diversity at a depth of millions of sequences per sample. Proc Natl Acad Sci U S A. 2011 Mar 15;108 Suppl 1(Suppl 1):4516-22. doi: 10.1073/pnas.1000080107. Epub 2010 Jun 3. PMID: 20534432; PMCID: PMC3063599.
- Cheng, L. K., O'Grady, G., Du, P., Egbuji, J. U., Windsor, J. A., & Pullan, A. J. (2010). Gastrointestinal system. *Wiley interdisciplinary reviews. Systems biology and medicine*, *2*(1), 65–79. https://doi.org/10.1002/wsbm.19
- Choi, J., Rakhilin, N., Gadamsetty, P. et al. Intestinal crypts recover rapidly from focal damage with coordinated motion of stem cells that is impaired by aging. Sci Rep 8, 10989 (2018). https://doi.org/10.1038/s41598-018-29230-y.
- Clark RI, Walker DW. Role of gut microbiota in aging-related health decline: insights from invertebrate models. Cell Mol Life Sci. 2018 Jan;75(1):93-101. doi: 10.1007/s00018-017-2671-1. Epub 2017 Oct 12. PMID: 29026921; PMCID: PMC5754256.
- Conway J, A Duggal N. Ageing of the gut microbiome: Potential influences on immune senescence and inflammageing. Ageing Res Rev.

2021 Jul;68:101323. doi: 10.1016/j.arr.2021.101323. Epub 2021 Mar 23. PMID: 33771720.

- Crost, E. H., Le Gall, G., Laverde-Gomez, J. A., Mukhopadhya, I., Flint, H. J., & Juge, N. (2018). Mechanistic Insights Into the Cross-Feeding of Ruminococcus gnavus and Ruminococcus bromii on Host and Dietary Carbohydrates. Frontiers in microbiology, 9, 2558. https://doi.org/10.3389/fmicb.2018.02558
- Cryan JF, O'Riordan KJ, Cowan CSM, Sandhu KV, Bastiaanssen TFS, Boehme M, Codagnone MG, Cussotto S, Fulling C, Golubeva AV, Guzzetta KE, Jaggar M, Long-Smith CM, Lyte JM, Martin JA, Molinero-Perez A, Moloney G, Morelli E, Morillas E, O'Connor R, Cruz-Pereira JS, Peterson VL, Rea K, Ritz NL, Sherwin E, Spichak S, Teichman EM, van de Wouw M, Ventura-Silva AP, Wallace-Fitzsimons SE, Hyland N, Clarke G, Dinan TG. The Microbiota-Gut-Brain Axis. Physiol Rev. 2019 Oct 1;99(4):1877-2013. doi: 10.1152/physrev.00018.2018. PMID: 31460832.
- Davis S, Meltzer PS, GEOquery: a bridge between the Gene Expression Omnibus (GEO) and BioConductor, Bioinformatics, Volume 23, Issue 14, 15 July 2007, Pages 1846–1847, https://doi.org/10.1093/bioinformatics/btm254
- De Palma G, Lynch MD, Lu J, Dang VT, Deng Y, Jury J, Umeh G, Miranda PM, Pigrau Pastor M, Sidani S, Pinto-Sanchez MI, Philip V, McLean PG, Hagelsieb MG, Surette MG, Bergonzelli GE, Verdu EF, Britz-McKibbin P, Neufeld JD, Collins SM, Bercik P. Transplantation of fecal microbiota from patients with irritable bowel syndrome alters gut function and behavior in recipient mice. Sci Transl Med. 2017 Mar 1;9(379):eaaf6397. doi: 10.1126/scitranslmed.aaf6397. PMID: 28251905.
- Delva E, Tucker DK, Kowalczyk AP. The desmosome. Cold Spring Harb Perspect Biol. 2009 Aug;1(2):a002543. doi: 10.1101/cshperspect.a002543. PMID: 20066089; PMCID: PMC2742091.
- Diao, D., Wang, H., Li, T., Shi, Z., Jin, X., Sperka, T., Zhu, X., Zhang, M., Yang, F., Cong, Y., Shen, L., Zhan, Q., Yan, J., Song, Z., & Ju, Z. (2018). Telomeric epigenetic response mediated by Gadd45a regulates stem cell aging and lifespan. EMBO reports, 19(10), e45494. https://doi.org/10.15252/embr.201745494
- Diaz Heijtz R, Wang S, Anuar F, Qian Y, Björkholm B, Samuelsson A, Hibberd ML, Forssberg H, Pettersson S. Normal gut microbiota modulates brain development and behavior. Proc Natl Acad Sci U S A. 2011 Feb 15;108(7):3047-52. doi: 10.1073/pnas.1010529108. Epub 2011 Jan 31. PMID: 21282636; PMCID: PMC3041077.
- Dinan TG, Cryan JF. Gut instincts: microbiota as a key regulator of brain development, ageing and neurodegeneration. J Physiol. 2017 Jan 15;595(2):489-503. doi: 10.1113/JP273106. Epub 2016 Dec 4. PMID: 27641441; PMCID: PMC5233671.

- Elderman M, Sovran B, Hugenholtz F, Graversen K, Huijskes M, Houtsma E, Belzer C, Boekschoten M, de Vos P, Dekker J, Wells J, Faas M. The effect of age on the intestinal mucus thickness, microbiota composition and immunity in relation to sex in mice. PLoS One. 2017 Sep 12;12(9):e0184274. doi: 10.1371/journal.pone.0184274. PMID: 28898292; PMCID: PMC5595324.
- Elinav E, Strowig T, Kau AL, Henao-Mejia J, Thaiss CA, Booth CJ, Peaper DR, Bertin J, Eisenbarth SC, Gordon JI, Flavell RA. NLRP6 inflammasome regulates colonic microbial ecology and risk for colitis. Cell. 2011 May 27;145(5):745-57. doi: 10.1016/j.cell.2011.04.022. Epub 2011 May 12. PMID: 21565393; PMCID: PMC3140910.
- Erny D, Hrabě de Angelis AL, Jaitin D, Wieghofer P, Staszewski O, David E, Keren-Shaul H, Mahlakoiv T, Jakobshagen K, Buch T, Schwierzeck V, Utermöhlen O, Chun E, Garrett WS, McCoy KD, Diefenbach A, Staeheli P, Stecher B, Amit I, Prinz M. Host microbiota constantly control maturation and function of microglia in the CNS. Nat Neurosci. 2015 Jul;18(7):965-77. doi: 10.1038/nn.4030. Epub 2015 Jun 1. PMID: 26030851; PMCID: PMC5528863.Exp Gerontol. 2011 Aug;46(8):643-59. doi: 10.1016/j.exger.2011.03.003. Epub 2011
- Fachi JL, Felipe JS, Pral LP, da Silva BK, Corrêa RO, de Andrade MCP, da Fonseca DM, Basso PJ, Câmara NOS, de Sales E Souza ÉL, Dos Santos Martins F, Guima SES, Thomas AM, Setubal JC, Magalhães YT, Forti FL, Candreva T, Rodrigues HG, de Jesus MB, Consonni SR, Farias ADS, Varga-Weisz P, Vinolo MAR. Butyrate Protects Mice from Clostridium difficile-Induced Colitis through an HIF-1-Dependent Mechanism. Cell Rep. 2019 Apr 16;27(3):750-761.e7. doi: 10.1016/j.celrep.2019.03.054. PMID: 30995474.
- Feige JN, Gelman L, Michalik L, Desvergne B, Wahli W. From molecular action to physiological outputs: peroxisome proliferator-activated receptors are nuclear receptors at the crossroads of key cellular functions. Prog Lipid Res. 2006 Mar;45(2):120-59. doi: 10.1016/j.plipres.2005.12.002. Epub 2006 Jan 25. PMID: 16476485.
- Fernandes, A.D., Reid, J.N., Macklaim, J.M. et al. Unifying the analysis of high-throughput sequencing datasets: characterizing RNA-seq, 16S rRNA gene sequencing and selective growth experiments by compositional data analysis. Microbiome 2, 15 (2014). https://doi.org/10.1186/2049-2618-2-15
- Franceschi, C., Garagnani, P., Parini, P. et al. Inflammaging: a new immune–metabolic viewpoint for age-related diseases. Nat Rev Endocrinol 14, 576–590 (2018).
- Fransen F, van Beek AA, Borghuis T, Aidy SE, Hugenholtz F, van der Gaast-de Jongh C, Savelkoul HFJ, De Jonge MI, Boekschoten MV, Smidt H, Faas MM, de Vos P. Aged Gut Microbiota Contributes to Systemical

Inflammaging after Transfer to Germ-Free Mice. Front Immunol. 2017 Nov 2;8:1385. doi: 10.3389/fimmu.2017.01385. PMID: 29163474; PMCID: PMC5674680.

- Funk MC, Zhou J, Boutros M. Ageing, metabolism and the intestine. EMBO Rep. 2020 Jul 3;21(7):e50047. doi: 10.15252/embr.202050047. Epub 2020 Jun 21. PMID: 32567155; PMCID: PMC7332987.
- Furuse M. Molecular basis of the core structure of tight junctions. Cold Spring Harb Perspect Biol. 2010 Jan;2(1):a002907. doi: 10.1101/cshperspect.a002907. PMID: 20182608; PMCID: PMC2827901.
- Galenza A, Foley E. A glucose-supplemented diet enhances gut barrier integrity in Drosophila. Biol Open. 2021 Mar 8;10(3):bio056515. doi: 10.1242/bio.056515. PMID: 33579694; PMCID: PMC7969588.
- Galloway, D. A., Phillips, A., Owen, D., & Moore, C. S. (2019). Phagocytosis in the Brain: Homeostasis and Disease. Frontiers in immunology, 10, 790. https://doi.org/10.3389/fimmu.2019.00790
- Gervais L, Bardin AJ. Tissue homeostasis and aging: new insight from the fly intestine. Curr Opin Cell Biol. 2017 Oct;48:97-105. doi: 10.1016/j.ceb.2017.06.005. Epub 2017 Jul 16. PMID: 28719867.
- Goehler LE, Gaykema RPA, Opitz N, Reddaway R, Badr N, Lyte M. Activation in vagal afferents and central autonomic pathways: early responses to intestinal infection with Campylobacter jejuni. Brain Behav Immun. (2005) 19:334–44. doi: 10.1016/j.bbi.2004.09.002
- Gordon S, Hamann J, Lin HH, Stacey M. F4/80 and the related adhesion-GPCRs. Eur J Immunol. 2011 Sep;41(9):2472-6. doi: 10.1002/eji.201141715. PMID: 21952799.
- Greicius G, Virshup DM. Stromal control of intestinal development and the stem cell niche differentiation. 2019 Jul-Aug;108:8-16. doi: 10.1016/j.diff.2019.01.001. Epub 2019 Jan 8. PMID: 30683451.
- Gwak, M. G., & Chang, S. Y. (2021). Gut-Brain Connection: Microbiome, Gut Barrier, and Environmental Sensors. Immune network, 21(3), e20. https://doi.org/10.4110/in.2021.21.e20
- Harach, T., Marungruang, N., Duthilleul, N., Cheatham, V., Mc Coy, K. D., Frisoni, G., Neher, J. J., Fåk, F., Jucker, M., Lasser, T., & Bolmont, T. (2017). Reduction of Abeta amyloid pathology in APPPS1 transgenic mice in the absence of gut microbiota. Scientific reports, 7, 41802. https://doi.org/10.1038/srep41802
- Hart, A. D., Wyttenbach, A., Perry, V. H., & Teeling, J. L. (2012). Age related changes in microglial phenotype vary between CNS regions: grey versus white matter differences. Brain, behavior, and immunity, 26(5), 754–765. https://doi.org/10.1016/j.bbi.2011.11.006
- Hartsock A, Nelson WJ. Adherens and tight junctions: structure, function and connections to the actin cytoskeleton. Biochim Biophys Acta. 2008;1778(3):660-669. doi:10.1016/j.bbamem.2007.07.012.

- Hölter SM, Einicke J, Sperling B, Zimprich A, Garrett L, Fuchs H, Gailus-Durner V, Hrabé de Angelis M, Wurst W. Tests for Anxiety-Related Behavior in Mice. Curr Protoc Mouse Biol. 2015 Dec 2;5(4):291-309. doi: 10.1002/9780470942390.mo150010. PMID: 26629773.
- Hou Q, Dong Y, Yu Q, Wang B, Le S, Guo Y, Zhang B. Regulation of the Paneth cell niche by exogenous L-arginine couples the intestinal stem cell function. FASEB J. 2020 Aug;34(8):10299-10315. doi: 10.1096/fj.201902573RR. Epub 2020 Jun 17. PMID: 32725957.
- Huang Z, Chen J, Li B, Zeng B, Chou CH, Zheng X, Xie J, Li H, Hao Y, Chen G, Pei F, Shen B, Kraus VB, Wei H, Zhou X, Cheng L. Faecal microbiota transplantation from metabolically compromised human donors accelerates osteoarthritis in mice. Ann Rheum Dis. 2020 May;79(5):646-656. doi: 10.1136/annrheumdis-2019-216471. Epub 2020 Mar 23. PMID: 32205337; PMCID: PMC7384301
- Iliev ID, Spadoni I, Mileti E, Matteoli G, Sonzogni A, Sampietro GM, Foschi D, Caprioli F, Viale G, Rescigno M. Human intestinal epithelial cells promote the differentiation of tolerogenic dendritic cells. Gut. 2009 Nov;58(11):1481-9. doi: 10.1136/gut.2008.175166. Epub 2009 Jun 30. PMID: 19570762.
- Jeffery V, Goldson AJ, Dainty JR, Chieppa M, Sobolewski A. IL-6 Signaling Regulates Small Intestinal Crypt Homeostasis. J Immunol. 2017 Jul 1;199(1):304-311. doi: 10.4049/jimmunol.1600960. Epub 2017 May 26. PMID: 28550196; PMCID: PMC6485663.
- Jiang X, Hao X, Jing L, Wu G, Kang D, Liu X, Zhan P. Recent applications of click chemistry in drug discovery. Expert Opin Drug Discov. 2019 Aug;14(8):779-789. doi: 10.1080/17460441.2019.1614910. Epub 2019 May 16. PMID: 31094231.
- Juan SMA, Adlard PA. Ageing and Cognition. Subcell Biochem. 2019;91:107-122. doi: 10.1007/978-981-13-3681-2_5. PMID: 30888651
- Kaminsky LW, Al-Sadi R, Ma TY. IL-1β and the Intestinal Epithelial Tight Junction Barrier. Front Immunol. 2021;12:767456. Published 2021 Oct 25. doi:10.3389/fimmu.2021.767456
- Kang DW, Adams JB, Coleman DM, Pollard EL, Maldonado J, McDonough-Means S, Caporaso JG, Krajmalnik-Brown R. Long-term benefit of Microbiota Transfer Therapy on autism symptoms and gut microbiota. Sci Rep. 2019 Apr 9;9(1):5821. doi: 10.1038/s41598-019-42183-0. PMID: 30967657; PMCID: PMC6456593.
- Kapetanovic R, Bokil NJ, Sweet MJ. Innate immune perturbations, accumulating DAMPs and inflammasome dysregulation: A ticking time bomb in ageing. Ageing Res Rev. 2015 Nov;24(Pt A):40-53. doi: 10.1016/j.arr.2015.02.005. Epub 2015 Feb 25. PMID: 25725308.

- Kawanishi H, Kiely J. Immune-related alterations in aged gut-associated lymphoid tissues in mice. Dig Dis Sci. 1989 Feb;34(2):175-84. doi: 10.1007/BF01536048. PMID: 2914536.
- Kelly, D., Campbell, J., King, T. et al. Commensal anaerobic gut bacteria attenuate inflammation by regulating nuclear-cytoplasmic shuttling of PPAR-γ and RelA. Nat Immunol 5, 104–112 (2004). https://doi.org/10.1038/ni1018
- Khounlotham M, Kim W, Peatman E, Nava P, Medina-Contreras O, Addis C, Koch S, Fournier B, Nusrat A, Denning TL, Parkos CA. Compromised intestinal epithelial barrier induces adaptive immune compensation that protects from colitis. Immunity. 2012 Sep 21;37(3):563-73. doi: 10.1016/j.immuni.2012.06.017. Epub 2012 Sep 13. PMID: 22981539; PMCID: PMC3564580.
- Kim YS, Ho SB. Intestinal goblet cells and mucins in health and disease: recent insights and progress. Curr Gastroenterol Rep. 2010 Oct;12(5):319-30. doi: 10.1007/s11894-010-0131-2. PMID: 20703838; PMCID: PMC2933006.
- Kitteringham E, Zhou Z, Twamley B, Griffith DM. Au(III) and Pt(II) Complexes of a Novel and Versatile 1,4-Disubstituted 1,2,3-Triazole-Based Ligand Possessing Diverse Secondary and Tertiary Coordinating Groups. Inorg Chem. 2018 Oct 1;57(19):12282-12290. doi: 10.1021/acs.inorgchem.8b01994. Epub 2018 Sep 7. PMID: 30192529.
- Knoop KA, Kumar N, Butler BR, et al. RANKL is necessary and sufficient to initiate development of antigen-sampling M cells in the intestinal epithelium. J Immunol. 2009;183(9):5738-5747. doi:10.4049/jimmunol.0901563
- Kobayashi A, Donaldson DS, Erridge C, Kanaya T, Williams IR, Ohno H, Mahajan A, Mabbott NA. The functional maturation of M cells is dramatically reduced in the Peyer's patches of aged mice. Mucosal Immunol. 2013 Sep;6(5):1027-37. doi: 10.1038/mi.2012.141. Epub 2013 Jan 30. PMID: 23360902; PMCID: PMC3747980.
- Korbecki J, Bobiński R, Dutka M. Self-regulation of the inflammatory response by peroxisome proliferator-activated receptors. Inflamm Res. 2019 Jun;68(6):443-458. doi: 10.1007/s00011-019-01231-1. Epub 2019 Mar 29. PMID: 30927048; PMCID: PMC6517359.
- Kothari C, Clemenceau A, Ouellette G, Ennour-Idrissi K, Michaud A, Diorio C, Durocher F. Is Carboxypeptidase B1 a Prognostic Marker for Ductal Carcinoma In Situ? Cancers (Basel). 2021 Apr 6;13(7):1726. doi: 10.3390/cancers13071726. PMID: 33917306; PMCID: PMC8038727.
- Kurokawa K, Hayakawa Y, Koike K. Plasticity of Intestinal Epithelium: Stem Cell Niches and Regulatory Signals. Int J Mol Sci. 2020;22(1):357. Published 2020 Dec 31. doi:10.3390/ijms22010357

- Langille, M.G., Meehan, C.J., Koenig, J.E. et al. Microbial shifts in the aging mouse gut. Microbiome 2, 50 (2014). https://doi.org/10.1186/s40168-014-0050-9
- Le Gall G, Noor SO, Ridgway K, Scovell L, Jamieson C, Johnson IT, Colquhoun IJ, Kemsley EK, Narbad A. Metabolomics of fecal extracts detects altered metabolic activity of gut microbiota in ulcerative colitis and irritable bowel syndrome. J Proteome Res. 2011 Sep 2;10(9):4208-18. doi: 10.1021/pr2003598. Epub 2011 Aug 8. PMID: 21761941.
- Lee E, Lee DH. Emerging roles of protein disulfide isomerase in cancer. BMB Rep. 2017 Aug;50(8):401-410. doi: 10.5483/bmbrep.2017.50.8.107. PMID: 28648146; PMCID: PMC5595169.
- Levy M, Thaiss CA, Zeevi D, Dohnalová L, Zilberman-Schapira G, Mahdi JA, David E, Savidor A, Korem T, Herzig Y, Pevsner-Fischer M, Shapiro H, Christ A, Harmelin A, Halpern Z, Latz E, Flavell RA, Amit I, Segal E, Elinav E. Microbiota-Modulated Metabolites Shape the Intestinal Microenvironment by Regulating NLRP6 Inflammasome Signaling. Cell. 2015 Dec 3;163(6):1428-43. doi: 10.1016/j.cell.2015.10.048. PMID: 26638072; PMCID: PMC5665753.
- Li H, Ni J, Qing H. Gut Microbiota: Critical Controller and Intervention Target in Brain Aging and Cognitive Impairment. Front Aging Neurosci. 2021 Jun 25;13:671142. doi: 10.3389/fnagi.2021.671142. PMID: 34248602; PMCID: PMC8267942
- Libina N, Berman JR, Kenyon C. Tissue-specific activities of C. elegans DAF-16 in the regulation of lifespan. Cell. 2003 Nov 14;115(4):489-502. doi: 10.1016/s0092-8674(03)00889-4. PMID: 14622602.
- Lin YR, Parikh H, Park Y. Stress resistance and lifespan enhanced by downregulation of antimicrobial peptide genes in the Imd pathway. Aging (Albany NY). 2018 Apr 19;10(4):622-631. doi: 10.18632/aging.101417. PMID: 29677000; PMCID: PMC5940113.
- Loch G, Zinke I, Mori T, Carrera P, Schroer J, Takeyama H, Hoch M. Antimicrobial peptides extend lifespan in Drosophila. PLoS One. 2017 May 17;12(5):e0176689. doi: 10.1371/journal.pone.0176689. PMID: 28520752; PMCID: PMC5435158.
- Lucchetta EM, Ohlstein B. The Drosophila midgut: a model for stem cell driven tissue regeneration. Wiley Interdiscip Rev Dev Biol. 2012;1(5):781-788. doi:10.1002/wdev.51
- Luo Y, Xie C, Brocker CN, Fan J, Wu X, Feng L, Wang Q, Zhao J, Lu D, Tandon M, Cam M, Krausz KW, Liu W, Gonzalez FJ. Intestinal PPARα Protects Against Colon Carcinogenesis via Regulation of Methyltransferases DNMT1 and PRMT6. Gastroenterology. 2019 Sep;157(3):744-759.e4. doi: 10.1053/j.gastro.2019.05.057. Epub 2019 May 30. PMID: 31154022; PMCID: PMC7388731.

- Mahlapuu M, Håkansson J, Ringstad L, Björn C. Antimicrobial Peptides: An Emerging Category of Therapeutic Agents. Front Cell Infect Microbiol. 2016 Dec 27;6:194. doi: 10.3389/fcimb.2016.00194. PMID: 28083516; PMCID: PMC5186781.
- Man AL, Bertelli E, Rentini S, Regoli M, Briars G, Marini M, Watson AJ, Nicoletti C. Age-associated modifications of intestinal permeability and innate immunity in human small intestine. Clin Sci (Lond). 2015 Oct;129(7):515-27. doi: 10.1042/CS20150046. Epub 2015 May 7. PMID: 25948052.
- Man AL, Gicheva N, Nicoletti C. The impact of ageing on the intestinal epithelial barrier and immune system, Cellular Immunology, Volume 289, Issues 1–2, 2014, Pages 112-118, ISSN 0008-8749. https://doi.org/10.1016/j.cellimm.2014.04.001.
- Man AL., Lodi F., Bertelli E., Regoli M, Pin C., Mulholland F., Satoskar A.R., Taussig M.J., Nicoletti C. The Journal of Immunology October 15, 2008, 181 (8) 5673-5680; DOI: 10.4049/jimmunol.181.8.5673
- Mann ER, Li X. Intestinal antigen-presenting cells in mucosal immune homeostasis: crosstalk between dendritic cells, macrophages and B-cells. World Journal of Gastroenterology. 2014 Aug;20(29):9653-9664. DOI: 10.3748/wjg.v20.i29.9653. PMID: 25110405; PMCID: PMC4123356.
  Mar 29. PMID: 21453768; PMCID: PMC3664302
- McDonald KG, Leach MR, Huang C, Wang C, Newberry RD. Aging impacts isolated lymphoid follicle development and function. Immun Ageing. 2011 Jan 7;8(1):1. doi: 10.1186/1742-4933-8-1. PMID: 21214915; PMCID: PMC3023758.
- McMurdie PJ, Holmes S. phyloseq: an R package for reproducible interactive analysis and graphics of microbiome census data. PLoS One. 2013 Apr 22;8(4):e61217. doi: 10.1371/journal.pone.0061217. PMID: 23630581; PMCID: PMC3632530.
- Mikolašević I, Hauser G, Abram M, et al. Fecal microbiota transplantation - where are we? Croatian Medical Journal. 2021 Feb;62(1):52-58. PMID: 33660961; PMCID: PMC7976890.
- Miyoshi J, Leone V, Nobutani K, et al. Minimizing confounders and increasing data quality in murine models for studies of the gut microbiome. PeerJ. 2018;6:e5166. Published 2018 Jul 12. doi:10.7717/peerj.5166
- Moorefield EC, Andres SF, Blue RE, Van Landeghem L, Mah AT, Santoro MA, Ding S. Aging effects on intestinal homeostasis associated with expansion and dysfunction of intestinal epithelial stem cells. Aging (Albany NY). 2017 Aug 29;9(8):1898-1915. doi: 10.18632/aging.101279. PMID: 28854151; PMCID: PMC5611984.
- Moses JE, Moorhouse AD. The growing applications of click chemistry. Chem Soc Rev. 2007 Aug;36(8):1249-62. doi: 10.1039/b613014n. Epub

2007 May 3. Erratum in: Chem Soc Rev. 2016 Dec 21;45(24):6888. PMID: 17619685.

- Mowat AM. Anatomical basis of tolerance and immunity to intestinal antigens. Nat Rev Immunol. 2003 Apr;3(4):331-41. doi: 10.1038/nri1057. PMID: 12669023.
- Nagafusa, H., Sayama, K. Age-related chemokine alterations affect IgA secretion and gut immunity in female mice. Biogerontology 21, 609–618 (2020). https://doi.org/10.1007/s10522-020-09877-9
- Nagpal R, Mainali R, Ahmadi S, Wang S, Singh R, Kavanagh K, Kitzman DW, Kushugulova A, Marotta F, Yadav H. Gut microbiome and aging: Physiological and mechanistic insights. Nutr Healthy Aging. 2018 Jun 15;4(4):267-285. doi: 10.3233/NHA-170030. PMID: 29951588; PMCID: PMC6004897.
- Nalapareddy K, Nattamai KJ, Kumar RS, et al. Canonical Wnt Signaling Ameliorates Aging of Intestinal Stem Cells. Cell Rep. 2017;18(11):2608-2621. doi:10.1016/j.celrep.2017.02.056.
- Nászai M, Carroll LR, Cordero JB. Intestinal stem cell proliferation and epithelial homeostasis in the adult Drosophila midgut. Insect Biochemistry and Molecular Biology, Volume 67, 2015, Pages 9-14, ISSN 0965-1748, https://doi.org/10.1016/j.ibmb.2015.05.016.
- National Cancer Institute, NIH. Surveillance, epidemiology and end results program. https://seer.cancer.gov/explorer/application.html?site=20&data_type=1&graph_type=3&compareBy=sex&chk_sex_1=1&rate_type=2&race=1&advopt_precision=1&advopt_show_ci=on&advopt_display=2
- Newton JL, Jordan N, Pearson J, Williams GV, Allen A, James OF. The adherent gastric antral and duodenal mucus gel layer thins with advancing age in subjects infected with Helicobacter pylori. Gerontology. 2000 May-Jun;46(3):153-7. doi: 10.1159/000022151. PMID: 10754373.
- Nicoletti C, Borghesi-Nicoletti C, Yang XH, Schulze DH, Cerny J. Repertoire diversity of antibody response to bacterial antigens in aged mice. II. Phosphorylcholine-antibody in young and aged mice differ in both VH/VL gene repertoire and in specificity. J Immunol. 1991 Oct 15;147(8):2750-5. PMID: 1918989.
- Nicoletti C, Yang X, Cerny J. Repertoire diversity of antibody response to bacterial antigens in aged mice. III. Phosphorylcholine antibody from young and aged mice differ in structure and protective activity against infection with Streptococcus pneumoniae. J Immunol. 1993 Jan 15;150(2):543-9. PMID: 8419487.
- Nicoletti C. Unsolved mysteries of intestinal M cells. Gut. 2000 Nov;47(5):735-739. DOI: 10.1136/gut.47.5.735. PMID: 11034595; PMCID: PMC1728097.

- O'Toole PW, Jeffery IB. Gut microbiota and aging. Science. 2015; 350:1214–1215. doi: 10.1126/science.aac8469
- Ohno H, Intestinal M cells, The Journal of Biochemistry, Volume 159, Issue 2, February 2016, Pages 151–160, https://doi.org/10.1093/jb/mvv121
- Park JS, Jeon HJ, Pyo JH, Kim YS, Yoo MA. Deficiency in DNA damage response of enterocytes accelerates intestinal stem cell aging in Drosophila. Aging (Albany NY). 2018 Mar 7;10(3):322-338. doi: 10.18632/aging.101390. PMID: 29514136; PMCID: PMC5892683.
- Parker, A., Maclaren, O. J., Fletcher, A. G., Muraro, D., Kreuzaler, P. A., Byrne, H. M., Maini, P. K., Watson, A. J., & Pin, C. (2017). Cell proliferation within small intestinal crypts is the principal driving force for cell migration on villi. FASEB journal : official publication of the Federation of American Societies for Experimental Biology, 31(2), 636–649. https://doi.org/10.1096/fj.201601002.
- Pelaseyed, T., Bergström, J. H., Gustafsson, J. K., Ermund, A., Birchenough, G. M., Schütte, A., van der Post, S., Svensson, F., Rodríguez-Piñeiro, A. M., Nyström, E. E., Wising, C., Johansson, M. E., & Hansson, G. C. (2014). The mucus and mucins of the goblet cells and enterocytes provide the first defense line of the gastrointestinal tract and interact with the immune system. Immunological reviews, 260(1), 8–20. https://doi.org/10.1111/imr.12182.
- Pellegrini C, D'Antongiovanni V, Ippolito C, Segnani C, Antonioli L, Fornai M, Bernardini N. From the intestinal mucosal barrier to the enteric neuromuscular compartment: an integrated overview on the morphological changes in Parkinson's disease. Eur J Histochem. 2021 Nov 22;65(s1):3278. doi: 10.4081/ejh.2021.3278. PMID: 34802221; PMCID: PMC8636839.
- Perez-Riverol Y, Csordas A, Bai J, Bernal-Llinares M, Hewapathirana S, Kundu DJ, Inuganti A, Griss J, Mayer G, Eisenacher M, Pérez E, Uszkoreit J, Pfeuffer J, Sachsenberg T, Yilmaz S, Tiwary S, Cox J, Audain E, Walzer M, Jarnuczak AF, Ternent T, Brazma A, Vizcaíno JA. The PRIDE database and related tools and resources in 2019: improving support for quantification data. Nucleic Acids Res. 2019 Jan 8;47(D1):D442-D450. doi: 10.1093/nar/gky1106. PMID: 30395289; PMCID: PMC6323896.
- Peters BA, Dominianni C, Shapiro JA, Church TR, Wu J, Miller G, Yuen E, Freiman H, Lustbader I, Salik J, Friedlander C, Hayes RB, Ahn J. The gut microbiota in conventional and serrated precursors of colorectal cancer. Microbiome. 2016 Dec 30;4(1):69. doi: 10.1186/s40168-016-0218-6.
- Petrella C, Farioli-Vecchioli S, Cisale GY, Strimpakos G, Borg JJ, Ceccanti M, Fiore M, Monteleone G, Nisticò R. A Healthy Gut for a Healthy Brain: Preclinical, Clinical and Regulatory Aspects. Curr Neuropharmacol.

2021;19(5):610-628. doi: 10.2174/1570159X18666200730111528. PMID: 32744976; PMCID: PMC8573748.

- Pitts MW. Barnes Maze Procedure for Spatial Learning and Memory in Mice. Bio Protoc. 2018 Mar 5;8(5):e2744. doi: 10.21769/bioprotoc.2744. PMID: 29651452; PMCID: PMC5891830.
- Qi Y, Goel R, Kim S, Richards EM, Carter CS, Pepine CJ, Raizada MK, Buford TW. Intestinal Permeability Biomarker Zonulin is Elevated in Healthy Aging. J Am Med Dir Assoc. 2017 Sep 1;18(9):810.e1-810.e4. doi: 10.1016/j.jamda.2017.05.018. Epub 2017 Jul 1. PMID: 28676292; PMCID: PMC5581307.
- Ragonnaud E, Biragyn A. Gut microbiota as the key controllers of "healthy" aging of elderly people. Immun Ageing. 2021 Jan 5;18(1):2. doi: 10.1186/s12979-020-00213-w. PMID: 33397404; PMCID: PMC7784378.
- Regan JC, Khericha M, Dobson AJ, Bolukbasi E, Rattanavirotkul N, Partridge L. Sex difference in pathology of the ageing gut mediates the greater response of female lifespan to dietary restriction. Elife. 2016 Feb 16;5:e10956. doi: 10.7554/eLife.10956. PMID: 26878754; PMCID: PMC4805549.
- Rokavec M, Kaller M, Horst D, Hermeking H. Pan-cancer EMT-signature identifies RBM47 down-regulation during colorectal cancer progression. Sci Rep. 2017 Jul 5;7(1):4687. doi: 10.1038/s41598-017-04234-2. PMID: 28680090; PMCID: PMC5498532.
- Santiago AF, Fernandes RM, Santos BP, Assis FA, Oliveira RP, Carvalho CR, Faria AM. Role of mesenteric lymph nodes and aging in secretory IgA production in mice. Cell Immunol. 2008 May-Jun;253(1-2):5-10. doi: 10.1016/j.cellimm.2008.06.004. Epub 2008 Jul 15. PMID: 18632091.
- Santoro A, Zhao J, Wu L, Carru C, Biagi E, Franceschi C. Microbiomes other than the gut: inflammaging and age-related diseases. Semin Immunopathol. 2020 Oct;42(5):589-605. doi: 10.1007/s00281-020-00814-z. Epub 2020 Sep 30. PMID: 32997224; PMCID: PMC7666274.
- Sasaki, A., Nishimura, T., Takano, T. et al. white regulates proliferative homeostasis of intestinal stem cells during ageing in Drosophila. Nat Metab 3, 546–557 (2021). https://doi.org/10.1038/s42255-021-00375-x.
- Schmucker DL, Owen RL, Outenreath R, Thoreux K. Basis for the age-related decline in intestinal mucosal immunity. Clin Dev Immunol. 2003 Jun-Dec;10(2-4):167-72. doi: 10.1080/10446670310001642168. PMID: 14768948; PMCID: PMC2485420.
- Schmucker DL. Intestinal mucosal immunosenescence in rats. Exp Gerontol. 2002 Jan-Mar;37(2-3):197-203. doi: 10.1016/s0531-5565(01)00184-x. PMID: 11772504.
- Seishima R, Barker N. A contemporary snapshot of intestinal stem cells and their regulation. Differentiation. 2019 Jul-Aug;108:3-7. doi: 10.1016/j.diff.2019.01.004. Epub 2019 Jan 25. PMID: 30711339.

- Shoji H, Takao K, Hattori S, Miyakawa T. Age-related changes in behavior in C57BL/6J mice from young adulthood to middle age. Mol Brain. 2016 Jan 28;9:11. doi: 10.1186/s13041-016-0191-9. PMID: 26822304; PMCID: PMC4730600.
- Shunsuke, Tachibana, Tomo, Hayase, Michiaki, & Yamakage (2020). Dexmedetomidine attenuates surgery-induced cognitive deficit and hippocampal Mapt expression in aged mice. doi ： 10.15114/smj.88.65
- Silva YP, Bernardi A, Frozza RL. The Role of Short-Chain Fatty Acids From Gut Microbiota in Gut-Brain Communication. Front Endocrinol (Lausanne). 2020 Jan 31;11:25. doi: 10.3389/fendo.2020.00025. PMID: 32082260; PMCID: PMC7005631.
  Simen AA. Parallel declines in cognition, motivation, and locomotion in aging
- Stevens, B. R., Goel, R., Seungbum, K., Richards, E. M., Holbert, R. C., Pepine, C. J., & Raizada, M. K. (2018). Increased human intestinal barrier permeability plasma biomarkers zonulin and FABP2 correlated with plasma LPS and altered gut microbiome in anxiety or depression. Gut, 67(8), 1555–1557. https://doi.org/10.1136/gutjnl-2017-314759
- Thursby E, Juge N. Introduction to the human gut microbiota. Biochem J. 2017;474(11):1823-1836. Published 2017 May 16. doi:10.1042/BCJ20160510
- Tran L, Greenwood-Van Meerveld B. Age-associated remodeling of the intestinal epithelial barrier. J Gerontol A Biol Sci Med Sci. 2013 Sep;68(9):1045-56. doi: 10.1093/gerona/glt106. Epub 2013 Jul 20. PMID: 23873964; PMCID: PMC3738030.
- Tran TTT, Corsini S, Kellingray L, Hegarty C, Le Gall G, Narbad A, et al. APOE genotype influences the gut microbiome structure and function in humans and mice: relevance for Alzheimer's disease pathophysiology. FASEB J. 2019;33(7):8221–31
- Tremblay S, Côté NML, Grenier G, Duclos-Lasnier G, Fortier LC, Ilangumaran S, Menendez A. Ileal antimicrobial peptide expression is dysregulated in old age. Immun Ageing. 2017 Aug 29;14:19. doi: 10.1186/s12979-017-0101-8. PMID: 28855949; PMCID: PMC5575895.
- Unger MM, Spiegel J, Dillmann KU, Grundmann D, Philippeit H, Bürmann J, et al. Short chain fatty acids and gut microbiota differ between patients with Parkinson’s disease and age-matched controls. Park Relat Disord. (2016) 32:66–72. doi: 10.1016/j.parkreldis.2016.08.019
- van Beek, A. A., Sovran, B., Hugenholtz, F., Meijer, B., Hoogerland, J. A., Mihailova, V., van der Ploeg, C., Belzer, C., Boekschoten, M. V., Hoeijmakers, J. H., Vermeij, W. P., de Vos, P., Wells, J. M., Leenen, P. J., Nicoletti, C., Hendriks, R. W., & Savelkoul, H. F. (2016). Supplementation with Lactobacillus plantarum WCFS1 Prevents Decline of Mucus Barrier

in Colon of Accelerated Aging Ercc1-/Δ7 Mice. Frontiers in immunology, 7, 408.

- Van der Sluis M, De Koning BA, De Bruijn AC, Velcich A, Meijerink JP, Van Goudoever JB, Büller HA, Dekker J, Van Seuningen I, Renes IB, Einerhand AW. Muc2-deficient mice spontaneously develop colitis, indicating that MUC2 is critical for colonic protection. Gastroenterology. 2006 Jul;131(1):117-29. doi: 10.1053/j.gastro.2006.04.020. PMID: 16831596.
- Varela, E., Muñoz-Lorente, M., Tejera, A. et al. Generation of mice with longer and better preserved telomeres in the absence of genetic manipulations. Nat Commun 7, 11739 (2016). https://doi.org/10.1038/ncomms11739
- Venugopal S, Anwer S, Szászi K. Claudin-2: Roles beyond Permeability Functions. Int J Mol Sci. 2019 Nov 12;20(22):5655. doi: 10.3390/ijms20225655. PMID: 31726679; PMCID: PMC6888627.
- Wang Q, Qi Y, Shen W, et al. The Aged Intestine: Performance and Rejuvenation. Aging Dis. 2021;12(7):1693-1712. Published 2021 Oct 1. doi:10.14336/AD.2021.0202.
- Wang RX, Henen MA, Lee JS, Vögeli B, Colgan SP. Microbiota-derived butyrate is an endogenous HIF prolyl hydroxylase inhibitor. Gut Microbes. 2021 Jan-Dec;13(1):1938380. doi: 10.1080/19490976.2021.1938380. PMID: 34190032; PMCID: PMC8253137.
- Wang X, Wang BR, Zhang XJ, Xu Z, Ding YQ, Ju G. Evidences for vagus nerve in maintenance of immune balance and transmission of immune information from gut to brain in STM-infected rats. World J Gastroenterol. (2002) 8:540–5. doi: 10.3748/wjg.v8.i3.540
- Wen L, Zhang X, Zhang J, Chen S, Ma Y, Hu J, Yue T, Wang J, Zhu J, Wu T, Wang X. Paxillin knockdown suppresses metastasis and epithelial-mesenchymal transition in colorectal cancer via the ERK signaling pathway. Oncol Rep. 2020 Sep;44(3):1105-1115. doi: 10.3892/or.2020.7687. Epub 2020 Jul 14. PMID: 32705241; PMCID: PMC7388420
- Wilson QN, Wells M, Davis AT, Sherrill C, Tsilimigras MCB, Jones RB, Fodor AA, Kavanagh K. Greater Microbial Translocation and Vulnerability to Metabolic Disease in Healthy Aged Female Monkeys. Sci Rep. 2018 Jul 27;8(1):11373. doi: 10.1038/s41598-018-29473-9. PMID: 30054517; PMCID: PMC6063974.
- Yang H, Wu J, Zhang J, Yang Z, Jin W, Li Y, Jin L, Yin L, Liu H, Wang Z. Integrated bioinformatics analysis of key genes involved in progress of colon cancer. Mol Genet Genomic Med. 2019 Apr;7(4):e00588. doi: 10.1002/mgg3.588. Epub 2019 Feb 11. PMID: 30746900; PMCID: PMC6465657.

- Yang X, Yu D, Xue L, Li H, Du J. Probiotics modulate the microbiota-gut-brain axis and improve memory deficits in aged SAMP8 mice. Acta Pharm Sin B. 2020 Mar;10(3):475-487. doi: 10.1016/j.apsb.2019.07.001. Epub 2019 Jul 7. PMID: 32140393; PMCID: PMC7049608.
- Zhao CJ, Du SK, Dang XB, Gong M. Expression of Paxillin is Correlated with Clinical Prognosis in Colorectal Cancer Patients. Med Sci Monit. 2015;21:1989-1995. Published 2015 Jul 10. doi:10.12659/MSM.893832
- Zhao Y, Scott A, Zhang P, Hao Y, Feng X, Somasundaram S, Khalil AM, Willis J, Wang Z. Regulation of paxillin-p130-PI3K-AKT signaling axis by Src and PTPRT impacts colon tumorigenesis. Oncotarget. 2017 Jul 25;8(30):48782-48793. doi: 10.18632/oncotarget.10654. PMID: 27447856; PMCID: PMC5564724
- Zhuang X, Lv M, Zhong Z, Zhang L, Jiang R, Chen J. Interplay between intergrin-linked kinase and ribonuclease inhibitor affects growth and metastasis of bladder cancer through signaling ILK pathways. J Exp Clin Cancer Res. 2016 Aug 30;35(1):130. doi: 10.1186/s13046-016-0408-x. PMID: 27576342; PMCID: PMC5006283.

Acknowledgments

This work was supported by the Doctorate Degree program PEGASO of the Tuscany region.

I would like to thank all members of the Bertelli laboratory: Prof. Eugenio Bertelli, Dr. Marì Regoli and Dr. Daniela Orazioli; they have been my second family during the past three years. I want to thank my supervisor Prof. Bertelli who gave me the big opportunity to work on this interesting project. Thanks for believing in me, for all the support, patience and help. A special thanks to Dr. Regoli who has always been present to help answer my questions and to give me support with experiments. Thanks to both for being inspiring scientists. Most importantly I want to thank you all also for being supportive in all aspects of my life.

I want to thanks my co-supervisor Prof. Claudio Nicoletti who has given me the opportunity to work on this project. Thanks for all the time spent to help me, for all the advices and suggestions.

I also want to thanks to all the collaborators who have made this work be possible.

Thanks to Prof. Arjan Narbad who accepted me as a visitor in his group in Quadram Institute Bioscience. It has been a great experience for me. In particular I want to thanks Dr. Stefano Romano who supervised me and gave me the opportunity to learn a lot. I will never forget his advices!

Last but not least I want to thanks my family no words will ever be enough!